UNIVERSIDADE FEDERAL DE SANTA CATARINA
DEPARTAMENTO DE CIÊNCIAS FARMACÊUTICAS
PROGRAMA DE PÓS-GRADUAÇÃO EM FARMÁCIA

Jadel Müller Kratz

IMPLEMENTAÇÃO E APLICAÇÃO DO MODELO *IN VITRO*
COM CÉLULAS CACO-2 PARA ESTUDO DA
PERMEABILIDADE INTESTINAL DE FÁRMACOS

Florianópolis

2011

Jadel Müller Kratz

IMPLEMENTAÇÃO E APLICAÇÃO DO MODELO *IN VITRO* COM CÉLULAS CACO-2 PARA ESTUDO DA PERMEABILIDADE INTESTINAL DE FÁRMACOS

Esta Tese foi julgada e aprovada em sua forma final pela Orientadora e membros da Banca Examinadora, composta pelos Professores Doutores:

Banca Examinadora:

_____
Prof.ª Dr.ª Simone Gonçalves Cardoso (UFSC – Membro Titular)

_____
Prof.ª Dr.ª Ângela Machado de Campos (UFSC – Membro Titular)

_____
Prof. Dr. João Batista Calixto (UFSC – Membro Titular)

_____
Prof.ª Dr.ª Bibiana Verlindo de Araújo (UFRGS – Membro Titular)

_____
Prof.ª Dr.ª Sílvia Storpirtis (USP – Membro Titular)

_____
Prof.ª Dr.ª Cláudia Maria Oliveira Simões (UFSC – Orientadora)

Prof. Dr. Eloir Paulo Schenkel
Coordenador do Programa de Pós-Graduação em Farmácia da UFSC

Florianópolis, 14 de Julho de 2011.

À minha família – Delso, Jacinta e Mahil

AGRADECIMENTOS

You can't always get what you want
But if you try sometimes, well you just might find
You get what you need...

(M. Jagger/K. Richards – The Rolling Stones, 1969)

RESUMO

Implementação e aplicação do modelo *in vitro* com células caco-2 para estudo da permeabilidade intestinal de fármacos

A absorção oral de um fármaco é controlada fundamentalmente por dois fatores: a solubilidade aquosa/dissolução e a permeabilidade intestinal. Portanto, a determinação dessas características ainda nas fases de descoberta e desenvolvimento de fármacos pode prover moléculas com ótimo perfil biofarmacêutico. Nesse sentido, esta tese teve dois objetivos: implementar e validar o modelo de avaliação da permeabilidade *in vitro* com células Caco-2 no Laboratório de Virologia Aplicada da UFSC, e aplicar esse modelo na determinação da permeabilidade de fármacos e compostos em estudo. Na implementação do modelo Caco-2 foi demonstrada a adequação morfológica das células, através do monitoramento da resistência elétrica transepitelial e da permeabilidade do *Lucifer yellow*. Através da avaliação da permeabilidade de fármacos marcadores (aciclovir, carbamazepina, hidroclorotiazida, propranolol, vimblastina e verapamil) em experimentos de transporte bi-direcional foi demonstrado que o modelo foi devidamente validado, já que foi estabelecida correlação entre a permeabilidade *in vitro* e a absorção em humanos. Adicionalmente, uma metodologia por CLAE-UV foi desenvolvida e validada para a determinação concomitante de todos esses fármacos marcadores. Na segunda etapa, avaliou-se o complexo talidomida:hidroxipropil-β-ciclodextrina, desenvolvido e caracterizado no estado sólido por diferentes técnicas, que comprovaram a complexação do fármaco e a redução da sua cristalinidade. Essas alterações culminaram em um leve aumento da solubilidade aparente do fármaco, bem como propiciaram um perfil de dissolução superior, quando comparado ao da talidomida isolada. No entanto, nenhuma alteração na permeabilidade foi detectada. Esses resultados sugerem que esta complexação poderia aumentar a biodisponibilidade oral da talidomida, através do aumento da sua solubilidade nos fluídos gastrointestinais, bem como facilitando a sua dissolução a partir de uma forma farmacêutica sólida. Também foi avaliado o composto anti-herpético galato de pentila, e foi demonstrado que ele apresenta perfis de permeabilidade intestinal e cutânea favoráveis para sua absorção oral e permeação tópica, respectivamente. Assim, após administração oral, sua biodisponibilidade não seria limitada pela permeabilidade intestinal, e no que se refere à administração tópica, ele ficaria restrito às camadas da pele no local de aplicação. Esses dados fornecem informações valiosas para o desenvolvimento de formas farmacêuticas e para a avaliação da atividade antiviral *in vivo*. Em suma, o modelo com células Caco-2 foi implementado, validado e aplicado satisfatoriamente, o que permitirá a execução de estudos colaborativos, sobretudo com o enfoque do Sistema de Classificação Biofarmacêutica.

Palavras-chave: permeabilidade intestinal, células Caco-2, talidomida, ciclodextrina, galato de pentila, Sistema de Classificação Biofarmacêutica

ABSTRACT

Implementation and application of the *in vitro* model with Caco-2 cells for the study of intestinal permeability of drugs

The oral drug absorption is fundamentally controlled by two factors: the aqueous solubility/dissolution and the permeability. Therefore, the early determination of these characteristics during drug discovery and development can secure the construction of molecules with optimal biopharmaceutical profiles. In this view, this thesis had two main objectives: to implement and validate the *in vitro* permeability model with Caco-2 cells in the Applied Virology Laboratory at UFSC, and employ this validated model in the permeability determination of cyclodextrin complexes of thalidomide, developed and characterized within this work, and pentyl gallate, a compound with promising anti-herpetic activity. During the Caco-2 model implementation, the cell monolayers morphologic adequacy was demonstrated by the measurement of the transepitelial electrical resistance and lucifer yellow permeability. The results obtained in bi-directional transport experiments with marker drugs (acyclovir, carbamazepine, hydrochlorothiazide, propranolol, vinblastine and verapamil) corroborated the assay suitability, given that a good correlation between *in vitro* permeability coefficients and human absorption was established. Additionally, an HPLC-UV method was developed and validated for the simultaneous determination of this group of drugs. In the second phase of this thesis, thalidomide:hydroxypropyl-β-cyclodextrin complexes were obtained and characterized in the solid state through different techniques. The results confirmed the inclusion of the drug and the reduction of its cristallinity. These modifications slightly improved thalidomide apparent solubility and enhanced the *in vitro* dissolution rate in comparison to the drug alone, even though the *in vitro* permeability was not affected. These findings suggest that the complexation could improve the bioavailability of orally administered thalidomide through the improvement of its solubility in the intestinal fluids and dissolution from the dosage form. The study with pentyl gallate showed that this compound presents favorable intestinal and cutaneous permeability profiles. Its oral bioavailability would not be jeopardized by limited intestinal permeability, and would be restricted to the application site when administered by the topical route. These findings provide valuable information for the formulation development and *in vivo* antiviral experiments. In summary, the *in vitro* permeability model with Caco-2 cells was implemented, validated and employed suitably. This assay is of great importance for our research group since it permits future collaborative studies regarding the Biopharmaceutics Classification System.

Keywords: intestinal permeability; Caco-2 cells; thalidomide; cyclodextrin, pentyl gallate; Biopharmaceutic Classification System

LISTA DE FIGURAS

SUMÁRIO

INTRODUÇÃO

DESCOBERTA E DESENVOLVIMENTO DE NOVOS FÁRMACOS

Nos últimos anos, os avanços tecnológicos ocorridos mudaram drasticamente as estratégias da pesquisa, desenvolvimento e inovação de fármacos. Essa é uma área em contínuo aperfeiçoamento, conforme novos conhecimentos, técnicas, métodos e estratégias são introduzidos. O que no passado era um processo basicamente empírico, atualmente avalia amostras em grande escala, principalmente após a introdução de modelos farmacológicos *in vitro*, da química combinatória, do estabelecimento de relações estrutura-atividade quantitativas, e modelos computacionais, associados ao forte crescimento do conhecimento relacionado ao desenvolvimento racional de fármacos (LIPINSKI et al., 1997; HOUGHTON, 2000; WATERBEEMD, GIFFORD, 2003; GANESAN, 2008; KERNS, DI, 2008).

Basicamente, novas moléculas ativas são sintetizadas ou isoladas de fontes naturais e têm sua atividade farmacológica identificada. Passam então para o desenvolvimento clínico e, se aprovados pelas agências regulatórias, tornam-se medicamentos disponíveis para o tratamento de pacientes. Esse é um processo excessivamente complexo e dispendioso. Os pesquisadores envolvidos interagem em múltiplas linhas de investigação, que envolvem diversas disciplinas, muitas vezes conflitantes, e por fim devem integrar os dados obtidos com o objetivo de obter um composto balanceado e com bom potencial terapêutico (HIDALGO, 2001; CHEN et al., 2006; KERNS, DI, 2008).

A pesquisa de novos fármacos pode ser dividida em dois estágios: descoberta e desenvolvimento (Figura 1). A descoberta compreende os passos iniciais onde alvos farmacológicos (enzimas ou receptores) são identificados e moléculas são isoladas de fontes naturais e/ou modificadas e/ou sintetizadas e otimizadas. Através da química combinatória, um grande número de compostos é produzido e paralelamente avaliado no que se refere à sua interação com o alvo desejado, o que determina a atividade intrínseca da molécula. Outras propriedades também são avaliadas, tais como pKa, solubilidade, permeabilidade, instabilidade química e metabólica, interação com enzimas, entre outras (WHITE, 2000; BLEICHER et al., 2003; BALIMANE, HAN, CHONG, 2006; KERNS, DI, 2008).

Em uma plataforma de descobrimento de fármacos são tomadas numerosas decisões no que se refere à possível progressão de uma molécula ativa às diferentes etapas da pesquisa. Somente moléculas

tidas como adequadas passarão para as fases seguintes. Decisões baseadas nas características físico-químicas são normalmente mais fáceis do que aquelas que envolvem propriedades biológicas, uma vez que essas têm interpretação mais problemática, considerando a complexidade dos sistemas biológicos. Como se tratam de decisões irrevogáveis, com julgamento de "sim ou não", é crucial que se obtenham informações meticulosas e acuradas, a fim de minimizar a ocorrência de falsos positivos ou negativos durante esse processo (WHITE, 2000; BLEICHER et al., 2003; BALIMANE, HAN, CHONG, 2006; KERNS, DI, 2008).
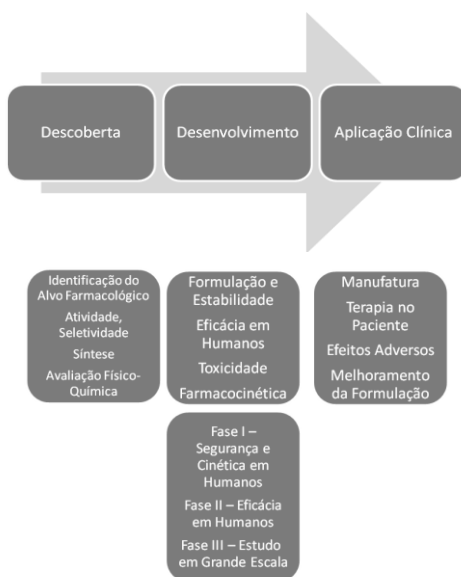
Figura 1. Representação esquemática da progressão da descoberta e desenvolvimento de fármacos. Adaptado de Kerns e Di (2008).

Um pequeno número de moléculas identificadas como sendo as que possuem as características mais desejáveis será então selecionado para progredir para a fase de desenvolvimento. Essa etapa é subdividida em pré-clínica e clínica. Durante a fase pré-clínica, estudos em animais são conduzidos com o objetivo de reunir a maior quantidade possível de dados acerca da segurança da molécula. Em paralelo, inúmeros experimentos *in vitro* são realizados visando à completa caracterização dos perfis físico-químico e farmacológico da molécula. Posteriormente,

os ensaios clínicos iniciais são conduzidos em pequena escala e englobam apenas voluntários sadios (fase 1), porém à medida que a molécula apresenta um efeito promissor, os estudos evoluem e passam a ser incluídos também pacientes (fases 2 e 3) (NEERVANNAN, 2006; KERNS, DI, 2008).

Em média, 50 projetos de descoberta de fármacos geram em torno de 10 moléculas candidatas à fase de desenvolvimento, que por fim levam a um medicamento comercializável, uma vez que a taxa de sucesso nos ensaios clínicos varia entre 10 e 20%, em um longo processo que leva em média 12 anos e consome diversos milhões de dólares. Esse custo tremendo não inclui apenas as despesas diretamente associadas com o medicamento em questão, mas também os custos de todas as moléculas que falharam durante as fases anteriores, das quais não se pode obter lucro algum (DIMASI, HANSEN, GRABOWSKI 2003; DICKSON, GAGNON, 2004; LOMBARDINO, LOWE, 2004; PREZIOSI, 2004; DIMASI et al., 2010; KAITIN, DIMASI, 2011).

Um estudo realizado na década de 90 revelou que, naquele período, em torno de 40% dos candidatos eliminados na fase de desenvolvimento eram descartados devido às propriedades farmacocinéticas precárias (KENNEDY, 1997). Por isso, a indústria farmacêutica decidiu concentrar esforços na investigação da absorção, distribuição, metabolismo e excreção (ADME) durante as fases iniciais do processo de descoberta de fármacos. Tradicionalmente, as corporações farmacêuticas focavam apenas na otimização da atividade farmacológica, baseada em ensaios biológicos *in vitro* e *in vivo*, atitude essa que foi modificada através da implementação da avaliação precoce do perfil ADME. Como resultado dessa mudança de paradigma, um estudo mais recente mostrou que as falhas associadas à ADME na fase de desenvolvimento reduziram de 40 para 10%. À medida que as falhas associadas às propriedades ADME foram reduzindo, o foco da indústria passou a ser o perfil toxicológico das moléculas, responsável atualmente pelo maior número de reprovações (KOLA, LANDIS, 2004).

Portanto, a avaliação, ainda na fase de descoberta, das propriedades biofarmacêuticas, tais como solubilidade, permeabilidade, metabolismo e estabilidade, pode prover importantes informações aos pesquisadores, esclarecendo dúvidas, predizendo e diagnosticando resultados *in vivo*, guiando relações estrutura-atividade e, sobretudo, fornecendo uma base sólida para a tomada de decisões. Fármacos bem sucedidos podem ser desenvolvidos quando as propriedades farmacológicas são otimizadas em paralelo com as propriedades farmacêuticas (DI, KERNS, 2005).

ABSORÇÃO INTESTINAL DE FÁRMACOS

Segundo a Organização Mundial da Saúde, em 2001, dos cinqüenta medicamentos mais vendidos 84% eram de administração oral (LENNERNÄS, ABRAHAMSOM, 2005). Essa via é considerada a mais segura e conveniente, entretanto, um fármaco administrado oralmente necessita chegar à circulação sistêmica para que alcance o local de ação na concentração e velocidade apropriadas a fim de exercer seu efeito terapêutico (STORPIRTIS, GAI, 2009).

Muitos são os fatores que afetam a biodisponibilidade oral de um fármaco (Figura 2); entretanto, a absorção intestinal é controlada fundamentalmente por dois fatores: (I) a solubilidade e a taxa de dissolução (que determinam a velocidade na qual o fármaco atinge sua concentração máxima nos fluídos intestinais), e (II) a permeabilidade (que está relacionada com a taxa de fármaco dissolvido que atravessa a parede intestinal e entra na circulação portal) (AMIDON et al., 1995; BOHETS et al., 2001).
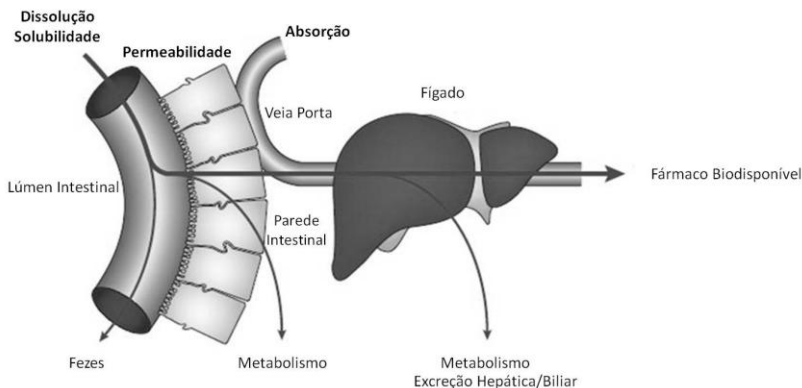
Figura 2. Representação esquemática dos fatores que influenciam a biodisponibilidade oral de um fármaco. Adaptado de Waterbeemd (2003).

Portanto, a determinação dos **perfis de dissolução** e de **solubilidade** (em diferentes pHs), e das propriedades de **permeabilidade** de fármacos pode fornecer informações valiosas sobre sua absorção oral (BOHETS et al., 2001). Um dos grandes avanços nessa área foi a criação, por Amidon e colaboradores (1995), do Sistema de Classificação Biofarmacêutica (SCB). O principal objetivo do SCB é

estimar o desempenho farmacocinético *in vivo* de um medicamento a partir de dados de permeabilidade e de solubilidade/dissolução (KARALIS et al., 2008). Com base nesses parâmetros, o SCB divide os fármacos em quatro classes:

- Classe 1 – fármacos com alta solubilidade e alta permeabilidade. Considera-se que o fármaco é bem absorvido e que o fator limitante para a absorção é a dissolução a partir da forma farmacêutica ou o esvaziamento gástrico, caso a dissolução seja muito rápida.
- Classe 2 – fármacos com baixa solubilidade e alta permeabilidade. A dissolução *in vivo* é o fator que controla a absorção oral, que normalmente é inferior à obtida com fármacos da primeira classe.
- Classe 3 – fármacos com alta solubilidade e baixa permeabilidade. Nesta classe a permeabilidade é o fator limitante, sendo que o perfil de dissolução apresentado será bem definido e simplificado.
- Classe 4 – fármacos com baixa solubilidade e baixa permeabilidade, ou seja, fármacos que apresentam problemas significativos para a administração oral (AMIDON et al., 1995).

Dessa forma, a utilização dos parâmetros considerados pelo SCB durante a descoberta e desenvolvimento de novos produtos farmacêuticos pode reduzir gastos e tempo. Esse sistema também representa uma ferramenta regulatória importante, possibilitando a substituição de determinados estudos de bioequivalência por testes de dissolução *in vitro*, podendo assim reduzir a exposição de voluntários sadios a fármacos em desenvolvimento (LENNERNÄS, ABRAHAMSSON, 2005).

Os **testes de dissolução** objetivam avaliar a liberação do fármaco a partir de uma forma farmacêutica para um meio aquoso, que mimetiza as condições *in vivo* (exceto nos casos de avaliação da dissolução intrínseca, onde é avaliada a dissolução do fármaco no estado sólido sem a presença da forma farmacêutica), e representam uma ferramenta indispensável nas etapas de desenvolvimento farmacotécnico de medicamentos. A importância da avaliação dos perfis de dissolução é enorme, uma vez que é possível afirmar que se o processo de dissolução de um medicamento (fármaco/forma farmacêutica sólida de liberação

imediata) é rápido, então a velocidade e a extensão da absorção oral deste fármaco é primariamente dependente da sua permeabilidade na mucosa intestinal (LENNERNÄS, ABRAHAMSSON, 2005; SOUZA et al., 2007; KERNS, DI, 2008).

Na área de produção farmacêutica e controle de qualidade, os resultados dos testes de dissolução podem ser empregados para detectar desvios na fabricação, para assegurar uniformidade durante a produção, e para avaliar diferenças entre polimorfos cristalinos de um mesmo fármaco. Eles também podem ser utilizados para avaliar mudanças após o registro do produto e podem auxiliar na decisão para a realização de estudos de bioequivalência e quando do estabelecimento de correlações *in vitro − in vivo* (SOUZA et al., 2007; KOVACEVIC et al., 2008; CARINI et al., 2009; YANG, 2010).

A **solubilidade** é outro fator determinante para a liberação do fármaco a partir da sua forma farmacêutica, bem como para sua absorção, já que o fármaco precisa estar em solução aquosa para ser absorvido na mucosa intestinal (STORPIRTIS, GAI, 2009). Essa propriedade está intimamente ligada às características moleculares, sendo que a baixa solubilidade aquosa é causada essencialmente por dois fatores: alta lipofilicidade e estrutura de rede cristalina muito rígida (geralmente identificada por um alto ponto de fusão), o que torna a solubilização do fármaco no estado sólido um processo altamente energético (MARTINEZ, AMIDON, 2002; FALLER, ERTL, 2007; MULLERTZ, 2010).

As definições de alta e baixa solubilidade são relativas, e dependem da dose terapêutica esperada e também da potência do fármaco. Como regra geral, uma molécula com potência moderada (1 mg/kg) deve apresentar um valor de solubilidade aparente de, ao menos, 0,1 g/L para ser adequadamente solúvel. Se uma molécula de mesma potência apresentar solubilidade menor que 0,01 g/L, então ela será considerada pouco solúvel (FALLER, ERTL, 2007). O SCB considera um fármaco altamente solúvel se a maior dose terapêutica for solúvel em volume igual ou menor que 250 mL na faixa de pH de 1,0 – 7,5. A fim de ser enquadrado na classe I, também é necessário que o fármaco apresente 85% de dissolução em 30 min para garantir a sua bioequivalência (US FDA, 2000).

Em geral, fármacos pouco solúveis podem ser divididos em dois grupos, dependendo da sua lipofilicidade: (1) fármacos não-lipofílicos e hidrofóbicos, conhecidos como "pó de tijolo" (do inglês *brick dust*) apresentam forte rede cristalina e são pouco solúveis também em lipídeos, tais como os triglicerídeos; eles podem apresentar uma

solubilidade razoável quando em formulações contendo surfactantes ou co-solventes; (2) fármacos lipofílicos e hidrófobicos, conhecidos como "bolas gordurosas" (do inglês *grease balls*), de baixa molhabilidade, solúveis em lipídeos, e que podem ter sua solubilidade melhorada quando formulados em sistemas lipídicos de liberação (MULLERTZ et al., 2010).

A **permeabilidade** também tem importante papel na absorção oral e penetração tecidual de fármacos (por exemplo, o sistema nervoso central). Uma vez que o fármaco tenha sido liberado da sua forma farmacêutica e seja solúvel nos fluidos gastrointestinais, ele está disponível para o transporte através da mucosa intestinal (BALIMANE, HAN, CHONG, 2006).

A permeabilidade intestinal é um processo complexo e envolve múltiplas vias (Figura 3).
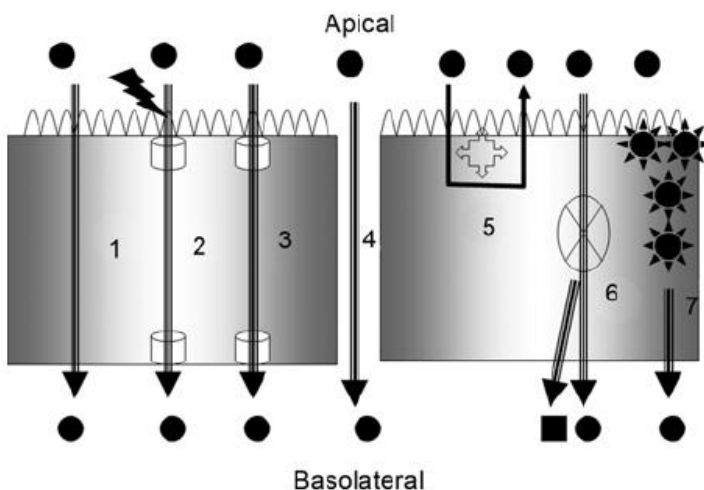
Figura 3. Esquema representativo das rotas e mecanismos de transporte através do epitélio intestinal (BALIMANE, HAN, CHONG, 2006).

A absorção passiva pela rota transcelular (1) é a mais comum entre os fármacos, e ocorre pelo interior dos enterócitos, sem gasto energético. A via passiva também compreende o transporte pelos espaços intercelulares (rota paracelular – 4). A absorção mediada por carreadores ocorre via processo ativo (transporte ativo – 2) ou por

difusão facilitada (3). Vários transportadores de membrana, muitos deles bombas de efluxo, tais como a glicoproteína-P (P-gp), estão localizados na porção apical dos enterócitos, atuando na proteção do organismo contra xenobióticos (5). Além disso, enzimas intestinais podem estar envolvidas na metabolização de fármacos na parede intestinal (6), e, por fim, a endocitose mediada por receptor (7) também desempenha um importante papel na absorção intestinal (BALIMANE, HAN, CHONG, 2006; PRESS; DI GRANDI, 2008). De forma geral, a permeabilidade é dependente da concentração do fármaco no lúmen intestinal, e é diretamente afetada por outros fatores, tais como a presença de transportadores de membrana, efeitos provocados pelos constituintes da forma farmacêutica, e outros fatores fisiológicos e bioquímicos (AMIDON et al., 1995; HIDALGO, 2001).

Existem diversos métodos disponíveis para a avaliação da permeabilidade intestinal, entre eles modelos físico-químicos, modelos computacionais (*in silico*), modelos *in vitro* (células ou tecidos), modelos de perfusão in situ e modelos *in vivo*, cada um apresentando vantagens e desvantagens perante os demais. (para uma revisão completa ver BOHETS et al., 2001; MIRET et al., 2004).

Entre os modelos mais amplamente reconhecidos e utilizados pela indústria farmacêutica estão o ensaio PAMPA (*Parallel Artificial Membrane Permeability Assay*) e o modelo que emprega células Caco-2. Com o ensaio PAMPA é possível avaliar apenas a permeabilidade passiva, uma vez que esse modelo baseia-se na separação de dois compartimentos por uma bicamada lipídica simples, enquanto que as células Caco-2 representam um modelo de mecanismos múltiplos, já que esta linhagem se diferencia e passa a exibir características morfológicas e funcionais similares às dos enterócitos (ARTURSSON, PALM, LUTHMAN, 2001; BOHETS et al., 2001; MIRET et al., 2004).

A combinação dessas duas metodologias fornece uma avaliação diagnóstica da permeabilidade. Caso haja uma correlação entre os resultados obtidos nos dois ensaios, um perfil de permeabilidade passiva é esperado. Entretanto, se os valores de permeabilidade em Caco-2 forem inferiores ou superiores aos obtidos no PAMPA, é possível que o fármaco seja substrato de algum transportador de efluxo ou absorção, respectivamente (DI, KERNS, 2005). As indústrias farmacêuticas costumam utilizar primeiramente o ensaio PAMPA como uma ferramenta de triagem, pois ele é relativamente mais barato, rápido e simples. O modelo com células Caco-2 é empregado, em um segundo momento, com o objetivo de identificar um possível mecanismo de transporte ativo (BOHETS et al., 2001; MIRET et al., 2004).

O LABORATÓRIO DE VIROLOGIA APLICADA DA UFSC

O Laboratório de Virologia Aplicada da UFSC, sob coordenação da Profa. Dra. Cláudia Maria Oliveira Simões, há vários anos avalia as atividades citotóxica e antiviral de produtos naturais e compostos sintéticos, incluindo a elucidação dos mecanismos de ação, através de diferentes estratégias experimentais. A equipe do laboratório vem buscando constantemente a implementação de metodologias diferenciadas, a fim de complementar os estudos realizados no referido laboratório, propiciando a prática da multidisciplinaridade e uma formação mais completa dos recursos humanos envolvidos.

Desde que a predição da absorção oral de fármacos se tornou um importante critério de decisões na descoberta e desenvolvimento de fármacos, tornou-se imprescindível o estabelecimento de métodos confiáveis e padronizados de avaliação das propriedades associadas à absorção, tais como os parâmetros fundamentais descritos pelo SCB, dissolução, solubilidade e permeabilidade. Por exemplo, é previsível que compostos com permeabilidade ou solubilidade extremamente baixas irão resultar em baixa disponibilidade oral, limitando o seu desenvolvimento clínico (LENNERNÄS, ABRAHAMSSON, 2005).

Nesse sentido, e conforme o projeto de pesquisa apresentado inicialmente ao Programa de Pós-Graduação em Farmácia, o presente trabalho teve como objetivo principal a implementação e validação do modelo de avaliação da permeabilidade intestinal *in vitro* com células Caco-2, e a sua aplicação na avaliação do perfil de permeabilidade *in vitro* de complexos do fármaco talidomida com ciclodextrinas, e do galato de pentila, um composto cuja atividade anti-herpética já havia sido detectada em estudos prévios.

De acordo com os resultados obtidos, esta tese foi elaborada na forma de capítulos, que apresentam uma breve revisão da literatura do tema abordado em cada capítulo e os respectivos resultados na forma de manuscritos. O primeiro capítulo descreve os procedimentos realizados e resultados obtidos durante a implementação e validação do modelo de permeabilidade com células Caco-2. No capítulo 2 estão descritos os resultados obtidos com os estudos de complexação do fármaco talidomida com ciclodextrinas, e no capítulo 3 é apresentada a avaliação dos perfis *in vitro* de permeabilidade intestinal e cutânea do galato de pentila. Na forma de apêndices, são apresentados o artigo publicado referente ao capítulo 1, e dois manuscritos que são fruto de estudos colaborativos realizados durante o período do estágio sanduíche no Departamento de Farmácia da Universidade de Uppsala, na Suécia.

OBJETIVOS

1.1.1 Objetivo Geral

Implementar e validar a metodologia de avaliação da permeabilidade intestinal *in vitro* com células Caco-2, e explorar a sua aplicabilidade no estabelecimento da permeabilidade intestinal *in vitro* de fármacos.

1.1.2 Objetivos Específicos

- Padronizar técnicas de cultura celular no Laboratório de Virologia Aplicada da UFSC a fim de possibilitar a implementação do modelo de avaliação da permeabilidade intestinal *in vitro* com células Caco-2. (Capítulo 1)
- Desenvolver e validar método analítico por cromatografia líquida de alta eficiência para determinação de fármacos marcadores empregados na padronização do modelo de avaliação da permeabilidade intestinal *in vitro* com células Caco-2. (Capítulo 1)
- Preparar e caracterizar complexos de inclusão do fármaco talidomida com diferentes ciclodextrinas. (Capítulo 2)
- Avaliar a influência da complexação sobre os perfis *in vitro* de solubilidade, dissolução e permeabilidade intestinal do fármaco talidomida. (Capítulo 2)
- Avaliar os perfis de permeabilidade intestinal e cutânea do composto anti-herpético galato de pentila, a fim de prover bases para estudos futuros de atividade antiviral *in vivo*. (Capítulo 3)
- Estabelecer correlações entre os resultados obtidos com diferentes metodologias de avaliação da permeabilidade implementadas no Laboratório de Virologia Aplicada. (Capítulo 3)

CAPÍTULO 01

IMPLEMENTAÇÃO DO MODELO DE PERMEABILIDADE INTESTINAL *IN VITRO* COM CÉLULAS CACO-2:
Padronização do cultivo celular e desenvolvimento de metodologia analítica para detecção de fármacos marcadores

APRESENTAÇÃO

Existem diversos métodos que podem ser utilizados na avaliação da permeabilidade de compostos. Entre eles estão modelos físico-químicos, modelos computacionais *in silico*, modelos *in vitro* (células, membranas artificiais), modelos de perfusão in situ e modelos *ex vivo*, cada um apresentando vantagens e desvantagens perante os demais. Dentre esses modelos, um dos mais populares e reconhecidos pela indústria farmacêutica e agências regulatórias da área de medicamentos é o modelo de permeabilidade *in vitro* com células Caco-2 (BALIMANE, HAN, CHONG, 2006; EHRHARDT; KIM, 2008).

Tendo em vista a importância da avaliação de permeabilidade de compostos ainda nas etapas iniciais da pesquisa e desenvolvimento de novos fármacos, bem como a representatividade do modelo com células Caco-2, o mesmo foi selecionado para ser implementado e validado no Laboratório de Virologia Aplicada da UFSC. Seguindo as diretrizes da agência regulatória norte-americana de medicamentos e alimentos (FDA)(US FDA, 2000, 2006) e as recomendações de especialistas (HUBATSCH et al., 2007), diversos aspectos foram monitorados durante esse processo, a fim de se garantir as condições ideais para os experimentos.

Os esforços empregados culminaram na validação do ensaio, possibilitando a avaliação dos perfis de permeabilidade de compostos com estruturas químicas diversas e ações farmacológicas distintas. Até o momento, este é o primeiro relato de implementação e validação do modelo de células Caco-2 para avaliação da permeabilidade *in vitro* no Brasil, o que ressalta o caráter inovador da proposta.

Por fim, os resultados obtidos nesta etapa inicial foram publicados na forma de artigo original no periódico *Brazilian Journal of Medical and Biological Research*, Volume 44, Série 6, Páginas 531-537, 2011. Essa publicação é apresentada na íntegra no Apêndice 1.

REVISÃO DA LITERATURA

Nos anos 70, uma coleção de linhagens celulares foi estabelecida a partir de tumores gastrointestinais, com o objetivo de realizar estudos acerca dos mecanismos do câncer e suas terapias citostáticas relacionadas (FOGH et al., 1977). Uma década depois, devido às dificuldades encontradas em se obter culturas de células intestinais diferenciadas a partir de tecidos normais, atenção especial foi dada às propriedades de algumas linhagens de células intestinais tumorais. Na maioria dos casos, a diferenciação era induzida através do tratamento com fatores de indução sintéticos ou biológicos adicionados ao meio de cultura (PINTO et al., 1983). Contudo, uma destas linhagens celulares, chamada de Caco-2, mostrou uma diferenciação espontânea, quando cultivada em longo prazo, sob condições normais de cultura.

Os primeiros estudos com as células Caco-2 demonstraram que essa linhagem, derivada de um adenocarcinoma de cólon humano, diferenciava-se e passava a exibir características morfológicas e funcionais similares às dos enterócitos, ou seja, capacidade absortiva (via microvilosidades), junções oclusivas e expressão de enzimas intestinais (aminopeptidases, esterases, sulfatases, enzimas do complexo citocromo P450, entre outras) e de transportadores (carreadores de biotina e de ácidos monocarboxílicos, PEPT1, glicoproteína P (P-gp), entre outros) (MIRET et al., 2004; SAMBUY et al., 2005; DEFERME, ANNAERT, AUGUSTIJNS, 2008; LI et al., 2008).

No intestino, uma única camada de células epiteliais recobre a parede intestinal interna e forma uma barreira seletiva para a absorção dos nutrientes, fármacos e demais xenobióticos dissolvidos no líquido gastrointestinal. Através da reconstituição adequada de uma monocamada celular diferenciada *in vitro* é possível predizer a absorção oral em humanos (HIDALGO et al., 1989; ARTURSSON et al., 1990).

A partir do momento em que as condições de cultivo foram otimizadas, proporcionando a diferenciação morfológica e funcional estável, tais células têm sido extensivamente utilizadas como um modelo para estudos de transporte de fármacos *in vitro* (HIDALGO et al., 1989; ARTURSSON et al., 1990; HILGERS et al., 1990; WILSON et al., 1990; PRESS; DI GRANDI, 2008).

O transporte de fármacos através da membrana intestinal é um processo complexo e envolve múltiplas vias (BALIMANE, HAN, CHONG, 2006). A absorção passiva ocorre mais comumente através dos enterócitos (rota transcelular) ou via junções oclusivas presentes entre estas células (rota paracelular). A absorção mediada por

carreadores ocorre via processo ativo (transporte ativo) ou por difusão facilitada. Vários transportadores de efluxo localizados na porção apical da célula, tais como a P-gp, são funcionais e podem limitar a absorção. Além disso, enzimas metabólicas podem estar envolvidas já nesta etapa (ARTURSSON et al., 2001; BALIMANE, HAN, CHONG, 2006; PRESS; DI GRANDI, 2008).

Com a verificação, por diversos laboratórios, de que através do uso de células Caco-2 podia-se estabelecer uma correlação entre a permeabilidade *in vitro* de um fármaco e a sua absorção oral (AMIDON et al., 1995; ARTURSSON et al., 2001), este modelo tornou-se uma ferramenta valiosa em estudos de permeabilidade intestinal de compostos farmacologicamente ativos (a título ilustrativo, são citados aqui alguns trabalhos: ZUO et al., 2000; KONISHI et al., 2003; TAMMELA et al., 2004; ZHOU et al., 2005; BALIMANE, HAN, CHONG, 2006; ZERROUK et al., 2006; BANSAL et al., 2007; KOLJONEN et al., 2008; PRESS; DI GRANDI, 2008; PANG et al., 2009; SIISSALO et al., 2010; KIMURA, et al., 2011).

Do ponto de vista experimental, as células são cultivadas por, pelo menos, 21 dias para formarem uma monocamada de células diferenciadas sobre um filtro poroso do inserto, como ilustrado na Figura 4. O filtro deve ser de natureza inerte (geralmente policarbonato) e possuir poros com diâmetro de até 0.4 µm para evitar a migração celular do lado apical para o basolateral. O tempo relativamente grande de cultivo é necessário para garantir a formação das junções oclusivas, obtenção da polaridade celular e alta expressão de transportadores de membrana (BOHETS et al., 2001).
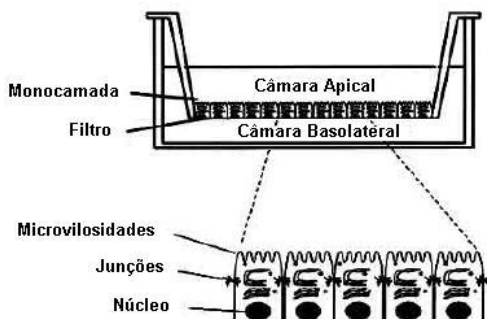
Figura 4. Representação esquemática do experimento de transporte utilizando o modelo de células Caco-2. Fonte: Adaptado de Bohets e colaboradores (2001).

Nos experimentos de transporte os compostos são adicionados em uma das câmaras separadas pela monocamada celular, e sua taxa de passagem para a outra câmara pode ser medida por cromatografia líquida de alta eficiência (CLAE) acoplada a diferentes detectores, tais como o ultravioleta ou espectrômetros de massa. Rotineiramente, o transporte em ambos os sentidos, tanto absortivo (apical para basolateral) quanto secretório (basolateral para apical) são investigados para determinar se algum mecanismo de efluxo está envolvido no processo avaliado. Os resultados obtidos são expressos como coeficiente de permeabilidade aparente (P_{app}, cm/s) (BOHETS et al., 2001; SAMBUY et al., 2005; PRESS; DI GRANDI, 2008).

Embora o modelo de permeabilidade com células Caco-2 apresente diversas vantagens, condições variáveis de cultura podem gerar características celulares inconsistentes, baixa reprodutibilidade, e variabilidade intra- e interlaboratorial. Portanto, as técnicas de cultivo celular e as condições experimentais precisam ser muito bem definidas e rigidamente controladas, a fim de garantir a validade dos dados obtidos nesses experimentos (US FDA, 2000; VOLPE, 2008).

Para demonstrar a funcionalidade e adequação do modelo, é necessário estabelecer uma classificação entre fármacos com diferentes coeficientes de permeabilidade, em função da sua absorção em humanos. Para ser considerado adequado, o modelo deve ser capaz de diferenciar perfis de alta e baixa permeabilidade passiva, bem como apresentar características morfológicas consistentes. Adicionalmente, o desempenho do ensaio deve ser monitorado continuamente, através do uso de fármacos marcadores (alta e baixa permeabilidade)(US FDA, 2000).

A fim de se avaliar a funcionalidade dos transportadores, também são utilizados substratos de transportadores ativos, tal como o transportador de oligopeptídeos (PEPT-1) (ADIBI, 1997), ou de bombas de efluxo, tais como digoxina (VERSCHRAAGEN et al., 1999), vimblastina (HUNTER et al., 1993; SHIRASAKA et al., 2008) ou ciclosporina A (AUGUSTIJNS et al., 1993).

No quesito avaliação da morfologia, diversos métodos estão disponíveis para avaliar a integridade da monocamada celular. Comumente, utiliza-se a medida da resistência elétrica transepitelial (em inglês, *Trans Epithelial Electrical Resistance* – TEER) é utilizada, uma vez que células confluentes com junções oclusivas formadas constituem uma barreira para a troca de eletrólitos e, consequentemente, geram uma resistência elétrica. As medidas de TEER são realizadas através de um voltímetro acoplado a microeletrodos colocados em ambos os

compartimentos (apical e basolateral) dos insertos, onde são cultivadas as células, e devem ser feitas antes e após a realização dos experimentos (PRESS; DI GRANDI, 2008).

Para garantir a qualidade dos resultados dos experimentos de transporte, também é desejável incluir um composto marcador da integridade da monocamada de células Caco-2, ou seja, um composto que possua baixíssimo coeficiente de permeabilidade. Vários compostos são utilizados nesse sentido, dentre eles o manitol, a dextrana conjugada ao isotiocianato de fluoresceína e o marcador de permeabilidade paracelular *Lucifer yellow* (YAMASHITA et al., 2002).

Apesar da reconhecida aplicabilidade desse modelo na predição da absorção oral, ele apresenta uma série de limitações que devem ser levadas em consideração, tais como a ausência de muco, a camada aquosa estática (*UWL*), a expressão variável de enzimas metabólicas, a superestimação do papel dos transportadores de efluxo *in vitro*, e a inviabilidade de estudos que busquem avaliar o impacto das diferenças entre as regiões do intestino sobre a absorção oral (INGELS, AUGUSTIJNS, 2003; LENNERNÄS, ABRAHAMSSON, 2005). Adicionalmente, condições variáveis de cultura podem gerar características celulares inconsistentes, baixa reprodutibilidade, e variabilidade intra- e interlaboratorial (HAYESHI et al., 2008; VOLPE, 2008).

Dessa forma, o modelo *in vitro* de permeabilidade com células Caco-2, quando corretamente implementado e monitorado, é capaz de fornecer informações valiosas sobre a permeabilidade de fármacos, possibilitando a realização de experimentos mecanísticos, que contribuem de forma decisiva para a pesquisa e o desenvolvimento racional de novos fármacos. Por esse motivo, este ensaio é amplamente aceito pela indústria farmacêutica e pelas agências regulatórias internacionais de medicamentos, sendo considerado o ensaio padrão para a predição da absorção oral.

PUBLICAÇÃO – APÊNDICE 1

An HPLC-UV method for the measurement of permeability of marker drugs in the Caco-2 cell assay

J.M. Kratz[1], M.R. Teixeira[1], L.S. Koester[2], C.M.O. Simões[1]

[1] Departamento de Ciências Farmacêuticas, Universidade Federal de Santa Catarina, UFSC, Florianópolis, SC, Brasil
[2] Faculdade de Farmácia, Universidade Federal do Rio Grande do Sul, UFRGS, Porto Alegre, RS, Brasil

CAPÍTULO 02

COMPLEXOS DE INCLUSÃO DA TALIDOMIDA:
Influência da complexação com ciclodextrinas sobre a solubilidade, dissolução e permeabilidade intestinal *in vitro*

APRESENTAÇÃO

A talidomida foi introduzida no mercado farmacêutico por suas atividades sedativas e antieméticas. A correlação de seu uso com o surgimento de focomelia em recém-nascidos fez com que esse fármaco fosse retirado dos mercados de alguns países. Desde então, muitas pesquisas vêm sendo realizadas com o intuito de avaliar novas potencialidades, explorando suas propriedades antiinflamatórias, imunomodulatórias e antineoplásicas (MATTHEWS; MCCOY, 2003; FRANKS et al., 2004; TEO, 2005; MELCHERT; LIST, 2007), abrindo novas possibilidades de aplicações clínicas para este fármaco.

A absorção da talidomida a partir do trato gastrointestinal é lenta e limitada, com taxa de eliminação superior à de absorção, e biodisponibilidade variável (TEO et al., 2004). Na forma de mistura racêmica, apresenta baixa solubilidade em água e alto grau de cristalinidade, estando suas moléculas agrupadas em arranjos cristalinos que conduzem à formação de duas formas polimórficas (ALLEN; TROTTER, 1970; CAIRA, BOTHA, FLANANGAR, 1994; REEPMEYER et al., 1994; LARA-OCHOA et al., 2007). Apesar do grande número de estudos envolvendo novas indicações de uso para a talidomida, pouco tem sido investigado no que se refere ao melhoramento de suas propriedades biofarmacêuticas. Nesse sentido, a proposta deste trabalho consistiu na avaliação da influência da complexação da talidomida com várias ciclodextrinas, adotando a hipótese de que esta complexação promoveria um aumento da solubilidade aquosa, taxa de dissolução e permeabilidade intestinal. A complexação deste fármaco também serviu como ferramenta para a avaliação da influência de adjuvantes no modelo Caco-2 implementado.

Este projeto foi aprovado pela Fundação de Amparo à Pesquisa e Inovação do Estado de Santa Catarina (FAPESC), no âmbito do Edital PPSUS 2006, com apoio financeiro do CNPq, Ministério da Saúde, e SES/SC. Os resultados obtidos foram compilados e submetidos para publicação no periódico *Journal of Pharmacy and Pharmacology*. Esse manuscrito encontra-se sob revisão e é apresentado na íntegra no final deste capítulo.

REVISÃO DA LITERATURA

A talidomida foi sintetizada em 1954 e lançada no mercado farmacêutico em 1957 pela empresa *German Company Chemie Grunental* como medicamento sedativo e antiemético, prescrito rotineiramente para o enjôo matinal de gestantes. Nos estudos de toxicidade em ratos, coelhos e cobaias, realizados naquela época, a taxa de letalidade não foi significativa, mesmo com doses altas. Esse fato fez com que o fármaco fosse considerado de baixa toxicidade e de maior segurança, quando comparado aos barbitúricos, o que contribuiu para que a talidomida se transformasse em um sedativo popular e de venda livre em diversos países, inclusive no Brasil. (OLIVEIRA, BERMUDEZ, SOUZA, 1999; MATTHEWS; MCCOY, 2003; MELCHERT; LIST, 2007).

Anos mais tarde, malformações congênitas em recém-nascidos foram associadas ao consumo de talidomida pelas gestantes durante o primeiro trimestre de gestação. Após a confirmação da teratogenicidade, o medicamento foi retirado do mercado, contabilizando-se milhares de vítimas de anormalidades (FRANKS et al., 2004). Nos Estados Unidos, o FDA não liberou a comercialização do medicamento, pois, preocupado com a neurotoxicidade, considerou que as evidências disponíveis na época não garantiam a segurança do mesmo, saindo desse episódio muito fortalecido, passando a coordenar a política de regulação de medicamentos naquele país através da emenda Kefauver-Harris, de 1962 (KELSEY, 1988; OLIVEIRA, BERMUDEZ, SOUZA, 1999). A partir dessa emenda, estudos de eficácia de novos e antigos medicamentos foram regulamentados pelo FDA, passando a ser exigido o cumprimento de um longo e rigoroso processo de comprovação da segurança e eficácia de cada substância candidata a medicamento (KELSEY, 1988; ABRAHAM, 1995; OLIVEIRA, BERMUDEZ, SOUZA, 1999).

No Brasil, a talidomida começou a ser comercializada em 1958, e os primeiros casos de malformações foram relatados em 1960. Apesar de ter sido banida dos mercados europeu e canadense em 1961, a talidomida continuou sendo comercializada no Brasil até 1965 (OLIVEIRA, BERMUDEZ, SOUZA, 1999).

Nesse mesmo ano, um dermatologista israelense relatou a administração da talidomida em um paciente com eritema nodoso leprótico (ENL), a princípio com o intuito de tratar sua insônia, mas acabou obtendo como resposta a melhora do quadro inflamatório cutâneo, com cicatrização total das feridas (OLIVEIRA, BERMUDEZ,

SOUZA, 1999; MATTHEWS; MCCOY, 2003). Após a descoberta de sua aplicação terapêutica no tratamento do ENL, ela voltou a ser comercializada em alguns países incluindo o Brasil (OLIVEIRA, BERMUDEZ, SOUZA, 1999). Em Julho de 1998, o FDA aprovou seu uso no tratamento do ENL moderado a grave, e na terapia de manutenção para supressão de manifestações recorrentes do ENL (MATTHEWS; MCCOY, 2003; FRANKS et al., 2004). No Brasil tal uso foi regulamentado em 1997 (BRASIL, 1997), sendo sua distribuição restrita a alguns programas governamentais de saúde. As indicações são para tratamento da hanseníase (reação hansênica tipo II ou ENL), de úlceras aftóides idiopáticas em pacientes portadores HIV+ ou com AIDS, de doenças crônico-degenerativas (lúpus eritematoso, doença enxerto contra hospedeiro) (BRASIL, 1997) e de mielomas múltiplos refratários à quimioterapia convencional (BRASIL, 2002).

Atualmente, o medicamento é produzido exclusivamente pelo Laboratório Farmacêutico da Fundação Ezequiel Dias (FUNED, Belo Horizonte, MG), sob a forma de comprimidos de 100 mg de talidomida. Esse medicamento é de uso controlado, restrito a hospitais, sendo classificado como imunossupressor da classe C3 pela Portaria 344 da SNVS/MS (BRASIL, 1998). Além disso, a Portaria 354 da SNVS/MS regulamenta o registro, a produção, a fabricação, a comercialização, a exposição à venda, a prescrição e a dispensação dos produtos à base de talidomida. O medicamento só pode ser dispensado com notificação de receita para medicamento especial, contendo dados sobre sua dispensação, sendo que o médico prescritor deve assumir formalmente o compromisso, a responsabilidade e o esclarecimento ao paciente dos riscos inerentes ao seu uso, sendo que o paciente também deve assinar um termo de esclarecimento (BRASIL, 1997).

Do ponto de vista físico-químico, a talidomida é um fármaco neutro, derivado do ácido glutâmico. Possui em sua estrutura um anel ftalimida e um anel glutarimida, que possui um carbono quiral, gerando dois enantiômeros: a forma (+)-(R), à qual as propriedades hipnótico-sedativas e antieméticas são atribuídas, e a forma (-)-(S), com propriedade antiinflamatória, imunomodulatória e antineoplásica, bem como potencial teratogênico. Entretanto, os enantiômeros sofrem rápida interconversão quiral *in vivo* e *in vitro*. Dessa forma, a administração exclusiva de uma forma enantiomérica não evita os efeitos teratogênicos (ERIKSSON, BJÖRKMAN, HÖGLUND, 2001; MATTHEWS; MCCOY, 2003; FRANKS et al., 2004; TEO, 2005).

O mecanismo de ação da talidomida é bastante complexo e ainda não foi totalmente esclarecido. Os efeitos antiinflamatórios e

imunomodulatórios parecem estar relacionados com a redução dos níveis do fator de necrose tumoral α, que regula a cascata inflamatória e a conseqüente produção de interleucina-2 e interferon-γ (FRANKS et al., 2004). O efeito teratogênico, e paralelamente a propriedade antineoplásica, do fármaco está relacionado à sua capacidade de inibir a angiogênese em células jovens, resultando em uma disfunção no desenvolvimento dos vasos sanguíneos (FRANKS et al., 2004; TEO, 2005). Os mecanismos moleculares envolvidos nesse processo têm sido alvo de diversos estudos e ainda não estão completamente elucidados, entretanto diversos mecanismos podem estar envolvidos simultaneamente nas malformações congênitas, tais como a própria perda da rede vascular em si (THERAPONTOS et al., 2009) e a ligação da talidomida à uma proteína chamada cereblon (ITO et al., 2010).

Em relação à sua farmacocinética, a talidomida possui baixa solubilidade aquosa (45-60 μg/mL), o que resulta em uma absorção oral lenta a partir do trato gastrointestinal, sendo que a taxa de eliminação é mais lenta que a taxa de absorção (fenômeno "*flip-flop*"). Após administração oral de 200 mg de talidomida (cápsulas), sua cinética é melhor descrita por um modelo monocompartimental, com absorção e eliminação de primeira ordem, apresentando concentração plasmática máxima (C_{max}) de 1-2 mg/L em 3-4 h após à administração (t_{max}) (TEO et al., 2004). A biodisponibilidade absoluta da talidomida em humanos ainda não foi determinada devido à baixa hidrossolubilidade do fármaco que impede a veiculação intravenosa, entretanto em modelos animais ela varia entre 67 e 93 % (CHEN et al., 1989). Mais de 90% do fármaco absorvido é eliminado na urina e fezes em 48 h. Sua eliminação é predominantemente renal, sendo que o fármaco é rapidamente degradado no plasma por hidrólise espontânea em pH fisiológico, formando doze produtos de degradação, também eliminados de forma passiva na urina. A metabolização hepática do fármaco via enzimas do citocromo P450 é mínima (TEO et al., 1999, 2004; FRANKS et al., 2004).

Adicionalmente, a literatura descreve a existência de, pelo menos, duas formas polimórficas para a talidomida, denominadas de α e β (ALLEN; TROTTER, 1970; CAIRA, BOTHA, FLANANGAR, 1994; REEPMEYER et al., 1994). Mais recentemente, Lara-Ochoa e colaboradores (2007) sugeriram a existência de um novo polimorfo, β*, formado em condições específicas de aquecimento, sendo que esta forma polimórfica exibe enantiotropia com as outras duas formas. Adicionalmente, Carini e colaboradores (2009) demonstraram que as diferentes formas polimórficas da talidomida apresentam diferentes

perfis de dissolução intrínseca, que poderiam impactar na biodisponibilidade e, consequentemente, na ação farmacológica do fármaco.

Embora exista um grande número de estudos acerca das novas aplicações da talidomida, as propriedades biofarmacêuticas precárias desse fármaco geram perfis farmacocinéticos irregulares, afetando a eficácia do fármaco e comprometendo os tratamentos (TEO et al., 2004). Nesse sentido, dois enfoques básicos têm sido empregados para a obtenção de uma melhor solubilidade aquosa, uma vez que esse é o fator limitante, já que estudos demonstraram que a talidomida possui propriedades favoráveis de permeabilidade intestinal (ZHOU et al. 2005; ZIMMERMANN et al., 2006), outro componente importante na absorção oral. O primeiro enfoque envolve a síntese de derivados, como por exemplo, a lenalidomida, que encontra-se em fase clínica III (REVLIMID®) (MELCHERT; LIST, 2007). O segundo enfoque abrange a modulação da biodisponibilidade através de estratégias farmacotécnicas (ERIKSSON et al., 2000; CHEN, GU, HU, 2008; ARAÚJO et al., 2011), como a que foi utilizada neste trabalho, por meio da complexação com ciclodextrinas.

As ciclodextrinas são oligossacarídeos com uma superfície externa hidrofílica e uma cavidade central lipofílica, que são capazes de formar complexos de inclusão estáveis com compostos em solução aquosa, através da inserção da molécula ou de parte dela na sua cavidade central. Dessa forma, ciclodextrinas têm sido utilizadas como agentes complexantes para o aumento da solubilidade, biodisponibilidade e estabilidade de fármacos (LOFTSSON et al., 2005; LOFTSSON, DUCHENE, 2007). O aumento da solubilidade aquosa e da estabilidade da talidomida mediante a complexação com β-ciclodextrina e hidroxipropil-β-ciclodextrina já foram relatados (KOCH; STEINACKER, 1988; KRENN et al., 1992; ALVAREZ et al., 2008). Siefert e colaboradores (1999) relataram o aumento dos níveis de talidomida no humor aquoso dos olhos de coelhos, após a instilação de uma solução contendo de talidomida e de hidroxipropil- β-ciclodextrina, em comparação com a talidomida isolada. Mais recentemente, outro estudo relatou a administração oral da talidomida em combinação com a sulfobutil-éter-7-β-ciclodextrina, resultando numa significativa diminuição do tempo de surgimento e tamanho de tumores em um modelo de carcinoma em camundongos (KALE et al., 2008). Os autores sugeriram que tal efeito estaria teoricamente ligado a uma melhor absorção da talidomida a partir do trato gastrointestinal (KALE et al., 2008), embora estudos farmacocinéticos não tenham sido realizados.

PUBLICAÇÃO

Corresponding Author: Cláudia M O Simões

Corresponding Author's Institution:

First Author: Jadel Müller Kratz

Order of Authors: Jadel Müller Kratz;Marina R Teixeira;Karine Ferronato;Helder F Teixeira;Letícia S Koester;Cláudia M O Simões

Preparation, characterization and *in vitro* intestinal permeability of thalidomide inclusion complexes

J.M. Kratz[1], M.R. Teixeira[1], K. Ferronato[2], H.F. Teixeira[2], L.S. Koester[2], C.M.O. Simões[1]

[1] Departamento de Ciências Farmacêuticas, Universidade Federal de Santa Catarina, UFSC, Florianópolis, SC, Brasil
[2] Faculdade de Farmácia, Universidade Federal do Rio Grande do Sul, UFRGS, Porto Alegre, RS, Brasil

Abstract

Thalidomide is emerging as a therapeutic agent with broad clinical range, presenting anti-inflammatory, immunomodulatory, and antineoplasic properties. Although, it's poor aqueous solubility leads to erratic and incomplete absorption in humans. In order to circumvent solubility problems, the complexation of thalidomide with cyclodextrins has been regarded as a promising strategy. Therefore, the present study shows the preparation of inclusion complexes of thalidomide with different cyclodextrins. Hydroxypropyl-β-cyclodextrin complexes (1:1) were obtained in the solid state by kneading technique and were characterized by differential scanning calorimetry, powder x-ray diffractometry and scanning electronic microscopy. The influence of complexation over aqueous solubility, dissolution rate and *in vitro* permeability of thalidomide through Caco-2 cells were evaluated. In summary, our results demonstrated that complexation could improve the bioavailability of orally administered thalidomide through the enhancement of the aqueous solubility and dissolution rate of the drug, but not through its influence on the intestinal permeability.

Keywords: Thalidomide; Cyclodextrin; Solubility; Intestinal permeability; Caco-2.

Introduction

Thalidomide (TD − Fig. 1) is a glutamic acid derivative that was first synthesized in Germany in 1954. It was initially approved in many countries as a sedative and antiemetic drug. However, due to teratogenicity and neuropathy, it was withdrawn from the market in the early 1960's [1,2].
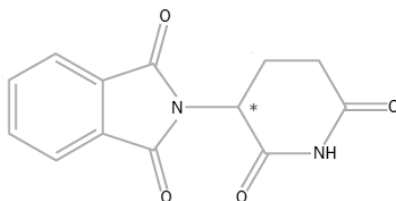
Figure 1 – Structure of thalidomide with the chiral center marked with an asterisk.

The pharmacological properties of TD extended beyond the neurosedative effects. Its subsequent establishment as an anti-inflammatory, immunomodulatory, and antineoplasic compound inspired researchers to define its clinical range. TD was approved by the FDA for the treatment of erythema nodosum leprosum and, more recently, in association with dexamethasone, for multiple myeloma [3-5].

TD is formulated as an equimolar racemate of two active enantiomers that rapidly interconvert under physiological conditions. The molecule contains a glutarimide moiety with a single chiral center, and undergoes spontaneous hydrolysis in aqueous solutions at pH 7.4 [6]. In addition to the chemical instability, TD exhibits diverse polymorphs [7] and absorption rate-limited pharmacokinetics. The low solubility and poor dissolution of the drug in the gastrointestinal tract leads to an erratic and incomplete absorption [6,8].

In order to circumvent instability and solubility issues, different pharmaceutical strategies have been employed. Isolation of pure enantiomers [9], association with polymeric carriers [10], incorporation into nanoemulsions [11] and complexation with cyclodextrins (CDs) [12-16].

CDs are cyclic oligosaccharides with a hydrophilic outer surface and a lipophilic central cavity which are able to form inclusion complexes. They have been extensively used in the pharmaceutical industry to improve bioavailability, especially of Class II drugs (low solubility, high permeability), according to the Biopharmaceutics Classification System (BCS). CDs may prove utility by both improving the solubility and the permeability [17].

While some studies have shown the improvement of the aqueous solubility of TD via complexation, there is a lack of information

regarding the intestinal permeability of the complexes. In this view, this work reports the preparation and characterization of TD inclusion complexes and the study of the effect of complexation over the aqueous solubility, dissolution rate and *in vitro* intestinal permeability of TD.

Material and Methods

Reagents and chemicals

TD produced by Microbiológica Química e Farmacêutica (Brazil) was a kind gift from Fundação Ezequiel Dias (MG, Brazil). All TD raw material used in this study consisted of an equimolar racemate of (+)-(R) and (−)-(S) enantiomers. α-cyclodextrin (αCD), γ-cyclodextrin (γCD) and phenacetin were purchased from Sigma (USA). β-cyclodextrin (βCD), hydroxypropyl-β-cyclodextrin (HPβCD) and methyl-β-cyclodextrin (MEβCD) were supplied by Roquette (France). Acetonitrile was obtained from Tedia (Brazil). All other reagents and solvents used in this study were of the highest purity commercially available. Ultrapure water from a Milli-Q system apparatus (Millipore – USA).

High Performance Liquid Chromatography (HPLC) Analysis

The method employed in this study was developed based on previous reports [18,19]. Quantitative determinations of TD were performed by HPLC on a Shimadzu LC-10A chromatographer. Chromatographic separations were obtained using a 150 mm x 4.6 mm C18 column (Phenomenex, USA) at 40 °C. Mobile phase consisted of acetonitrile, water and phosphoric acid in the ratio of 24:76:0.1 (v/v) under an isocratic flow rate of 1.0 ml/min. The analytical wavelength was set at 237 nm and samples of 20 μl were injected into the HPLC system. Phenacetin was used as an internal standard. The chromatographic method was validated according to ICH recommendations [20] and found specific, linear (y = 0.0073x + 0.0012, r2 = 0.9998), precise (RSD < 2.40 %) and accurate (97.7 – 101.6 %). A representative chromatogram is shown in Fig. 2.
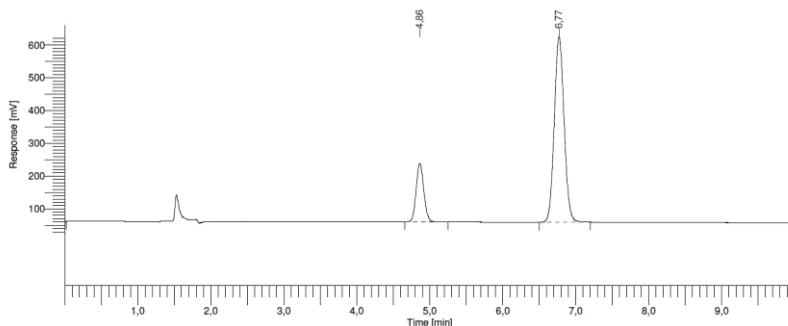
Figure 2 – Representative chromatogram of thalidomide (50 μM) and phenacetin (internal standard, 100 μM) in HBSS buffer. The retention times were 4.86 and 6.77 min, respectively.

Phase solubility studies

Phase solubility studies were carried out in aqueous medium as described earlier [21]. Excess amounts of TD (50 mg -7.7 mM) were added to 25 ml of water or aqueous solutions containing increasing concentrations of CDs (0 - 31 mM). Flasks were covered with aluminum foil and the pH of the dispersions was adjusted to 4-5 in order to avoid chemical degradation. Dispersions were magnetically stirred for 6 h, at room temperature (25 ºC), filtered through 0.45 μm membranes (Millipore, USA) and appropriately diluted.

Concentration of TD in the filtrates was determined by HPLC. The presence of CDs did not interfere with the assay as previously evaluated (data not shown). The apparent stability constants (K_s) of TD complexes were calculated from phase solubility diagrams according to the equation below, where S_0 is the intrinsic aqueous solubility of TD [21].

$$Ks = \frac{slope}{So\left(1 - slope\right)}$$

Preparation of the solid inclusion complexes

Inclusion Complexes (KN)

The solid TD/CD complex was obtained by the kneading technique. A mixture of 0.50 g of TD and an appropriate amount of CD

(molar ratio of 1:1) was wet in a mortar with a minimum volume of ethanol/water solution (1 ml, 1:1, v/v). The mixture was grounded thoroughly with a pestle for 30 min and afterward dried for 48 h at room temperature (25 ºC). The dried complex was pulverized into a fine powder.

Physical mixture (PM)

A physical mixture of TD and CD in the dry state was prepared at the same molar ratio as the complexes. The components were thoroughly mixed in a mortar for 30 min and afterward dried for 48 h at room temperature (25 ºC). All products were stored in a dessicator until further evaluation.

Characterization of the solid complexes

Differential scanning calorimetry (DSC)

DSC measurements were performed on a DSC-60 calorimeter (Shimadzu, Japan). Samples of 1 to 2 mg were accurately weighed in aluminum pans and crimped. The operating conditions were 10 ºC/min of heating rate, from 35 ºC up to 350 ºC, 50 ml/min of nitrogen gas flow. The temperature calibration was performed using Indium (mp 157 ºC) and Zinc (mp 420 ºC) as standards.

Powder X-ray diffractometry (XRD)

The XRD patterns were recorded on a Siemens D5000 diffractometer (Siemens, Germany) equipped with a curved graphite crystal, using Cu Kα radiation. The scanning rate employed was 0.05 ° per second over a 2θ range of 5 – 70 °. Generator tension and current were 40 kV and 30 mA, respectively.

Morphology evaluation

Surface morphology was analyzed in a JSM-6060 scanning electron microscope (SEM) (JEOL, USA). Samples were fixed on a brass stub using double-sided tape and then coated with a thin gold layer under vacuum. The photomicrographs were taken at a voltage of 10-20 kV and magnification factor from 500 to 1500.

Dissolution studies

In vitro dissolution profiles were evaluated as described previously [22], with some modifications, using the USP basket apparatus. Capsules containing 50 mg of TD, or its equivalent in KN or PM products, were added to 1000 ml of dissolution media (0.225 M HCl and 1 % of sodium lauryl sulphate) at 37.0 ± 0.5 °C and stirred at 100 rpm on standard dissolution equipment (Nova Ética, Brazil). About 5 ml of the test medium were sampled at 10, 20, 30, 45 and 60 min with medium reposition, and TD concentration was determined by HPLC.

In vitro intestinal permeability studies with Caco-2 cells

Cell culture

Caco-2 cells were obtained from the American Type Culture Collection (ATCC # HTB-37, USA). Cells were maintained in a humidified 5 % CO_2 air atmosphere at 37 °C and were cultured in DMEM containing 4.5 g/l glucose (Gibco, USA) with 20 % fetal bovine serum, 1% non essential amino acids, 100 U/ml of penicillin, 100 µg/ml of streptomycin and 25 µg/ml of amphotericin B (Gibco, USA). After reaching 80-90 % of confluence, cells were harvested and seeded into Millicell® polycarbonate inserts (0.6 cm^2, 0.4 µm pore size – Millipore, USA) at a density of 10^5 cells/insert.

Transport experiments

The experiments were carried out under sink conditions, according to recommendations described previously [23]. *In vitro* permeation studies were performed after 21-25 days of culture, using Caco-2 cells between passage 25 and 31. Hank's Balanced Salt Solution (HBSS) buffered at pH 6.0 (10 mM of methanesulfonic acid) and at pH 7.4 (10 mM of 4-(2-hydroxyethyl)-1-piperazineethanesulfonic acid) were used as transport buffers in the apical (AP – donor) and basolateral (BL – acceptor) side, respectively.

Transepithelial electrical resistance (TEER) measurements (Millicell® ERS meter – Millipore, USA) and Lucifer Yellow (LY, Sigma, USA), a fluorescent paracellular permeability marker, were used to control the integrity of Caco-2 monolayers.

Sample solutions containing 50 µM of TD or equivalents in KN or PM were added to the AP side and filters were incubated for 2 h at 37

°C in an orbital shaker (100 rpm). At suitable time intervals, samples were collected from the BL side by moving the cell monolayers to a new well containing fresh HBSS. A sample was also collected from the AP side at the final time point in order to perform the mass balance calculation.

After sample collection, all aliquots were mixed with two volumes of cold acetonitrile/methanol mixture containing 2 % acetic acid and 100 µM of phenacetin to prevent TD from spontaneous degradation [19]. Following, samples were dried using a SpeedVac concentrator (Thermo, USA) and the residues were reconstituted in mobile phase. The mean recovery value obtained in this process was 87.3 ± 2.5 %. TD was assayed by HPLC and the apparent permeability coefficients (P_{app}, cm/s) were calculated according to the following equation:

$$P_{app} = \frac{(\Delta Q)}{(\Delta t)} \times \frac{1}{A \times C_0}$$

where ($\Delta Q/\Delta t$) is the amount of TD permeated in the unit of time, A is the surface area of the monolayers and C_0 is the initial donor concentration [23].

Statistical analysis

The results were expressed as the mean ± SD of three independent experiments, unless otherwise stated. Statistical analyses were performed by one-way ANOVA followed by Tukey's post hoc test ($p < 0.05$). Calculations were performed with GraphPad Prism software (GraphPad, USA).

Results and Discussion

Phase solubility studies

A preliminary phase solubility study was performed to assess the inclusion of TD by parent CDs (αCD, βCD and γCD) (Fig. 3). An excess of 10 times the solubility of TD (2 mM) and two molar ratios (1:1 and 1:4) were employed. In the absence of CDs, the aqueous solubility of TD at pH 5 was found to be 51.4 ± 1.5 µg/ml. Two different stirring times were used (6 and 24 h) since operational conditions can affect the formation of complexes. No significant differences between stirring

times were found (p > 0.05). The comparative analysis of the parent CDs revealed important differences in their complexation capacity. βCD generated the most promising results among the three tested CDs (p < 0.001). This CD increased the solubility of TD by 1.3 and 1.8 fold for the 1:1 and 1:4 molar ratios, respectively. Accordingly, a phase solubility study was performed with βCD and two other β-derivatives with improved solubility, HPβCD and MEβCD.
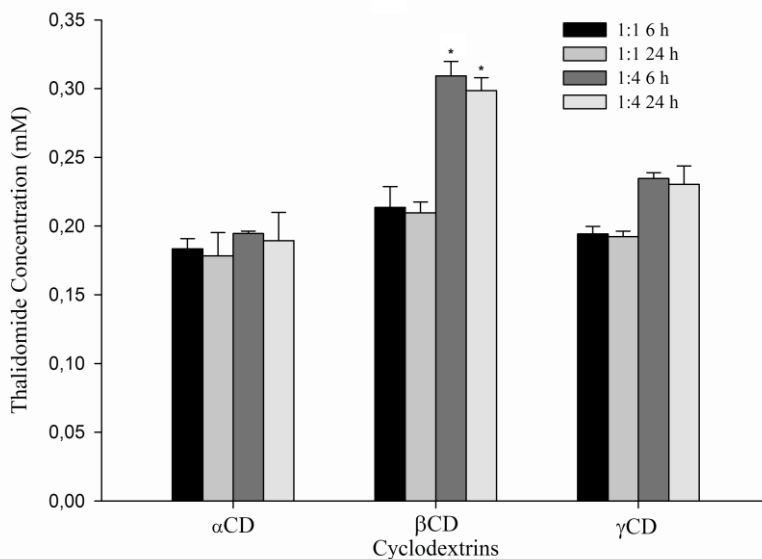
Figure 3 – Preliminary phase solubility study of thalidomide and α-, β- and γ-cyclodextrins. Experimental conditions: stirring time of 6 and 24 h at room temperature (25 °C), molar ratio of 1:1 and 1:4 and excess amount of 2 mM. Results are expressed as mean ± SD (n = 3) * Differs from other cyclodextrins and/or molar ratios (p < 0.001).

The phase solubility diagrams obtained for TD/HPβCD and TD/MEβCD systems are presented in Figure 4. A different excess was used (7.7 mM) since parallel experiments showed an improved solubilization of TD with this setup (data not shown). The form of diagrams followed an A_L-type profile [21], where a linear increase of TD solubility was observed as function of CDs concentration (r^2 = 0.9749 and 0.9974, respectively). In general, the modified CDs form A-type phase solubility profiles, whereas less soluble CDs frequently form

B-type profiles, indicative of the formation of complexes with limited solubility (βCD – Fig. 4). Since A_L-type phase solubility profiles were obtained, the stoichiometry 1:1 stability constants (K_s) were calculated and found to be 108.90 M^{-1} and 102.65 M^{-1} for HPβCD and MEβCD, respectively. Low stability constants such as the ones obtained indicate that TD can easily dissociate from the complexes and be available to permeate through biological membranes, such as the intestinal mucosa [24].
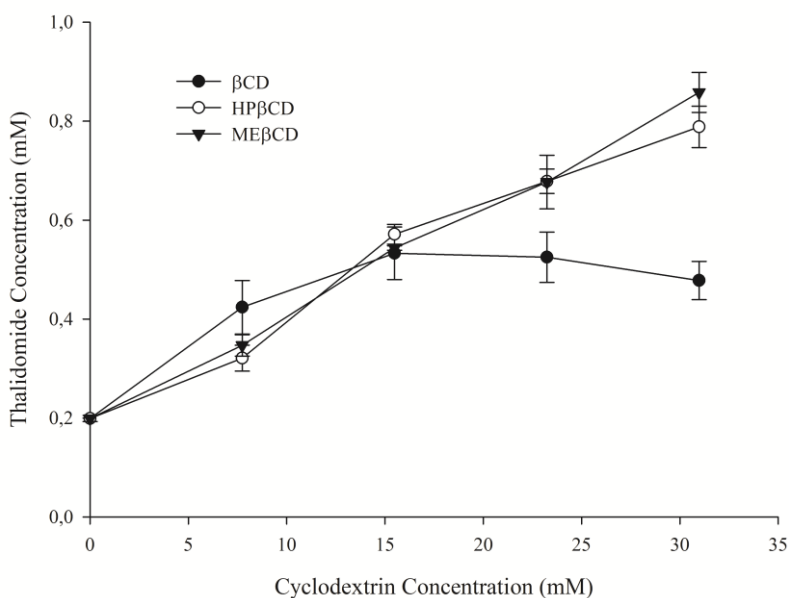
Figure 4 – Phase solubility diagrams of thalidomide and βCD, HPβCD and MEβCD. Experimental conditions: stirring time of 6 h at room temperature (25 °C) and excess amount of 7.7 mM. Results are expressed as mean ± SD (n = 3).

Preparation and characterization of solid inclusion complexes

HPβCD and MEβCD presented the best results with regard to aqueous solubility improvement of TD. HPβCD was selected as the most advantageous CD since is a widely studied alternative to βCD with improved water solubility. In addition, toxicological studies have

pointed out that this CD is well tolerated by the human body via intravenous and oral administrations [17,25,26].

Initially, a TD/HPβCD freeze-dried complex was obtained by lyophilization. This technique generated solid complexes containing < 1 % of TD, with little pharmaceutical usefulness (data not shown). Therefore, the solid 1:1 TD/HPβCD complex (KN) was obtained by the kneading technique.

The characterization of solid samples was carried out by several methods. DSC thermograms of TD, HPβCD, KN and PM are shown in Fig. 5.
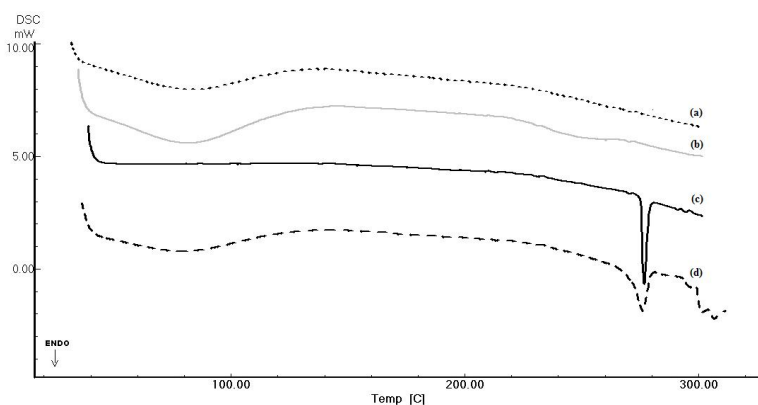
Figure 5 – DSC thermograms of (a) HPβCD, (b) thalidomide/ HPβCD complex (Kneading), (c) thalidomide, and (d) physical mixture.

Thermogram of TD presented a sharp endothermic peak at 276.7 °C corresponding to the melting point of the drug, while HPβCD showed only a broad endothermic peak near 80 °C, corresponding to the release of water from the CD cavity. The complete disappearance of TD endothermic peak in the KN thermogram indicates a strong interaction of TD into the HPβCD cavity in the solid state. The thermogram of PM presented a mixed profile, with characteristics from both HPβCD and TD. The fusion peak of the drug was broaden, with lower onset temperature (270.5 °C for PM and 275.3 °C for TD), indicative of a slight interaction in this simple mixture.

Additional evidence of the complexation of TD was obtained by XRD patterns (Fig. 6). Free drug presented sharp and intense peaks, indicating its crystalline nature. In contrast, HPβCD presented a

characteristic hollow pattern, representative of amorphous structures. Both diffraction patterns of KN and PM correspond to the superimposition of those of the pure components, with lower intensities of the diffraction peaks. These profiles were observed due to particle size reduction during grinding and dilution of the pure crystalline components, indicating partial amorphization of the material.
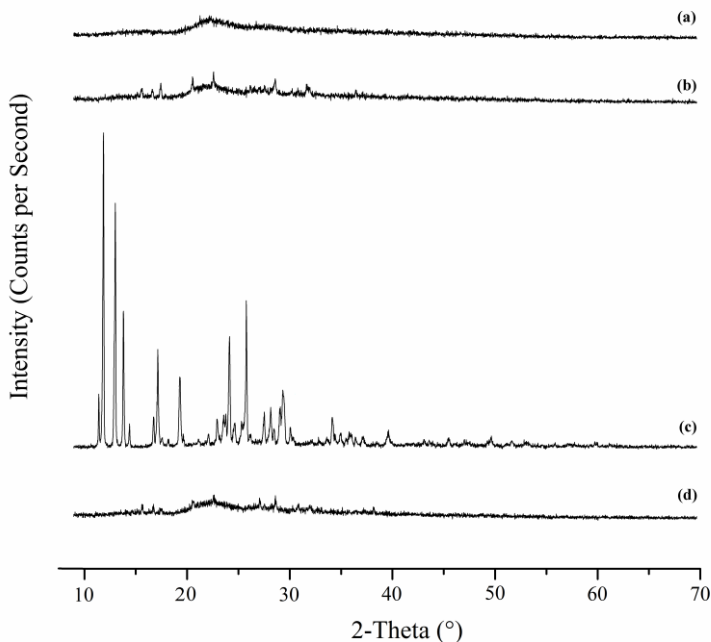
Figure 6 – Powder X-ray diffractograms of (a) HPβCD, (b) thalidomide/ HPβCD complex (Kneading), (c) thalidomide, and (d) physical mixture.

SEM photomicrographs of TD, HPβCD and the KN complex were taken with x500 and x1500 magnification (Fig. 7). The crystalline structure of TD is evidenced in Figure 7A, which presents characteristic format of big pointed plates, indicating that the raw material is formed mainly by the β polymorph [22]. This hypothesis was confirmed by Fourier transformed infrared spectroscopy (FTIR) analysis (data not shown). Alternatively, curved particles of various sizes with some concavities on the surface were revealed for HPβCD, whereas aggregate

formations occurred in the kneading process, as many small adhered formations can be observed in complexed product (Fig. 7C, D).
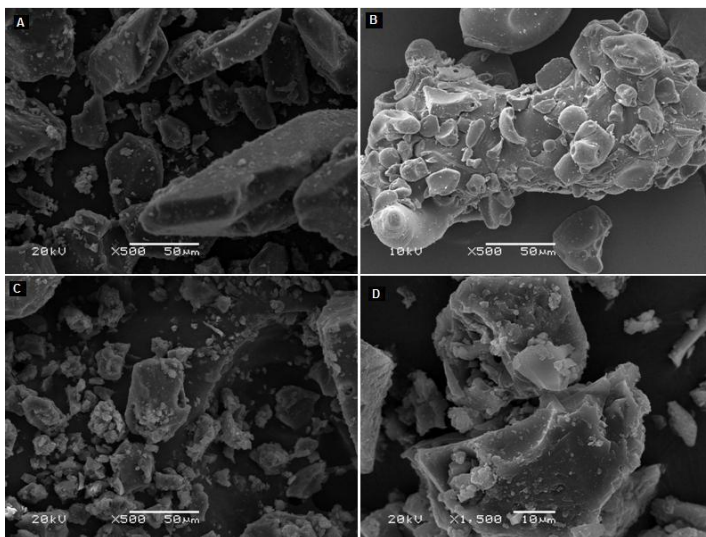
Figure 7 – Scanning electron microscopic (SEM) photomicrographs of (a) thalidomide, (b) HPβCD and (c, d) thalidomide/ HPβCD complex (Kneading).

Dissolution studies

Dissolution profiles of capsules containing 50 mg of free TD, or its equivalent amount in KN or PM products were assessed and the results expressed as the percent amount dissolved versus time. Fig. 8 shows that only $25.5 \pm 3.2\%$ of the free TD was dissolved after 60 min, while the percentage of TD dissolved from the PM was $54.9 \pm 4.7\%$. The enhancement in the drug dissolution rate from PM could be due to the surfactant-like properties of CDs, thus improving the wettability and dissolution of the drug, as reported previously [27]. The kneaded product presented higher dissolution rate when compared to PM and free TD ($p < 0.001$), with $77.3 \pm 0.1\%$ of TD dissolved after 60 min. This enhancement has been attributed to the formation of stable inclusion complexes in the solid state, improving the hydrophilicity of the molecule and reducing its cristallinity, as indicated by DSC, XRD and SEM studies.
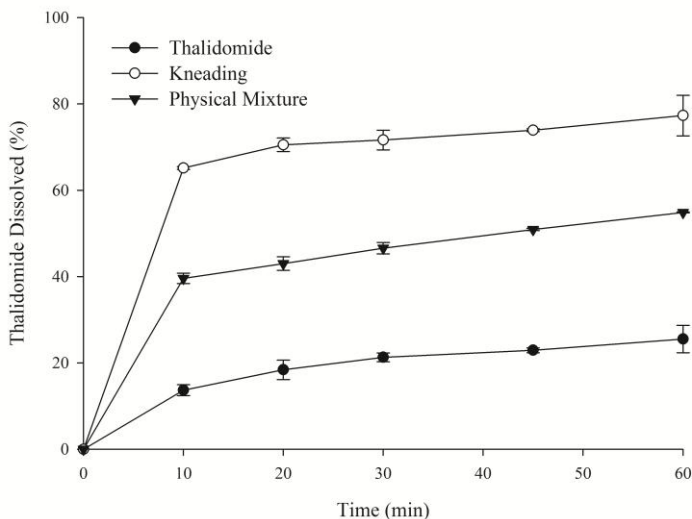
Figure 8 – Dissolution profiles of free thalidomide, thalidomide complexed with HPβCD (Kneading) and physical mixture in 0.225M HCl + 1% sodium lauryl sulphate at 37 °C. Results are expressed as mean ± SD (n = 3).

The *in vitro* dissolution results obtained with the free drug in this study were slightly different from those obtained by Kale and co-workers [13]. This variability was attributed to the use of different TD samples and experimental conditions. Raw materials may be composed by different polymorphs and present unrelated dissolution profiles [22]. Furthermore, different formulations and dissolution techniques may produce diverse results, as already described for TD [28].

In vitro permeability data

CDs are potential absorption enhancers and may alter epithelial barrier properties [24,29,30]. Both positive and negative outcomes have been achieved with the complexation of drugs with CDs in relation to the *in vitro* permeability [31-36]. In order to evaluate if the complexation may also affect the *in vitro* intestinal permeability of TD, transport experiments were performed on Caco-2 cells.

The apparent permeability of LY was not affected by the incubation of cells with samples, and TEER values were stable before

and after the experiments (data not shown). These findings show that cell monolayers were not destabilized during the permeability evaluation.

After 120 min of incubation, the accumulated transported amount of TD for all three samples presented a similar linear profile (Fig. 9). Free TD presented a P_{aap} value of $5.33 \pm 0.78 \times 10^{-5}$ cm/s, which categorizes TD as a highly permeable drug [37]. KN and PM (1:1 molar ratio) showed P_{app} values of $4.84 \pm 0.11 \times 10^{-5}$ and $4.98 \pm 0.77 \times 10^{-5}$ cm/s, respectively ($p > 0.05$). Stability of TD during the experiments was evaluated through the mass balance check. Results showed that TD was stable in the transport buffer for 2h, with a mean recovery value of $93.6 \pm 2.2 \%$.
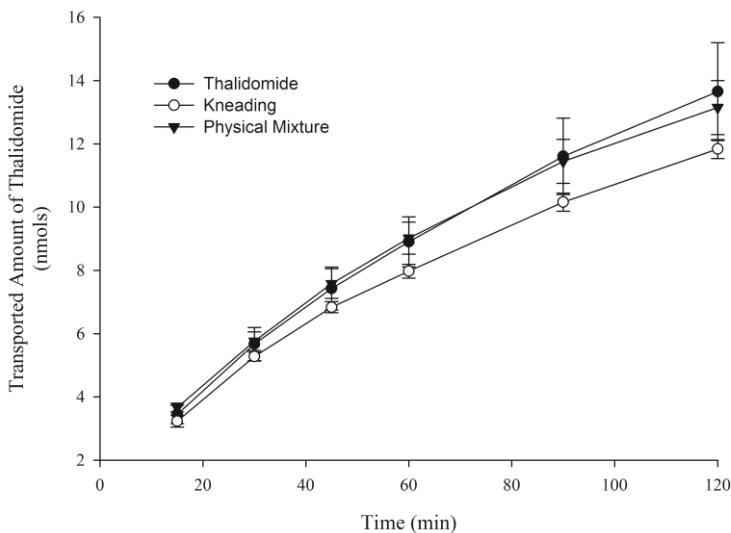
Figure 9 – Comparative *in vitro* permeability of free thalidomide, thalidomide complexed with HPβCD (Kneading) and physical mixture across Caco-2 cells in the apical to basolateral direction. Results are expressed as mean ± SD (n = 6).

These findings show that the complexation of TD with HPβCD, or the simple presence of the CD in solution, did not influence its permeability through intestinal epithelial cells. Previous reports evaluating the permeability in Caco-2 cells model showed that TD has favorable properties for biological membrane permeation, being rapidly

transported through cells [38,39]. Furthermore, Zimmermann and co-workers [39] also described that both enantiomers of TD are highly transported in both absorptive and secretory directions, with a linear passive profile. They also demonstrated that TD is not a substrate, an inhibitor, or an inducer of P-glycoprotein efflux transporter (P-gp) in Caco-2 cells.

Conclusion

Our results showed that the complexation of TD with HPβCD improved the aqueous solubility and the *in vitro* dissolution rate of the drug through the enhancement of its apparent solubility and reduction of cristallinity, both resulting from the formation of stable inclusion complexes in the solid state. It was demonstrated that TD was able to dissociate from the complexes and permeate across intestinal epithelial Caco-2 cells with a favorable high permeability profile equivalent to that of the free drug. In summary, these findings suggest that the TD/HPβCD complex obtained could improve the bioavailability of orally administered TD through the enhancement of its solubility and dissolution but not by the influence on the intestinal permeability of the drug.

Acknowledgements

References

1. Franks ME et al. Thalidomide. *Lancet* 2004; 363: 1802-1811.
2. Melchert M, List A. The thalidomide saga. *Int J Biochem Cell Biol* 2007; 39: 1489-1499.
3. Eriksson T et al. Clinical pharmacology of thalidomide. *Eur J Clin Pharmacol* 2001; 57: 365-376.
4. Matthews SJ, McCoy C. Thalidomide: A review of approved and investigational uses. *Clin Ther* 2003; 25: 342-395.
5. Teo SK. Properties of thalidomide and its analogues: Implications for anticancer therapy. *AAPS J* 2005; 7: E14-19.

6. Teo SK et al. Clinical pharmacokinetics of thalidomide. *Clin Pharmacokinet* 2004; 43: 311-327.

7. Lara-Ochoa F et al. Calorimetric determinations and theoretical calculations of polymorphs of thalidomide. *J Mol Struct* 2007; 840: 97-106.

8. Teo SK et al. Thalidomide dose proportionality assessment following single doses to healthy subjects. *J Clin Pharmacol* 2001; 41: 662-667.

9. Eriksson T et al. Intravenous formulations of the enantiomers of thalidomide: Pharmacokinetic and initial pharmacodynamic characterization in man. *J Pharm Pharmacol* 2000; 52: 807-817.

10. Chen H et al. Comparison of two polymeric carrier formulations for controlled release of hydrophilic and hydrophobic drugs. *J Mater Sci Mater Med* 2008; 19: 651-658.

11. Araujo FA et al. Development and characterization of parenteral nanoemulsions containing thalidomide. *Eur J Pharm Sci* 2011; 42: 238-245.

12. Alvarez C et al. Effects of hydroxypropyl-beta-cyclodextrin on the chemical stability and the aqueous solubility of thalidomide enantiomers. *Pharmazie* 2008; 63: 511-513.

13. Kale R et al. Molecular encapsulation of thalidomide with sulfobutyl ether-7 beta-cyclodextrin for immediate release property: Enhanced *in vivo* antitumor and antiangiogenesis efficacy in mice. *Drug Dev Ind Pharm* 2008; 34: 149-156.

14. Koch HP, Steinacker C. Improvement in solubility and stability of thalidomide by synthesis of inclusion complexes with cyclodextrins. *Arch Pharm (Weinheim)* 1988; 321: 371-373.

15. Krenn M et al. Improvements in solubility and stability of thalidomide upon complexation with hydroxypropyl-beta-cyclodextrin. *J Pharm Sci* 1992; 81: 685-689.

16. Siefert B et al. Influence of cyclodextrins on the *in vitro* corneal permeability and *in vivo* ocular distribution of thalidomide. *J Ocul Pharmacol Ther* 1999; 15: 429-438.

17. Loftsson T, Duchene D. Cyclodextrins and their pharmaceutical applications. *Int J Pharm* 2007; 329: 1-11.

18. Bosch ME et al. Recent advances in analytical determination of thalidomide and its metabolites. *J Pharm Biomed Anal* 2008; 46: 9-17.

19. Zhou S et al. Determination of thalidomide in transport buffer for caco-2 cell monolayers by high-performance liquid chromatography

with ultraviolet detection. *J Chromatogr B Analyt Technol Biomed Life Sci* 2003; 785: 165-173.

20. ICH. *International conference on harmonization. Validation of analytical procedures: Text and methodology q2(r1).* Geneva: ICH, 2005.

21. Higuchi T, Connors KA. Phase-solubility techniques. *Adv Anal Chem Instr* 1965; 4: 117-212.

22. Carini JP et al. Solid state evaluation of some thalidomide raw materials. *Int J Pharm* 2009; 372: 17-23.

23. Hubatsch I et al. Determination of drug permeability and prediction of drug absorption in caco-2 monolayers. *Nat Protoc* 2007; 2: 2111-2119.

24. Loftsson T et al. Effects of cyclodextrins on drug delivery through biological membranes. *J Pharm Sci* 2007; 96: 2532-2546.

25. Gould S, Scott RC. 2-hydroxypropyl-beta-cyclodextrin (hp-beta-cd): A toxicology review. *Food Chem Toxicol* 2005; 43: 1451-1459.

26. Loftsson T et al. Cyclodextrins in drug delivery. *Expert Opin Drug Deliv* 2005; 2: 335-351.

27. Badr-Eldin SM et al. Inclusion complexes of tadalafil with natural and chemically modified beta-cyclodextrins. I: Preparation and in-vitro evaluation. *Eur J Pharm Biopharm* 2008; 70: 819-827.

28. Fujita Y et al. Comparison of dissolution profile and plasma concentration-time profile of the thalidomide formulations made by japanese, mexican and british companies. *Yakugaku Zasshi* 2008; 128: 1449-1457.

29. Hamid KA et al. The effects of common solubilizing agents on the intestinal membrane barrier functions and membrane toxicity in rats. *Int J Pharm* 2009; 379: 100-108.

30. Lambert D et al. Methyl-beta-cyclodextrin increases permeability of caco-2 cell monolayers by displacing specific claudins from cholesterol rich domains associated with tight junctions. *Cell Physiol Biochem* 2007; 20: 495-506.

31. Maestrelli F et al. Microspheres for colonic delivery of ketoprofen-hydroxypropyl-beta-cyclodextrin complex. *Eur J Pharm Sci* 2008; 34: 1-11.

32. Monnaert V et al. Effects of gamma- and hydroxypropyl-gamma-cyclodextrins on the transport of doxorubicin across an *in vitro* model of blood-brain barrier. *J Pharmacol Exp Ther* 2004; 311: 1115-1120.

33. Udata C et al. Enhanced transport of a novel anti-hiv agent--cosalane and its congeners across human intestinal epithelial (caco-2) cell monolayers. *Int J Pharm* 2003; 250: 157-168.
34. Ventura CA et al. Preparation of celecoxib-dimethyl-beta-cyclodextrin inclusion complex: Characterization and *in vitro* permeation study. *Eur J Med Chem* 2005; 40: 624-631.
35. Zerrouk N et al. Influence of cyclodextrins and chitosan, separately or in combination, on glyburide solubility and permeability. *Eur J Pharm Biopharm* 2006; 62: 241-246.
36. Zuo Z et al. Flutamide-hydroxypropy-beta-cyclodextrin complex: Formulation, physical characterization, and absorption studies using the caco-2 *in vitro* model. *J Pharm Pharm Sci* 2000; 3: 220-227.
37. Bergstrom CA et al. Absorption classification of oral drugs based on molecular surface properties. *J Med Chem* 2003; 46: 558-570.
38. Zhou S et al. Transport of thalidomide by the human intestinal caco-2 monolayers. *Eur J Drug Metab Pharmacokinet* 2005; 30: 49-61.
39. Zimmermann C et al. Thalidomide does not interact with p-glycoprotein. *Cancer Chemother Pharmacol* 2006; 57: 599-606.

CAPÍTULO 03

ESTUDO DA PERMEABILIDADE DO GALATO DE PENTILA:
Avaliação dos perfis de permeabilidade intestinal e cutânea e correlação entre as diferentes metodologias empregadas

APRESENTAÇÃO

O Laboratório de Virologia Aplicada da UFSC vem há vários anos avaliando a citotoxicidade e a atividade antiviral de produtos naturais e de compostos sintéticos. Nesse âmbito, a atividade anti-herpética de uma série de ésteres alquílicos do ácido gálico, também conhecidos como galatos, foi avaliada. Em um estudo inicial, foram estabelecidas relações estrutura-atividade para esse grupo de moléculas, não somente no que diz respeito à ação anti-herpética, mas também à sua ação antioxidante e sua genotoxicidade (SAVI et al., 2005).

Mais recentemente, nosso grupo de trabalho aprofundou os estudos com essa série, e demonstrou o mecanismo de ação antiviral do galato de pentila. Esse composto mostrou-se mais ativo que os demais componentes testados, atuando em múltiplos estágios da replicação viral (KRATZ et al., 2008a, b).

Embora o galato de pentila seja um composto com atividade antiviral promissora, a natureza intrínseca de sua molécula pode acarretar alguns problemas biofarmacêuticos. Tammela e colaboradores (2004) demonstraram que os galatos de metila e propila (um e três carbonos na cadeia alquílica, respectivamente) foram capazes de permear células Caco-2, ainda que de forma lenta, enquanto que o galato de octila (oito carbonos na cadeia alquílica) possui afinidade à membrana plasmática muito forte, característica que impede seu transporte *in vitro*.

Nesse sentido, visando à realização de experimentos *in vivo* e a preparação de formas farmacêuticas contendo o galato de pentila, foi realizado um estudo no qual foram avaliados os perfis de permeabilidade intestinal e cutânea desse composto, através do uso de diferentes estratégias metodológicas. Os resultados obtidos foram compilados e submetidos para publicação no periódico *Biological and Pharmaceutical Bulletin*. Esse manuscrito encontra-se sob revisão e é apresentado na íntegra no final deste capítulo.

REVISÃO DA LITERATURA

O ácido gálico (ácido 3,4,5-trihidroxibenzóico) é um composto fenólico presente em diversas plantas, que pode ser obtido através de hidrólise ácida ou alcalina de taninos. Seus ésteres n-alquílicos, também conhecidos como galatos (Figura 5), em especial o galato de propila, octila e dodecila, são amplamente utilizados como antioxidantes em alimentos e cosméticos (VAN DER HEIJDEN et al., 1986; KUBO et al., 2002a; MUNOZ et al., 2002; HA; NIHEI; KUBO, 2004).
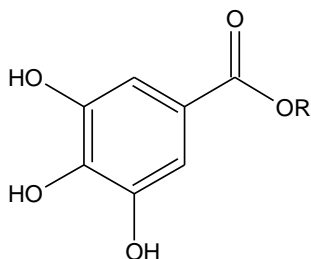
Figura 5. Estrutura básica dos galatos. No ácido gálico, o radical R = H e nos galatos, R = cadeia alquílica com número variável de carbonos.

A ação destes compostos sobre os radicais livres já foi bastante estudada, e algumas destas moléculas podem agir tanto como antioxidantes como pró-oxidantes (YOSHINO et al., 2002; HA; NIHEI; KUBO, 2004; AZMI et al., 2006).

Além da atividade antioxidante, diversas outras atividades biológicas já foram descritas para este grupo de compostos, e ficou evidente a influência do tamanho da cadeia alquílica sobre essas propriedades (SAVI et al., 2005; ROSSO et al., 2006; LOCATELLI et al., 2008; LEAL et al., 2009). Dentre as propriedades biológicas estudas estão: influência sobre enzimas hepáticas (OW; STUPANS, 2003), sobre 5-alfa-redutases envolvidas no processamento de hormônios (HIIPAKKA et al., 2002), e sobre a esqualeno epoxidase, enzima relacionada com a biossíntese do colesterol (ABE; SEKI; NOGUCHI, 2000); atividades antiinflamatória (MURASE et al., 1999), vaso-relaxante (PAULINO et al., 1999) e neuroprotetora (BASTIANETTO et al., 2006).

Entretanto, grande parte dos esforços na busca por atividades farmacológicas para esses compostos restringe-se à avaliação de suas propriedades citotóxicas e antitumorais, e antiinfecciosas (KANE et al.,

1988; BAER-DUBOWSKA, GNOJKOWSKI, FENRYCH, 1997; SAEKI et al, 2000; GNOJKOSWKI et al., 2001; KUBO et al., 2001, 2002b, 2003, 2004; FUJITA; KUBO, 2002a, b; FIUZA et al., 2004; STAPLETON et al., 2004; KREANDER et al., 2005; SAVI et al., 2005; SHIBATA et al., 2005; UOZAKI et al., 2006; VELURI et al., 2006; HSU et al., 2007; KRATZ et al., 2008a, b; LOCATELLI et al., 2008; LEAL et al., 2009; LOCATELLI et al., 2011).

Como citado anteriormente, um trabalho desenvolvido em nosso laboratório relatou a atividade anti-herpética de diversos galatos (SAVI et al., 2005). Nesse estudo, foi estabelecida uma série de relações estrutura-atividade para essas moléculas, não somente no que diz respeito à ação anti-herpética, mas também à sua ação antioxidante e sua genotoxicidade. Mais recentemente, nosso grupo também demonstrou (KRATZ et al., 2008a, b) o mecanismo da ação anti-herpética (anti-HSV-1 e anti-HSV-2) do galato de pentila. Kratz e colaboradores (2008a), após a triagem de 16 galatos, demonstraram que a atividade antiviral do galato de pentila mostrou-se superior aos demais, sendo que sua atividade anti-HSV-1 é exercida em múltiplos estágios da replicação viral, a saber: através da redução da infectividade viral, inibição da adsorção e da penetração dos vírus nas células, diminuição dos níveis das proteínas virais VP5, ICP27, gB, gC, gD e gE e interferência sobre a síntese da proteína gD, através do bloqueio da expressão do seu mRNA, e sobre a síntese de DNA viral.

Já em relação à sua atividade anti-HSV-2, Kratz e colaboradores (2008b) demonstraram que o galato de pentila também inibe a replicação desse vírus em diversas etapas, através da inibição da adsorção viral e da propagação da infecção (cell-to-cell spread), da interferência sobre a síntese das proteínas virais gB e gC e da síntese do DNA viral, além de reduzir a infectividade do vírus, ainda que esta atividade seja praticamente abolida em presença de soluções protéicas.

Embora os galatos sejam empregados nas formulações de alimentos e cosméticos já há algum tempo, os perfis de absorção desses compostos ainda não foram extensivamente avaliados. Em um estudo *in vitro*, Tammela e colaboradores (2004) demonstraram que o grau de hidroxilação, a configuração molecular e o tamanho da cadeia lateral de flavonóides e galatos tem um impacto importante na sua afinidade por membranas lipídicas e permeabilidade em células Caco-2. Dos três galatos avaliados, apenas os galatos de metila e propila (um e três carbonos na cadeia alquílica, respectivamente) foram capazes de permear células Caco-2, ainda que de forma lenta, enquanto que o galato de octila (oito carbonos na cadeia alquílica) acumulava

extensivamente no interior das células, o que impediu seu transporte através da monocamada celular e conseqüente detecção no compartimento receptor.

Já em relação à interação dos galatos com transportadores de membrana, Kitagawa e colaboradores (2005), através de um modelo de células KB-C2 que superexpressam a P-gp, verificaram um aumento no acúmulo dos substratos rodamina 123 e danorubicina em presença dos galatos de octila e dodecila através da inibição da P-gp, enquanto que o ácido gálico e o galato de butila não apresentavam esse efeito. Nesse estudo foi possível demonstrar que tanto o grupamento galoil (éster do ácido gálico), quanto uma cadeia lateral longa eram essenciais para a inibição do efluxo mediado pela P-gp.

Estudos com compostos relacionados estruturalmente aos galatos, em especial os flavonóides pertencentes à classe das catequinas (principalmente a epicatequina, epigalocatequina, e seus respectivos galatos) são mais abundantes. Esse grupo de moléculas presente no chá-verde tem recebido atenção devido às suas propriedades farmacológicas, que incluem efeitos cardio- e neuroprotetores e antineoplásicos. Entretanto, seu potencial terapêutico ainda é limitado devido à sua baixa disponibilidade oral, atribuída à instabilidade química, à baixa permeabilidade intestinal e ao possível efluxo por transportadores de membrana (VAIDYANATHAN, WALLE, 2001, 2003; ZHANG et al., 2004; DUBE, NICOLAZZO, LARSON, 2010).

Em relação à absorção cutânea, pouco se sabe acerca da permeação dos galatos. Em relação às catequinas relacionadas citadas acima, alguns estudos mostraram boas características de penetração e retenção cutânea para esses compostos, em especial aqueles que possuam o grupamento galoil na molécula, como o galato de epigalocatequina. Esse grupo de compostos foi capaz de permear em quantidades significativas nas camadas da pele, embora atingissem concentrações negligíveis sistemicamente, o que corrobora o seu potencial de aplicação local (DVORAKOVA et al., 1999; BATCHELDER et al., 2004; FANG et al., 2006; BELO et al., 2009).

Tendo em vista a falta de estudos acerca do perfil de permeabilidade do galato de pentila, e a existência de dados na literatura acerca de compostos relacionados, fica claro que a avaliação da permeabilidade intestinal e cutânea do galato de pentila é importante, não apenas para estabelecer o seu perfil de permeabilidade, mas também a fim de obter informações que permitirão uma análise mais consistente da possibilidade de se realizar estudos adicionais *in vivo* com esse composto. As propriedades físico-químicas de sua molécula podem

acarretar problemas biofarmacêuticos nesses estudos, tais como a baixa solubilidade aquosa e acúmulo inespecífico em tecidos (cadeia alquílica de cinco carbonos), e suscetibilidade à oxidação (presença de três hidroxilas livres).

O ensaio PAMPA é um modelo empregado na triagem de moléculas em larga escala, desenvolvido para avaliar a permeabilidade nos estágios iniciais da pesquisa e desenvolvimento de fármacos. (KANSY; SENNER; GUBERNATOR, 1998; AVDEEF, 2005;). Fundamentalmente, esse ensaio consiste em dois compartimentos (doador e aceptor) contendo tampões aquosos separados por uma membrana artificial disposta sobre um filtro poroso (AVDEEF, 2001, 2005). Devido à sua relativa versatilidade, essa técnica ganhou popularidade rapidamente nas indústrias farmacêuticas, e, desde então, surgiram diversas variações metodológicas (FALLER, 2008). Tais variações diferem entre si pela natureza da constituição química do filtro, da composição da membrana artificial, do pH nos compartimentos aceptores e doadores e do tempo de incubação (AVDEEF et al., 2007).

O ensaio PAMPA apresenta uma característica extremamente vantajosa, que é o seu alto rendimento (avaliação concomitante de grande número de moléculas), usando placas de 96 cavidades, aliado à possibilidade de quantificação por espectrofotometria no ultravioleta. O custo de cada ensaio é aproximadamente 5% do valor dos experimentos com células Caco-2. Entretanto, esse modelo avalia apenas a permeabilidade passiva, que é o mecanismo predominante do transporte de fármacos administrados por via oral. Adicionalmente, esse ensaio envolve procedimentos menos laboriosos do que nos experimentos com cultura de células e estudos *in vivo*, embora apresente um poder preditivo semelhante aos mesmos (AVDEEF, 2001, 2005; KERNS, DI, 2008). Porém, há algumas limitações relativas à predição da absorção em humanos, como por exemplo, a variação da composição das bicamadas lipídicas usadas nas diferentes variações deste modelo, que pode provocar alterações nos coeficientes de permeabilidade, tanto de fármacos transportados ativamente, quanto de pequenas moléculas hidrofóbicas transportadas passivamente através da via paracelular (MIRET et al., 2004; BALIMANE, HAN, CHONG, 2006; AVDEEF et al., 2007; KERNS, DI, 2008).

A utilização da pele como via de administração de fármacos é atrativa não apenas pelo seu efeito cutâneo (tratamento local), mas também pela possibilidade de obtenção de efeito sistêmico (terapias

transdérmicas)(PRAUSNITZ et al., 2004). Além disso, a rota de administração transdérmica tem como vantagens a limitada atividade metabólica, quando comparada à via oral que é susceptível ao metabolismo hepático de primeira passagem, bem como a possibilidade de se alcançar um perfil contínuo de liberação. A barreira de permeação exercida pelas diferentes camadas da pele representa a principal limitação dessa rota de administração (BOUWSTRA et al., 2003).

Geralmente, em preparações cutâneas, não é desejável que o fármaco alcance a circulação sistêmica, mas que se concentre nas camadas superficiais, promovendo um efeito local (por exemplo, antibióticos, antifúngicos, antivirais, corticosteróides, agentes antiinflamatórios, entre outros)(BARRY, 2002).

O processo de permeação cutânea envolve diferentes etapas que incluem, primeiramente, a liberação do fármaco da forma farmacêutica, seguida da sua penetração através das barreiras da pele, e, por fim, a ativação da resposta farmacológica. Todas essas etapas devem ser otimizadas para garantir a eficácia terapêutica. Adicionalmente, deve-se considerar aspectos relativos à natureza físico-química do fármaco, o tipo de veículo utilizado, as condições da pele, as interações pele/fármaco e pele/forma farmacêutica, entre outros (ANSEL, POPOVICH, ALLEN, 2000).

O desenvolvimento de formulações dermatológicas exige estimativas prévias da taxa e extensão de penetração dos fármacos através da pele. Modelos *in vivo* e *ex vivo* podem ser utilizados com esse propósito (MUHAMMAD, RIVIERE, 2006). Dentre os métodos animais, a pele de porco tem sido amplamente utilizada em função da sua similaridade estrutural e funcional com a pele humana, aliada à praticidade de obtenção desse material em abatedouros. Características comuns entre os dois tipos de pele incluem a distribuição esparsa de pêlos, pigmentação e vascularização, bem como a composição lipídica e propriedades biofísicas do estrato córneo (MUHAMMAD, RIVIERE, 2006). Diversos estudos têm mostrado a correlação entre os perfis de permeação entre as peles suína e humana (CHANG et al., 1994; SCHMOOK et al., 2001; HERKENNE et al., 2006).

Dessa forma, a utilização das câmaras de difusão, em especial a câmara da Franz, também conhecido como modelo estático, representa uma opção de ampla aplicabilidade para estudos de permeabilidade *ex vivo*. O tecido é colocado entre dois compartimentos preenchidos por tampões aquosos, sendo que o epitélio da pele encontra-se voltado para o compartimento doador, enquanto que a derme para o receptor (FRANTZ, 1990).

PUBLICAÇÃO

Biological & Pharmaceutical Bulletin

Current Status of Submitted Manuscript

Journal:	BPB
Manuscript ID:	b110393
Corresponding Author Name:	Simoes Claudia Maria Oliveira (Claudia Maria Oliveira Simoes)
Manuscript Title:	Intestinal and cutaneous permeability of pentyl gallate – PAMPA, Caco-2 cell line and pig ear skin permeation models
All Authors' Name:	Jadel Müller Kratz, Naira Fernanda Zanchett Schneider, Thiago Caon, Marina Rodrigues Teixeira, Alessandra Mascarello, Rosendo Augusto Yunes, Ricardo José Nunes, Letícia Scherer Koester, Cláudia Maria Oliveira Simões
Type of Manuscript:	Regular Article
Appropriate Section:	23. Biopharmacy and Pharmacokinetics
Date Submitted:	2011/6/10
Assigned to Editor:	2011/6/10
Under Review:	
Revision Request:	
Revised Manuscript Submitted:	
Under 2nd Review:	
2nd Revision Request:	
2nd Revised Manuscript Submitted:	
Under 3rd Review:	
Final Decision:	

Intestinal and cutaneous permeability of pentyl gallate – PAMPA, Caco-2 cell line and pig ear skin permeation models

J.M. Kratz[1], N.F.Z. Schneider[1], T. Caon[1], M.R. Teixeira[1], A. Mascarello[2], R.A. Yunes[2], R.J. Nunes[2], L.S. Koester[3], C.M.O. Simões[1]

[1] Departamento de Ciências Farmacêuticas, Universidade Federal de Santa Catarina, UFSC, Florianópolis, SC, Brasil
[2] Departamento de Química, Universidade Federal de Santa Catarina, UFSC, Florianópolis, SC, Brasil
[3] Faculdade de Farmácia, Universidade Federal do Rio Grande do Sul, UFRGS, Porto Alegre, RS, Brasil

Abstract

Pentyl gallate (PG) is a synthetic n-alkyl ester of gallic acid with significant anti-herpetic activity. The goal was to clarify the oral absorption and topical permeation of the compound, providing useful information for the design of pharmaceutical formulations and *in vivo* antiviral experiments. We evaluated the intestinal and cutaneous permeability profiles of PG through PAMPA, Caco-2 cells and pig ear skin permeation assays. Regarding the assessment of intestinal permeability, we have shown that PG has a high passive diffusion in different pH values, covering the physiological range. Data obtained in both PAMPA and Caco-2 models show that the oral absorption of PG will not be limited by permeability issues. On the other hand, in relation to the topical administration, we have shown that PG is not transported through the skin, and accumulates mainly in the epidermis. A correlation between PAMPA and pig ear skin model was not established in our study. The results obtained here show that both intestinal and cutaneous permeability profiles of PG are adequate for an anti-herpetic candidate, and provide important basis for future studies aiming the design of pharmaceutical formulations with PG.

Keywords: Pentyl gallate; Permeability; Caco-2; PAMPA; Pig ear skin.

Introduction

The synthetic n-alkyl esters of gallic acid, also called gallates, are frequently used as antioxidants by food and pharmaceutical industries [1]. These phytochemical derivatives present several additional

biological activities, mainly antibacterial [2], antifungal [3], antiviral [4-6] and anticancer [7] properties. Although this group of phenolic compounds has remarkable pharmacological potential, the quest for new chemical entities that will prove to be clinically useful drugs is challenging. The pharmaceutical industry experience has shown that the optimization of biopharmaceutical properties in parallel with the potency of drug candidates is the best way to produce drug-like molecules [8,9].

Ideal drug candidates should have adequate aqueous solubility, permeability and stability in order to distribute well and achieve effective concentrations in the tissue where the corresponding target is actually located [10-12]. Permeability is considered one of the most important features regarding the absorption of drugs. Mechanisms of permeation through biological barriers comprise passive diffusion (transcellular and paracellular), active uptake and efflux transports [13]. Among several techniques available for the permeability assessment, the Caco-2 cell line and the parallel artificial membrane permeability assay (PAMPA) are the most popular models [9].

Caco-2 cells are able to fully polarize into differentiated monolayers with well-established tight junctions and brush border membrane, as well as to express several membrane transporters and metabolizing enzymes, allowing the measurement of functional permeability (both passive diffusion and active transport) [14]. PAMPA is a filter-based assay that measures exclusively passive diffusion, with an artificial organic membrane that separates two compartments filled with aqueous buffer solutions [15]. Different adaptations of this assay have been developed in order to mimic specific tissues, such as the gastrointestinal tract [15] and skin [16]. These models employed synergistically can provide an efficient and rapid investigation of permeability mechanisms [17].

The absorption and bioavailability of polyphenolic compounds have been studied in different models [18-22]. In general, the molecular structure, degree of hydroxylation and interaction with biological membranes (accumulation and efflux) seem to play an important role in the permeability profiles [20,21]. In this view, the objective of this study was to perform *in vitro* and *ex vivo* assessments of intestinal and cutaneous permeability of pentyl gallate (PG – Fig. 1), a compound with anti-herpes activity [4,5]. PAMPA, Caco-2 cells and pig ear skin permeation assays were performed. These models could provide useful information regarding the absorption/permeation of PG, which could be further used for the design of pharmaceutical formulations and *in vivo*

experiments, looking for correlations between its antiviral activity and permeability profile.
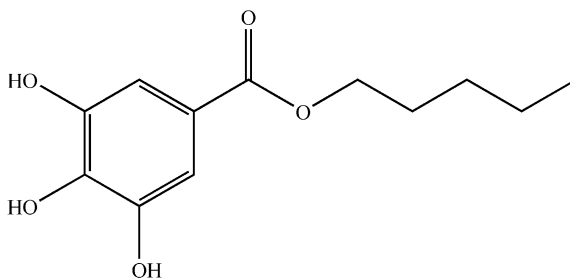
Figure 1 – Pentyl gallate (PG) structure.

Materials and Methods

Materials

PG was synthesized as previously described [23], dissolved in DMSO (50mM) and stored at -20°C protected from light. Dulbecco's modified Eagle's medium with high glucose (DMEM), fetal bovine serum (FBS), nonessential amino acids, and antibiotics/antimycotic were all purchased from Gibco (Carlsbad, CA, USA). Hank's balanced salt solution (HBSS), sodium 4-(2-hydroxyethyl)-1-piperazineethanesulfonate (HEPES), methanesulfonic acid (MES), DMSO, Lucifer yellow (LY), n-dodecane and silicone oil DC 200 were all purchased from Sigma Chemical Co. (St. Louis, MO, USA). Soy lecithin was purchased from Avanti Polar Lipids Inc. (Alabaster, AL, USA). Isopropyl myristate was purchased from Alfa Aesar (Karlsruhe, Baden-Wurttemberg, Germany). Hexane was purchased from Acros Organics (Geel, Vlaams Gewest, Belgium). Methanol was purchased from Tedia Co. (Fairfield, OH, USA). All other reagents and solvents used in this study were of the highest purity commercially available. Ultrapure water from a Milli-Q system apparatus (Millipore Corp. – Billerica, MA, USA) was used throughout the study.

Parallel Artificial Membrane Permeability Assay (PAMPA) studies

PAMPA studies were carried out to predict the oral and topical absorption of PG. Experiments were designed to mimic the intestinal

epithelium [15] and the human skin [16,24] as previously described. In both approaches, 96-well PVDF filter plates (Multiscreen, Millipore) and 96-well plates (MSSACEPTOR, Millipore) were used as donor and acceptor plates, respectively.

PAMPA Intestine model

In this model, each filter was coated with 5 µL of a 20% soy lecithin solution in n-dodecane (w/v). Donor solutions (150 µL) were prepared by dilution of PG stock solution in phosphate buffer (PBS) containing 0.5% DMSO to a final concentration of 500 µM. Different pH values (5.0, 6.2 and 7.4) were employed to mimic the different pH conditions of the gastrointestinal tract. All acceptor wells were filled with 300 µL of PBS/0.5% DMSO buffer at pH 7.4. The acceptor plate was placed on top of the donor plate to create a "sandwich" in which two compartments were separated by the coated filter. The sandwich was incubated for 1 h at room temperature under constant stirring (300rpm).

PAMPA Skin model

The lipid component of the membrane used for this model consisted of a mixture of silicone oil and isopropyl myristate (70:30, v/v). This mixture was further diluted in hexane (35%, v/v) and each filter was coated with 17 µL of this solution. Filter plates were incubated for 20 min at room temperature prior to the permeability assay to completely evaporate the solvent. Donor solution (150 µL) was prepared by dilution of PG stock solution in PBS/0.5% DMSO (pH 5.0) to a final concentration of 500 µM. Acceptor solution (300 µL) was PBS/0.5% DMSO buffer at pH 7.4. Sandwiches were assembled and incubated for 7 h at room temperature under gentle stirring (150 rpm).

For both methods, after incubation the contents of donor and acceptor plates were transferred to a 96-well UV quartz plate (SPECTRAplate, Molecular Devices, Sunnyvale, CA, USA) and PG determined as described in section 2.5. The effective permeability coefficients (P_e, cm/s) and mass retentions (R, %) were calculated as previously described [25], according to Equations 1-3:

$$P_e = \frac{-ln[\,1 - C_A(\,t\,)\,/\,C_{equilibrium}\,]}{A(1/V_D + 1/V_A)t} \qquad (1)$$

$$C_{equilibrium} = \frac{[C_D(t)V_D + C_A(t)V_A]}{V_D + V_A} \qquad (2)$$

$$R = \frac{1 - [C_D(t)V_D + C_A(t)V_A]}{C_0 V_D} \qquad (3)$$

where A is the effective filter area (0,3 cm^2), V_D is the donor volume (0.15 mL), V_A is the acceptor volume (0.3 mL), t is the incubation time (s), $C_A(t)$ is the compound concentration in acceptor well at time t, $C_D(t)$ is the compound concentration in donor well at time t and C_0 is the initial compound concentration in the donor well.

Caco-2 permeability studies

Cell culture

Caco-2 cells (HTB-37 – American Type Culture Collection, Manassas, VA, USA) were maintained in a humidified 5% CO_2 air atmosphere at 37 °C and were cultured in DMEM with 20% FBS, 1% non essential amino acids, 100 U/mL penicillin, 100 µg/mL streptomycin and 25 µg/mL amphotericin B, until cells reached 80 – 90% of confluence. For transport experiments, 1.0×10^5 cells between passages 28 and 30 were harvested and seeded into Millicell polycarbonate inserts (0.6 cm^2, 0.4 µm pore size – Millipore) and allowed to grow and differentiate for 21-25 days prior to the experiments.

Transport experiments

The determination of the *in vitro* intestinal permeability was carried out by transport experiments with Caco-2 cell monolayers, according to previous recommendations [26].
Stock solution of PG was diluted to a final concentration of 50 µM in HBSS at pH 6.0 (10 mM MES) or pH 7.4 (10 mM HEPES), which were used as transport buffers in the apical (400 µL) and basolateral (500 µL) compartments. Bi-directional experiments (AB and BA) were run for 1 h at 37 °C, in an orbital shaker (100 rpm). At suitable time intervals, 100 µL aliquots were sampled from the receiver

compartment and replenished with an equal volume of fresh buffer. At the end of the experiment, aliquots were collected from donor compartments in order to perform the mass balance calculation. Samples were analyzed by HPLC. Transport experiments were conducted under sink conditions and the apparent permeability coefficients (P_{app}, cm/s) were calculated from Equation 4:

$$P_{app} = \frac{\Delta Q}{\Delta t} \frac{1}{AC_0} \qquad (4)$$

where $\Delta Q/\Delta t$ is the steady-state flux (mol/s), A is the surface area of the filter (cm2) and C_0 is the initial concentration in the donor compartment (mol/mL).

Transepithelial electrical resistance (TEER) and permeability to Lucifer yellow (LY – paracellular marker) were used as indicators of the monolayer integrity. TEER was assessed before and after the experiments at 37 °C using a Millicell ERS meter (Millipore) connected to a WPI Endohm tissue resistance measurement chamber (Sarasota, FL, USA). The permeability of LY (100 µg/mL) was determined for 1h at 37 °C in the AB direction after the experiments. Only monolayers with TEER values over 200 Ωcm^2 and LY permeability $\leq 2.0 \times 10^{-7}$ cm/s were used.

Ex vivo skin permeation studies

Skin permeation experiments were conducted as previously described [27]. Full thickness pig ear skin (1.00 ± 0.05 mm) was obtained from young animals sacrificed at a local slaughterhouse (Antonio Carlos, SC, Brazil). Skin was initially cleaned up with tap water, hairs and subcutaneous fat tissue were removed, and the obtained membranes were stored at -80°C for up to two months. After thawing at room temperature, the skin was mounted in a two-chamber glass Franz diffusion cells with the stratum corneum towards the donor chambers (diffusion area of 1.77 cm^2). Receiver chambers were filled with 10 mL of PBS (pH 7.4) and kept under continuously stirring at 900 rpm. The system was stabilized at 37°C by circulating heated water through an external water jacket for 30 min.

Different PG concentrations (50, 250 and 500 µM) in PBS (pH 7.4) were added to the donor chamber and the diffusion cells were covered with aluminum foil to prevent evaporation. At fixed time

intervals (total time = 7 h), samples (400 µL) were withdrawn from the receiver chambers and replenished with an equal volume of fresh buffer. At the end of the permeation experiment, aliquots were also collected from donor compartments in order to perform the mass balance calculation.

Additionally, skins were carefully washed with PBS to remove residual donor solution, and epidermis was separated from dermis by using a scalpel and placed in separate pre-weighed tubes. PG was extracted from the tissues by vortexing with 5 mL of methanol and filtration through cellulose membranes (0.45 µm; Millipore). The extraction method was validated in blank experiments by spiking the skin with a known amount of PG (98% recovery). The permeated and retained amounts of PG were determined by HPLC.

Regarding the permeation parameters, the steady-state permeation fluxes (J_s) were calculated from the linear slope of the cumulative amount of PG permeated vs. time. The lag time (T_L) represented the time required to achieve the steady-state flux, and the permeability coefficient (P) was the relation between the flux and the initial concentration of PG added to the donor compartment (C_d), as described in Equation 5:

$$P = \frac{J_s}{C_d} \qquad (5)$$

Analytical methods

PAMPA samples were analyzed by UV spectrophotometry using a Tecan Infinite M200 microplate reader (Seestrasse, Lenzerheiden, Switzerland). The analytical wavelength was set at 270 nm. LY fluorescent samples were analyzed using the same equipment. The fluorescent absorbance was measured using wavelengths of 485 nm excitation and 520 nm emission.

For the Caco-2 and *ex vivo* skin permeation studies, an HPLC method was developed based on a previous published method [20]. Quantitative determinations of PG were performed on a Perkin Elmer Series 200 chromatographer (Waltham, MA, USA) consisted of quaternary pump, vacuum degasser, autosampler, and diode-array detector. Elution was carried out using a 150 mm x 4.6 mm C18 column (Phenomenex, Torrance, CA, USA). Mobile phase consisted of methanol and water/phosphoric acid (100:0.1) in the ratio of 70:30 (v/v)

under an isocratic flow rate of 1.2 mL/min. The analytical wavelength was set at 273 nm.

Statistical analysis

Results were expressed as the mean ± SD of three independent experiments unless otherwise stated. Statistical analyses were performed by one-way ANOVA followed by SNK post hoc test ($p < 0.05$).

Results

Oral absorption prediction

We evaluated the diffusion of PG across 20% soy lecithin membranes in the PAMPA intestine variation. Results are summarized in Table 1. PG showed a pH-independent high permeability profile, with P_e values ranging from 8.22×10^{-5} to 6.75×10^{-5} cm/s ($p > 0.05$). At pH 7.4, PG permeability was intermediary when compared to high and low permeability controls. Carbamazepine was highly permeable ($22.29 \pm 1.25 \times 10^{-5}$ cm/s), while furosemide was 56-times less permeable ($0.12 \pm 0.01 \times 10^{-5}$ cm/s) than PG. High retention was detected for PG, indicating elevated accumulation of the compound in the lipid monolayer.

Table 1. Effective permeability coefficients (P_e) of pentyl gallate (PG) obtained by parallel artificial membrane permeability assays (PAMPA).

PAMPA Assay	P_e $(10^{-5})(cm/s)$			Mass retention (%)		
	pH 5.0	pH 6.2	pH 7.4	pH 5.0	pH 6.2	pH 7.4
Intestine	8.22 ± 0.29	7.76 ± 0.72	6.75 ± 0.64	79.4 ± 8.2	78.6 ± 8.6	79.3 ± 13.7
Skin	4.43 ± 0.57	n.d.[a]	n.d.	1.5 ± 0.3	n.d.	n.d.

Lipid monolayers were prepared with a 20% soy lecithin solution in n-dodecane (w/v) and a mixture of silicone oil and isopropyl myristate (70:30, v/v) in hexane (35%, v/v) for the intestine and skin models, respectively. PG at 500 μM was incubated for 1 h or 7 h at 37 °C in the intestine and skin version, respectively. Permeability coefficients were calculated from equations 1-3 and the results are means ± SD of three independent experiments. ANOVA/SNK tests ($p < 0.05$). [a] Not determined.

Accordingly, PG transport across Caco-2 cell monolayers was assessed in a pH gradient approach (6.0/7.4) in order to mimic *in vivo* conditions. When PG at 50 µM was added to the donor compartment, it could be detected in the receiver compartment in significant amounts after only a few minutes. Figure 2 shows the cumulative amount permeated (nmol/cm2) in the AB and BA directions.

Transport of PG was essentially linear for a period of 1h, even though an initial transport burst could be noticed. Comparable P_{app} values were obtained in the absorptive (P_{app} AB − 2.09 ± 0.02 x 10^{-5} cm/s) and secretory directions (P_{app} BA − 1.54 ± 0.07 x 10^{-5} cm/s) ($p > 0.05$). The efflux ratio ($P_{app\ BA}/P_{app\ AB}$) of 0.73 is indicative of a passive diffusion mechanism. Similar to the PAMPA assay, PG had low mass balance values, with an average recovery of 57.9 ± 1.5 and 59.6 ± 1.9% in the experiments in the AB and BA directions, respectively.
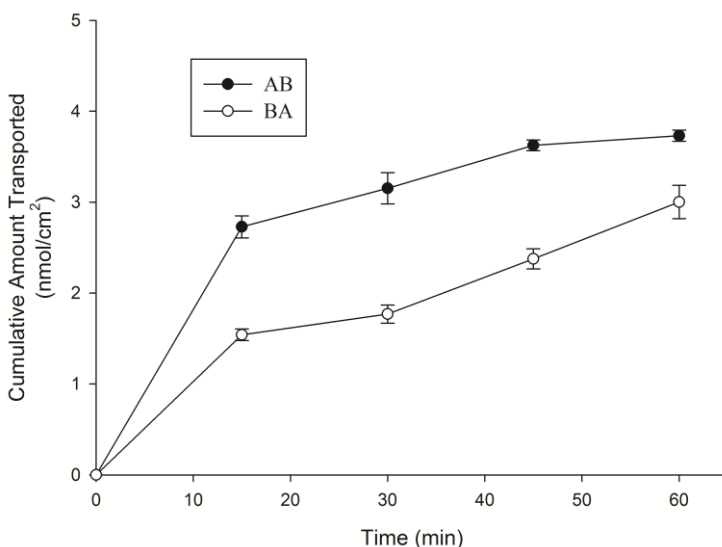
Figure 2 – Cumulative amount transported of pentyl gallate (PG) across Caco-2 cells in the apical to basolateral (AB) or basolateral to apical (BA) direction. Cell monolayers were incubated with 50 µM of PG for 1 h at 37°C and samples were collected from the opposite compartments at suitable times. In all experiments, the apical and basolateral media were HBSS pH 6.0 and pH 7.4, respectively. Data are means ± SD of six independent monolayers.

Topical absorption prediction

PAMPA Skin is able to mimic the barrier properties of human stratum corneum and can be used for the fast prediction of human skin permeability [16,24]. Table 1 shows that PG presented a high permeability coefficient across this membrane and low retention percentages. Controversially, the amount of PG permeated through the dermis and epidermis was lower than the quantification limit (1 μM) established during the validation of the HPLC method in the *ex vivo* experiments. Even with higher donor concentrations, it was not possible to detect PG in the receiver compartment after 7 h. Permeation parameters such as flux, lag time and the permeability coefficient were therefore not calculated. An average mass balance of 70.2 ± 7.4 % was obtained in this assay.

Figure 3 shows the accumulation of PG in the epidermis and dermis. At 50 μM, the amounts accumulated in both tissues were similar ($p > 0.05$). With higher donor concentrations, the amounts accumulated in the epidermis increased, ranging from 3.30 ± 0.64 to 24.21 ± 3.42 μg/g. On the other hand, this behavior was not observed in the dermis, where the accumulation remained constant with different donor concentrations ($p > 0.05$).
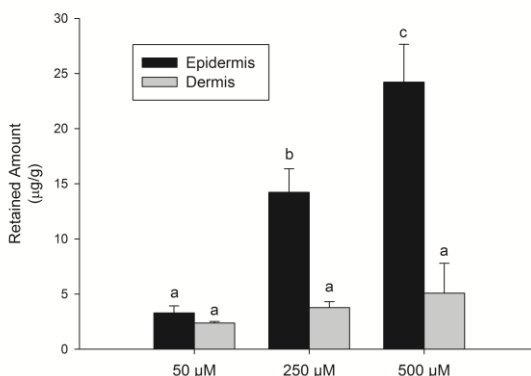
Figure 3 – Retained amount of pentyl gallate (PG) per gram of tissue after 7 h in the pig ear skin permeation assay. Epidermis was separated from dermis with a scalpel and PG was extracted from the tissues with methanol. Data are means ± SD of three independent experiments. ANOVA/SNK tests ($p < 0.05$) were performed and different letters indicate significant statistical differences among treatments.

Discussion

There is an urgent need to develop new anti-infective drugs in the face of a constant threat of resistance development, which can eventually lead to therapeutic failure [28,29]. The antiviral activity of PG has been recently characterized by our research group [4,5] and the results suggested that this compound could be regarded as a candidate for development as an anti-herpetic agent. For this reason, we evaluated the intestinal and cutaneous permeability profiles of PG, the most common administration routes of anti-herpetic drugs.

PG was first screened using PAMPA to assess passive transcellular permeability potential. This assay is relatively fast and inexpensive, and since the great majority of drugs are absorbed by passive diffusion, this model correlates well with human absorption [9,17]. Different pH values were employed in this initial screening. Fluctuations on the intestinal pH may impact on the oral absorption. The passive membrane permeability of uncharged species is much higher than that of the charged ones [30]. Table 1 shows that PG had similar high permeability coefficients at all pH values tested, indicating no influence of ionization on the physiologic pH range.

Further on, the permeability of PG across Caco-2 cells was investigated. This cell line is the most widely and successfully used permeation model in the drug discovery and early drug development [11]. The combination of PAMPA and Caco-2 cells can provide a mechanistic insight over the membrane permeability. This combo approach turned out to be important even in the correlation between the permeability and the activity of antiviral drug candidates [31].

The P_{app} values obtained for PG were much higher than the cut-off coefficient reported as indispensable for a complete intestinal absorption in humans ($\geq 1.0 \times 10^{-6}$ cm/s) [14,32]. This finding suggest that permeability may not impose a major obstacle in the oral bioavailability of PG. Additionally, the values obtained in PAMPA correlated well with the Caco-2 assay, fact that suppose a passive transcellular pathway. To check this assumption, Caco-2 bi-directional transport experiments were conducted. Figure 2 shows that similar profiles were obtained in the absorptive (AB) and secretory (BA) directions, supporting the passive diffusion. Different donor concentrations were used to discard transporters saturation, with no significant effect on the permeability coefficients (data not shown).

Lipophilic compounds are frequently problematic in permeability studies due to their non-specific adsorption to plastic surfaces and

membrane accumulation. This behavior may lead to inaccurate estimation of permeability and underestimation of human absorption [15,26]. The low mass balance values obtained in the Caco-2 assay and the high percentages of retention in the PAMPA clearly illustrate this issue. The biomembrane interactions of some alkyl esters have been previously studied. Tammela and co-workers [20] showed that the transport of methyl, propyl and octyl gallate across Caco-2 cells was governed by the length of the alkyl moiety. Gallates with shorter n-alkyl chains were detected in the receiver chamber, although these compounds permeated slower than PG in our study. Meanwhile, octyl gallate showed cellular uptake but no transport. This compound was extremely rapidly and almost totally (96%) reduced from the apical solution within 60 min. These findings support that the low mass balances of PG in our study could possibly be attributed to cellular accumulation, even though this hypothesis needs to be confirmed.

The topical delivery of drugs offer many advantages, including higher metabolic stability through avoidance of first-pass metabolism, lower fluctuations in plasma drug levels and higher safety by restricted local effect [33]. In the case of antiviral agents, the concentration in the skin lesion of a herpetic infection is expected to be higher than the one achieved by oral administration. In this view, one of the goals of this study was to evaluate the skin permeation of PG. The results obtained in the *ex vivo* experiments showed low permeation of PG through the skin layers, and a substantial accumulation in the epidermis and dermis (Fig. 3).

PG accumulated preferably in the epidermis. The amounts of PG found in the epidermis increased when higher donor concentrations were used. Although, in relation to the three different initial amounts of PG added to the system, the percentages retained in the epidermis were constant, around 8%. In the dermis, the accumulation was constant, with a mean value of 3.74 ± 1.36 µg/g, indicating a slow release rate from the epidermis, which supposes that the epidermis layer acts as a reservoir for this compound, preventing its access to deeper layers of skin and consequently to the blood stream. The greater retention in the epidermis, when compared to the dermis, could be associated to the high lipophilicity of this compound (Clog P = 2.84 − ChemAxon Kft.). This outcome is promising, since anti-infective topical agents are expected to remain confined in the skin and not to reach systemic circulation.

Controversially, the results obtained in the PAMPA assay indicated good skin permeation potential (Table 1). This PAMPA variation was developed by Ottaviani and co-workers [16] to rapidly

predict passive human skin permeation. For a determined set of thirty-one drugs, this model provided a good correlation between human skin permeability coefficients (log K_p) and those obtained by PAMPA Skin (log P_e).

In our study with PG this relationship could not be established. The discrepancy could be attributed to the membrane configuration in PAMPA. It has a lower thickness, only mimicking the behavior of the stratum corneum. The pig ear skin in contrast, possesses both viable epidermis and dermis as further barriers. In another diverse issue, higher mass balance was found for PAMPA when compared to the *ex vivo* model. The lower mass balance found in *ex vivo* experiments could be associated to the metabolism of the compound by enzymes of skin viable layers, particularly esterases [34].

In summary, PG presented adequate permeability profiles for both oral and topical administration. In the gastrointestinal tract, we have shown that the absorption of PG will not be limited to any larger extent by the intestinal permeability. PAMPA and Caco-2 cells models correlated well, showing a high permeability profile via passive diffusion pathway. It is noteworthy that other biopharmaceutical properties, for instance metabolic instability and protein binding, might impact in the oral bioavailability of PG, and require further investigations. In relation to the cutaneous permeability, even though a correlation between PAMPA and the pig ear skin model was not established, the *ex vivo* model provided good insights over the skin permeation of PG. The compound seems to accumulate in the skin layers, particularly in the epidermis, restricting its transport to blood circulation. This feature is valuable when a local delivery is necessary, like in the topical therapy of epithelial herpetic infections. These findings provide important information for the design of formulations, and corroborate that PG can be further considered as a topical and oral anti-herpetic candidate.

Acknowledgements

References

1. Kubo I, Masuoka N, Xiao P, Haraguchi H. Antioxidant activity of dodecyl gallate. J Agric Food Chem, 2002; 50:3533-3539.
2. Kubo I, Fujita K, Nihei K. Anti-Salmonella activity of alkyl gallates. J Agric Food Chem, 2002; 50:6692-6696.
3. Leal PC, Mascarello A, Derita M, Zuljan F, Nunes RJ, Zacchino S, Yunes RA. Relation between lipophilicity of alkyl gallates and antifungal activity against yeasts and filamentous fungi. Bioorg Med Chem Lett, 2009; 19:1793-1796.
4. Kratz JM, Andrighetti-Frohner CR, Kolling DJ, Leal PC, Cirne-Santos CC, Yunes RA, Nunes RJ, Trybala E, Bergstrom T, Frugulhetti IC, Barardi CR, Simoes CM. Anti-HSV-1 and anti-HIV-1 activity of gallic acid and pentyl gallate. Mem Inst Oswaldo Cruz, 2008; 103:437-442.
5. Kratz JM, Andrighetti-Frohner CR, Leal PC, Nunes RJ, Yunes RA, Trybala E, Bergstrom T, Barardi CR, Simoes CM. Evaluation of anti-HSV-2 activity of gallic acid and pentyl gallate. Biol Pharm Bull, 2008; 31:903-907.
6. Uozaki M, Yamasaki H, Katsuyama Y, Higuchi M, Higuti T, Koyama AH. Antiviral effect of octyl gallate against DNA and RNA viruses. Antiviral Res, 2007; 73:85-91.
7. Locatelli C, Carvalho DR, Mascarello A, de Cordova CA, Yunes RA, Nunes RJ, Pilati C, Creczynski-Pasa TB. Antimetastatic activity and low systemic toxicity of tetradecyl gallate in a preclinical melanoma mouse model. Invest New Drugs, 2011; in press.
8. Chen XQ, Antman MD, Gesenberg C, Gudmundsson OS. Discovery pharmaceutics--challenges and opportunities. AAPS J, 2006; 8:E402-408.
9. Di L, Kerns EH. Application of pharmaceutical profiling assays for optimization of drug-like properties. Curr Opin Drug Discov Devel, 2005; 8:495-504.
10. van De Waterbeemd H, Smith DA, Beaumont K, Walker DK. Property-based design: optimization of drug absorption and pharmacokinetics. J Med Chem, 2001; 44:1313-1333.
11. Balimane PV, Han YH, Chong S. Current industrial practices of assessing permeability and P-glycoprotein interaction. AAPS J, 2006; 8:E1-13.
12. Varma MV, Obach RS, Rotter C, Miller HR, Chang G, Steyn SJ, El-Kattan A, Troutman MD. Physicochemical space for optimum oral

bioavailability: contribution of human intestinal absorption and first-pass elimination. J Med Chem, 2010; 53:1098-1108.

13. Matsson P, Bergstrom CA, Nagahara N, Tavelin S, Norinder U, Artursson P. Exploring the role of different drug transport routes in permeability screening. J Med Chem, 2005; 48:604-613.

14. Artursson P, Karlsson J. Correlation between oral drug absorption in humans and apparent drug permeability coefficients in human intestinal epithelial (Caco-2) cells. Biochem Biophys Res Commun, 1991; 175:880-885.

15. Avdeef A, Bendels S, Di L, Faller B, Kansy M, Sugano K, Yamauchi Y. PAMPA--critical factors for better predictions of absorption. J Pharm Sci, 2007; 96:2893-2909.

16. Ottaviani G, Martel S, Carrupt PA. Parallel artificial membrane permeability assay: a new membrane for the fast prediction of passive human skin permeability. J Med Chem, 2006; 49:3948-3954.

17. Kerns EH, Di L, Petusky S, Farris M, Ley R, Jupp P. Combined application of parallel artificial membrane permeability assay and Caco-2 permeability assays in drug discovery. J Pharm Sci, 2004; 93:1440-1453.

18. Ferruzzi MG, Lobo JK, Janle EM, Cooper B, Simon JE, Wu QL, Welch C, Ho L, Weaver C, Pasinetti GM. Bioavailability of gallic acid and catechins from grape seed polyphenol extract is improved by repeated dosing in rats: implications for treatment in Alzheimer's disease. J Alzheimers Dis, 2009; 18:113-124.

19. Konishi Y, Kobayashi S, Shimizu M. Transepithelial transport of p-coumaric acid and gallic acid in Caco-2 cell monolayers. Biosci Biotechnol Biochem, 2003; 67:2317-2324.

20. Tammela P, Laitinen L, Galkin A, Wennberg T, Heczko R, Vuorela H, Slotte JP, Vuorela P. Permeability characteristics and membrane affinity of flavonoids and alkyl gallates in Caco-2 cells and in phospholipid vesicles. Arch Biochem Biophys, 2004; 425:193-199.

21. Tian XJ, Yang XW, Yang X, Wang K. Studies of intestinal permeability of 36 flavonoids using Caco-2 cell monolayer model. Int J Pharm, 2009; 367:58-64.

22. Vaidyanathan JB, Walle T. Cellular uptake and efflux of the tea flavonoid (-)epicatechin-3-gallate in the human intestinal cell line Caco-2. J Pharmacol Exp Ther, 2003; 307:745-752.

23. Wei B, Zhang Z, Wang L. Synthesis of alkyl gallates under microwave irradiation. Zhongguo Niangzao, 2009; 9:45-46.

24. Ottaviani G, Martel S, Carrupt PA. *In silico* and *in vitro* filters for the fast estimation of skin permeation and distribution of new chemical entities. J Med Chem, 2007; 50:742-748.

25. Chen X, Murawski A, Patel K, Crespi CL, Balimane PV. A novel design of artificial membrane for improving the PAMPA model. Pharm Res, 2008; 25:1511-1520.

26. Hubatsch I, Ragnarsson EG, Artursson P. Determination of drug permeability and prediction of drug absorption in Caco-2 monolayers. Nat Protoc, 2007; 2:2111-2119.

27. Caon T, Costa AC, de Oliveira MA, Micke GA, Simoes CM. Evaluation of the transdermal permeation of different paraben combinations through a pig ear skin model. Int J Pharm, 2010; 391:1-6.

28. Schmidt S, Barbour A, Sahre M, Rand KH, Derendorf H. PK/PD: new insights for antibacterial and antiviral applications. Curr Opin Pharmacol, 2008; 8:549-556.

29. De Clercq E. In search of a selective therapy of viral infections. Antiviral Res, 2010; 85:19-24.

30. Neuhoff S, Ungell AL, Zamora I, Artursson P. pH-dependent bidirectional transport of weakly basic drugs across Caco-2 monolayers: implications for drug-drug interactions. Pharm Res, 2003; 20:1141-1148.

31. Li C, Nair L, Liu T, Li F, Pichardo J, Agrawal S, Chase R, Tong X, Uss AS, Bogen S, Njoroge FG, Morrison RA, Cheng KC. Correlation between PAMPA permeability and cellular activities of hepatitis C virus protease inhibitors. Biochem Pharmacol, 2008; 75:1186-1197.

32. Bergstrom CA, Strafford M, Lazorova L, Avdeef A, Luthman K, Artursson P. Absorption classification of oral drugs based on molecular surface properties. J Med Chem, 2003; 46:558-570.

33. Williams, A., Transdermal and Topical Drug Delivery. Pharmaceutical Press, London, UK, 2003.

34. Jewell C, Prusakiewicz JJ, Ackermann C, Payne NA, Fate G, Williams FM. The distribution of esterases in the skin of the minipig. Toxicol Lett, 2007; 173:118-123.

DISCUSSÃO GERAL

O presente trabalho teve dois objetivos principais. O primeiro objetivo foi a implementação e validação do modelo de permeabilidade *in vitro* com células Caco-2 no Laboratório de Virologia Aplicada da UFSC. Esse modelo celular é um dos mais representativos no que se refere à predição da absorção de fármacos pela via oral, e nosso grupo de pesquisa é um dos pioneiros na implementação desse modelo no Brasil. A segunda etapa do projeto foi realizada após a conclusão do primeiro objetivo, uma vez que o plano de trabalho obedeceu a um planejamento linear. O segundo objetivo consistiu na aplicação desse modelo, já validado, na avaliação dos perfis de permeabilidade *in vitro* de duas amostras de interesse: um complexo do fármaco talidomida com ciclodextrina, desenvolvido e caracterizado durante este trabalho; e o galato de pentila, um composto com promissora atividade anti-herpética.

Portanto, inicialmente células Caco-2 foram adquiridas junto ao banco de células norte-americano *ATCC* (*American Type Culture Collection*), a cultura foi estabelecida e incorporada ao banco de células do nosso laboratório. A ausência de contaminantes (bactérias, fungos, leveduras e micoplasma) foi assegurada periodicamente, durante todo o período de realização deste trabalho, a fim de garantir a qualidade necessária.

Através de uma busca na literatura, e seguindo-se as recomendações de Hubatsch e colaboradores (2007), as condições de cultivo celular foram otimizadas e as células semeadas em insertos de policarbonato (Millicell®) para a realização dos experimentos de transporte. As técnicas de cultivo celular foram muito bem definidas e rigidamente controladas, a fim de garantir a reprodutibilidade dos dados de permeabilidade obtidos nos experimentos.

A fim de mimetizar as condições *in vivo*, foram considerados requisitos de conformidade a formação de uma monocamada de células viáveis, com valores de TEER adequados, na qual a formação de uma rede de junções oclusivas estável precisa ser confirmada (ARTURSSON et al., 2001; HUBATSCH et al., 2007). Para tal, a morfologia e a adequação da monocamada de células formada nos insertos, sob as condições padronizadas de cultivo, foram avaliadas através de diferentes técnicas.

Os valores médios obtidos de TEER, ao longo de todo o tempo de cultivo, estão apresentados na Figura 6.
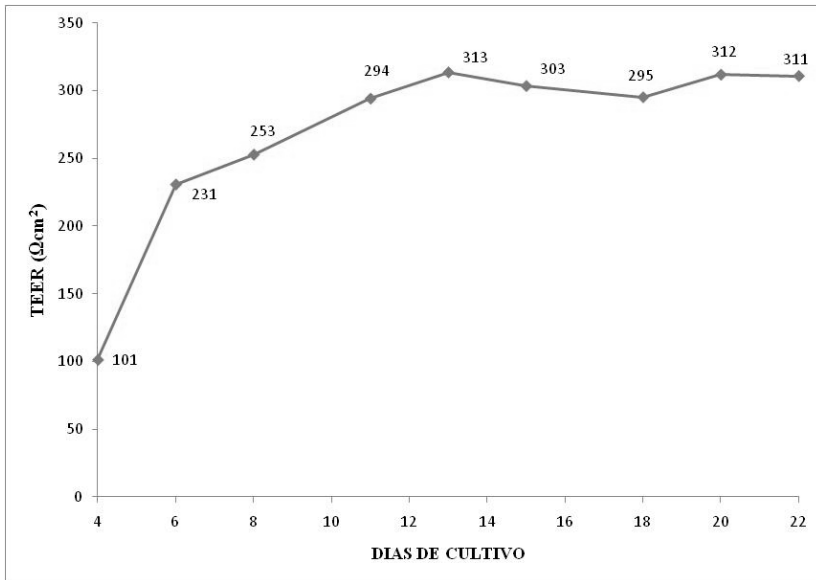
Figura 6. Avaliação da Resistência Elétrica Transepitelial (TEER) de células Caco-2 cultivadas sobre insertos de policarbonato ao longo de 22 dias.

Valores detectáveis de TEER foram obtidos a partir do quarto dia de cultivo (em torno de 100 Ωcm^2). Os valores continuaram a aumentar, indicando a formação de uma monocamada cada vez mais confluente e justaposta, atingindo um valor estável a partir do décimo segundo dia de cultivo. Os valores médios obtidos durante a realização deste trabalho foram de 297 $\pm$ 21 Ωcm^2. A fim de se definir valores-limite para a realização dos experimentos, o valor de 200 Ωcm^2 foi estabelecido como o mínimo adequado, portanto, apenas insertos que apresentaram este valor (antes e após os experimentos de transporte) foram utilizados ou considerados durante o cálculo dos coeficientes de permeabilidade.

Adicionalmente, também foi realizada a otimização da densidade celular a ser semeada nos insertos. Tendo em vista as variações interlaboratoriais amplamente discutidas na literatura relacionada (para uma discussão mais ampla sobre a variabilidade do modelo Caco-2 veja VOLPE, 2008), e a fim de evitar um número excessivo de células que poderia levar a formação de multicamadas celulares, foram testadas três densidades celulares ($0,8 \times 10^5$; $1,7 \times 10^5$ e $3,0 \times 10^5$ células/cm^2). Hubatsch e colaboradores (2007) recomendam um valor de aproximadamente $2,5 \times 10^5$ células/cm^2. Os melhores resultados foram

obtidos com a densidade de 1.7×10^5 células/cm^2, refletidos por valores de TEER estáveis. Além disso, imagens obtidas por microscopia de fluorescência, utilizando anticorpos primários para a proteína ZO-1 das junções oclusivas e iodeto de propídeo como coloração nuclear, possibilitaram a visualização direta da monocamada (Figura 7) e da rede de junções oclusivas formada, assegurando assim a obtenção da morfologia adequada.
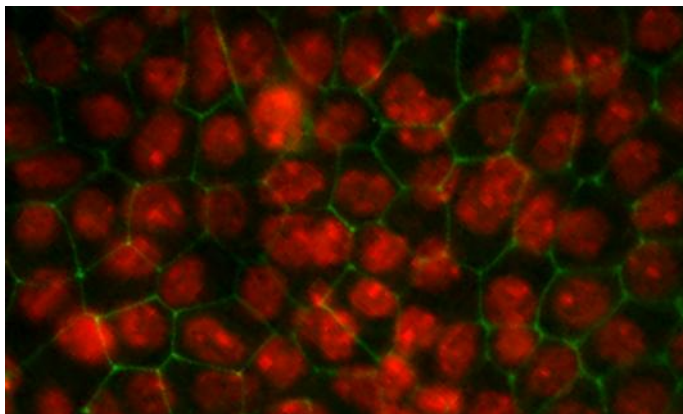
Figura 7. Microscopia de Fluorescência de uma monocamada de células Caco-2 sobre insertos de policarbonato cultivados sob as condições estabelecidas neste trabalho. Em verde, a proteína das junções oclusivas ZO-1 localizada preferencialmente nas bordas celulares, enquanto os núcleos são representados em vermelho. Aumento 40X.

A justaposição das células da monocamada também foi avaliada através da determinação da permeabilidade do *Lucifer yellow*. Esse composto fluorescente possui valores de coeficiente de permeabilidade muito baixos, uma vez que permeia somente através da via paracelular (PRESS; DI GRANDI, 2008), podendo ser utilizado como um marcador da integridade da monocamada celular. Os resultados obtidos em experimentos de transporte com esse composto (100 µg/mL – 60 min) em monocamadas diferenciadas (21-25 dias) demonstraram a adequação das condições de cultivo, uma vez que os valores de P_{app} obtidos foram $\leq 0.2 \times 10^{-6}$ cm/s, indicando um perfil de baixa permeabilidade. Dessa forma, a avaliação do transporte do *Lucifer Yellow* após todos os experimentos de permeabilidade foi utilizada, em conjunto com a avaliação da TEER, como forma de controle de qualidade da

monocamada celular existente nos insertos. Assim sendo, pôde-se garantir que as amostras não eram citotóxicas ou haviam perturbado a justaposição das células, e que o próprio pesquisador não tinha alterado tal morfologia durante a amostragem, comprometendo assim a fidedignidade dos resultados. Cabe ressaltar que a principal vantagem do emprego do *Lucifer yellow* é a não utilização de compostos radiomarcados, como o [14C]-manitol, que é também amplamente utilizado em ensaios com Caco-2.

Após a confirmação de que as condições de cultivo estabelecidas propiciavam a formação de uma monocamada celular com características capazes de mimetizar a mucosa intestinal, foi definido um grupo de fármacos com valores de permeabilidade e absorção orais já disponíveis na literatura, pertencentes às diferentes classes do Sistema de Classificação Biofarmacêutica, e com uma ampla diversidade estrutural (Figura 8) e físico-química (ver *Table 1* da publicação no apêndice 1). O objetivo foi estabelecer uma correlação entre os coeficientes de permeabilidade e as frações absorvidas em humanos (FA%), como forma de demonstrar a aplicabilidade do modelo na predição da absorção oral (US FDA, 2000).
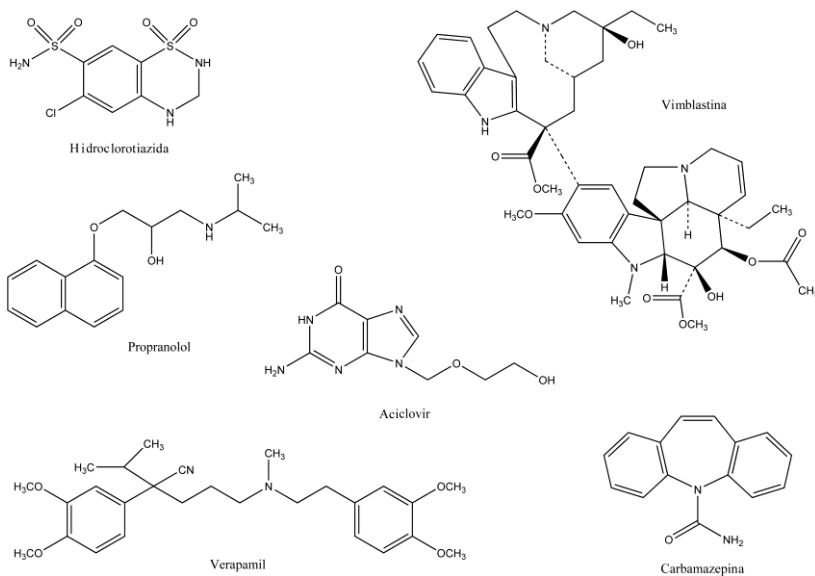
Figura 8. Fármacos utilizados durante a padronização do modelo de permeabilidade intestinal *in vitro* com células Caco-2.

Para tal, foram selecionados quatro fármacos com perfis de permeabilidade passiva (aciclovir, carbamazepina, hidroclorotiazida e propranolol), bem como um substrato (vimblastina) e um inibidor (verapamil) da P-gp, a fim de demonstrar a funcionalidade do transporte ativo mediado por transportadores de membrana. Um método por CLAE-UV foi desenvolvido e validado conforme recomendações do ICH (2005) para a determinação concomitante de todos os fármacos empregados nessa etapa do trabalho.

É importante ressaltar a importância desse método analítico, uma vez que é possível a análise quantitativa de uma mistura complexa de fármacos, com um bom nível de resolução entre eles, possibilitando dessa forma a realização de experimentos do tipo "coquetel", onde vários fármacos são adicionados concomitantemente aos insertos. Experimentos dessa natureza são importantes na redução dos gastos laboratoriais, uma vez que o ensaio com células Caco-2 ainda é considerado relativamente oneroso, sendo especialmente atrativos no ambiente industrial.

Este é o primeiro relato da literatura que apresentou a determinação quantitativa direta em tampão aquoso por CLAE-UV da vimblastina, concomitantemente ao verapamil, propranolol, carbamazepina, aciclovir e hidroclorotiazida. Este método pode ser aplicada para o doseamento de fármacos marcadores durante a avaliação rotineira do desempenho do modelo com células Caco-2 por outros laboratórios. Adicionalmente, sua aplicabilidade pode ser estendida para demais técnicas que utilizem esses fármacos em tampões aquosos, tal como o ensaio não celular PAMPA, que foi recentemente implementado em nosso laboratório (SCHNEIDER, 2011).

De posse do método analítico desenvolvido e validado, foram realizados experimentos de transporte bi-direcionais, a fim de determinar se o modelo era capaz de diferenciar compostos com diferentes perfis de permeabilidade. Os experimentos foram realizados sob condição de gradiente de pH (apical = 6,0 / basolateral = 7,4), buscando mimetizar as condições originais do trato gastrointestinal, mas sempre considerando o potencial de erro associado às diferentes concentrações das frações ionizadas dos fármacos (vide discussão da permeabilidade passiva do propranolol na publicação do capítulo 1)(NEUHOFF et al., 2003).

Também foi dada especial atenção no sentido de se manter as condições *sink* sempre que possível (menos de 10% da concentração inicial permeada a cada intervalo de amostragem, para evitar o refluxo

para o compartimento doador, e conseqüente inexatidão dos resultados), conforme recomendações (HUBATSCH et al., 2007).

Os resultados nos experimentos de transporte permitiram afirmar que o modelo foi devidamente validado, uma vez que pôde-se estabelecer uma correlação entre os valores de P_{app} obtidos e os valores de absorção em humanos existentes na literatura (US FDA, 2000). Os fármacos testados que são bem absorvidos em humanos (propranolol e carbamazepina) apresentaram valores elevados de P_{app}, enquanto que os fármacos testados reconhecidos por sua moderada e baixa absorção em humanos (hidroclorotiazida e aciclovir, respectivamente) apresentaram valores baixos de P_{app}.

Ademais, o fármaco marcador de transporte ativo, no caso o substrato da P-gp vimblastina, apresentou uma taxa de efluxo (razão do P_{app} BL/AP e P_{app} AP/BL) de 17,75, que é um valor representativo de fármacos cuja permeabilidade é influenciada por bombas de efluxo. Já na presença de um inibidor da P-gp, o verapamil, essa taxa de efluxo caiu drasticamente, atingindo o valor de 4,28, corroborando a adequação do modelo no quesito expressão de transportadores (US FDA, 2006).

Dessa forma, através do monitoramento das características morfológicas das células e da avaliação da permeabilidade de fármacos marcadores selecionados, foi possível concluir que o modelo de permeabilidade *in vitro* com células Caco-2 foi implementado e validado com sucesso em nosso laboratório. Uma vez mantidas as características essenciais do ensaio, este modelo poderá ser utilizado para a avaliação da permeabilidade intestinal *in vitro* de fármacos e compostos com diferentes atividades farmacológicas, além de poder ser utilizado na avaliação da influência de diferentes adjuvantes usados na preparação de formas farmacêuticas diversas.

De acordo com a necessidade, poderão ser estabelecidas adaptações no ensaio padrão, tais como a utilização de fluidos simulados, conhecidos como meios biorrelevantes (por exemplo, os fluidos intestinais simulados com alimentação – *FaSSIF* – ou jejum – *FeSSIF*) buscando mimetizar condições específicas. A simples utilização de muco simulado no tampão de transporte ou soluções protéicas no compartimento receptor, visando um melhor balanço de massas quando compostos altamente lipofílicos, que aderem às superfícies plásticas, também podem ser utilizados (YAMASHITA et al., 2000; ZAKI et al., 2010).

Os resultados obtidos nessa primeira etapa já foram publicados (KRATZ et al, 2011) e constituem o primeiro relato do modelo de permeabilidade *in vitro* com células Caco-2 no Laboratório de Virologia

Aplicada da UFSC. O próximo passo é a formação de um banco de dados *in house* com valores de permeabilidade *in vitro*, a fim de amparar estudos que objetivem a avaliação da solubilidade, dissolução e permeabilidade intestinal de fármacos sob a luz do Sistema de Classificação Biofarmacêutico (AMIDON et al., 1995).

Seguindo as premissas de aplicação do modelo recém-validado, a segunda parte do trabalho foi iniciada visando avaliar a influência da complexação da talidomida com ciclodextrinas sobre sua solubilidade, dissolução e perfil de permeabilidade intestinal *in vitro*.

Primeiramente, uma metodologia de CLAE para o doseamento de talidomida foi desenvolvida e validada. Uma mistura de acetonitrila, água e ácido fosfórico (24:76:0.1, v/v/v) foi empregada como fase móvel, e sob condições isocráticas, o analito de interesse foi eluído em 4.9 min, enquanto que o padrão interno (fenacetina) foi eluído em 6.8 min. As amostras submetidas ao doseamento foram previamente acidificadas para evitar hidrólise espontânea do fármaco, como descrito por Zhou e colaboradores (2003), secas sob vácuo, e reconstituídas em fase móvel no momento da análise para garantir a estabilidade.

Estudos de solubilidade de fase foram realizados a fim de se avaliar o potencial aumento da solubilidade aquosa aparente da talidomida mediante sua complexação com ciclodextrinas. Os resultados mostraram que, dentre as ciclodextrinas avaliadas, a hidroxipropil-β-ciclodextrina (HPβCD) apresentou maior capacidade de solubilização, e, por já possuir perfil de baixa toxicidade descrito (GOULD; SCOTT, 2005) foi escolhida para a preparação dos complexos no estado sólido. De certa forma, esse era um resultado esperado, uma vez que a HPβCD é uma ciclodextrina modificada, com solubilidade aquosa intrínseca superior às ciclodextrinas naturais testadas (α-, β- e γ-ciclodextrinas), e devido a esta característica, de uma forma geral, apresenta capacidade de complexação superior às demais (LOFTSSON, DUCHENE, 2007).

Para a obtenção dos complexos, inicialmente foi empregada a técnica de liofilização. Entretanto, os produtos obtidos possuíam teor de fármaco inferior a 1%. Dessa forma, seria praticamente impossível caracterizar os complexos no estado sólido, e a sua aplicabilidade como matéria-prima farmacêutica seria praticamente nula. Portanto, a técnica do kneading foi utilizada, já que com ela geralmente se produz produtos com teores superiores de fármaco. Esta técnica consiste na trituração do fármaco com a ciclodextrina, na presença de uma pequena quantidade de líquido, formando uma pasta (LOFTSSON et al., 2005; LOFTSSON, DUCHENE, 2007).

Os complexos de talidomida:HPβCD obtidos na proporção molar 1:1 foram então caracterizados através de técnicas de microscopia eletrônica de varredura, difração de raios X e calorimetria exploratória diferencial. Os resultados obtidos para o complexo, quando comparados aos dados obtidos com a talidomida isolada ou com a mistura física simples dos componentes, revelaram uma diminuição da cristalinidade do fármaco, resultante da formação de complexos estáveis em meio sólido. Foram feitas diversas análises por ressonância magnética nuclear de hidrogênios (Figura 9), considerada a técnica padrão para determinação da complexação, entretanto os resultados não foram conclusivos.
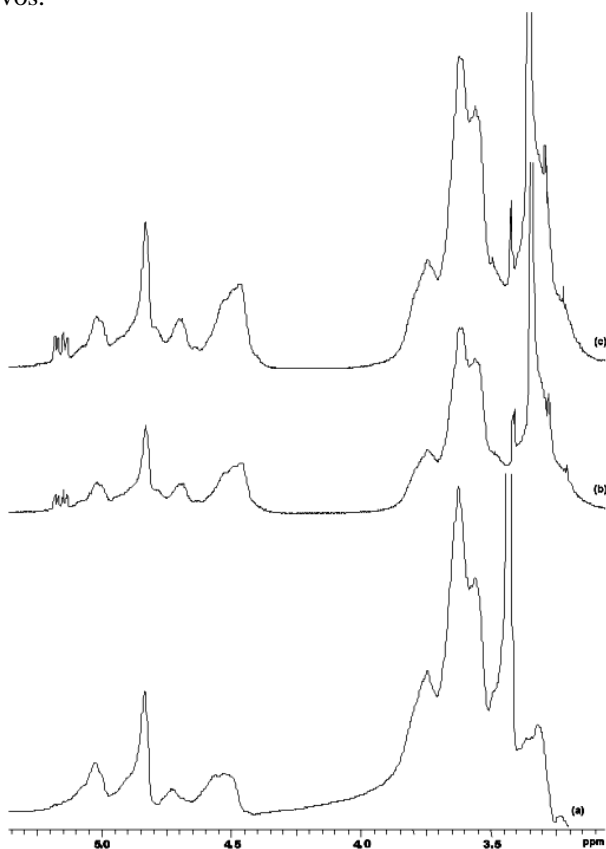
Figura 9. Exemplos de espectros de ressonância magnética nuclear de hidrogênios obtidos durante a caracterização dos complexos talidomida:HPβCD. (a) HPβCD, (b) complexo, (c) mistura física.

Após a caracterização dos complexos, foi realizada a avaliação da influência da complexação sobre a dissolução e permeabilidade intestinal, dois fatores intimamente ligados à biodisponibilidade de fármacos. Em relação aos perfis de dissolução, através da complexação, foi possível obter 77,3% do fármaco dissolvido após 60 min, enquanto que para a talidomida isolada, apenas 25,5% estavam dissolvidos, no mesmo período, ou seja, três vezes mais talidomida estava dissolvida quando complexada. Esse efeito pôde ser atribuído à redução da cristalinidade do fármaco, conforme detectado por difração de raios X e calorimetria exploratória diferencial (ver publicação do capítulo 2).

Já em relação à avaliação da permeabilidade em células Caco-2, a talidomida apresentou um perfil de alta permeabilidade passiva (P_{app} = 5,33 x 10^{-5} cm/s). Os dados obtidos nesse estudo corroboraram os achados de estudos prévios (ZHOU et al., 2005; ZIMMERMANN et al., 2006). Entretanto, a complexação da talidomida com HPβCD não acarretou melhora desse perfil, uma vez que os valores de P_{app} obtidos (4,84 x 10^{-5} cm/s) não foram estatisticamente diferentes entre si (ANOVA, $p > 0,05$).

Em suma, complexos de talidomida:HPβCD foram obtidos, caracterizados no estado sólido por diferentes técnicas, que indicam a complexação do fármaco (comprovar a inclusão não foi possível) e a redução da sua cristalinidade. Essas alterações culminaram em um leve aumento da solubilidade aparente do fármaco, bem como propiciaram um perfil de dissolução superior, quando comparado ao da talidomida isolada. No entanto, nenhuma alteração na permeabilidade *in vitro* foi detectada, pois não houve diferenças estatisticamente significativas entre os coeficientes de permeabilidade obtidos. Esses resultados sugerem que a complexação com ciclodextrinas poderia aumentar a biodisponibilidade oral da talidomida, através do aumento da sua solubilidade nos fluídos gastrointestinais, bem como facilitando a sua dissolução a partir de uma forma farmacêutica sólida, entretanto essa hipótese ainda precisa ser confirmada com estudos *in vivo*.

Estudos que busquem a melhora das propriedades biofarmacêuticas da talidomida são importantes devido à aplicabilidade terapêutica atual desse fármaco. Por possuir baixa solubilidade e alta permeabilidade esse fármaco se encaixa na classe II do Sistema de Classificação Biofarmacêutica. Formas farmacêuticas que promovam uma melhora da solubilidade e dissolução desse fármaco, através de uma correlação *in vitro – in vivo* podem, inclusive, serem trabalhadas buscando uma extensão dos limites de bioisenção, como já descrito para outros fármacos dessa classe (KOVACEVIC et al., 2008; YANG, 2010).

Complementando a segunda etapa deste trabalho, foram avaliados os perfis de permeabilidade intestinal e cutânea do galato de pentila. Por se tratar de um composto com atividade anti-herpética, com possível utilização em um quadro infeccioso onde a eficácia terapêutica pode ser atingida tanto pelo tratamento oral quanto pela aplicação tópica do fármaco sobre a lesão, os dois perfis de permeabilidade foram avaliados, objetivando principalmente prover bases para um possível estudo da atividade antiviral *in vivo*.

Além disso, esse estudo objetivou correlacionar os resultados obtidos com diferentes metodologias de predição da absorção disponíveis no laboratório. Como dito anteriormente, a validação e a implementação do ensaio PAMPA em nosso laboratório foi objeto de uma dissertação de Mestrado (SCHNEIDER, 2011). Essa é uma técnica rápida e relativamente barata, baseada na formação de uma bicamada fosfolipídica sobre uma membrana permeável, gerando dessa forma dois compartimentos, o doador, onde se adiciona o fármaco dissolvido em um tampão aquoso, e o receptor, onde se quantifica a fração do fármaco que foi capaz de permear a membrana. Esse método é muito utilizado para predizer a permeabilidade transcelular passiva, uma vez que apenas mimetiza a natureza físico-química da membrana celular (AVDEEF, 2001).

Diferentes composições da membrana lipídica podem ser empregadas nessa técnica, e dessa forma é possível mimetizar variadas condições fisiológicas. Nesse sentido, duas modalidades foram utilizadas nesse estudo, a saber, o PAMPA Intestinal, onde a bicamada lipídica é formada por uma solução de 20% de lecitina de soja dissolvida em dodecano, e cujos resultados foram comparados aos obtidos no modelo de células Caco-2; e o PAMPA Pele, onde a bicamada lipídica é composta de óleo de silicone e miristato de isopropila, cujos resultados foram comparados aos obtidos com o modelo clássico de permeação em pele de orelha suína, padronizado previamente no laboratório (CAON et al., 2010). Estudos têm mostrado uma importante correlação entre os dados de permeabilidade obtidos nos modelos PAMPA e os valores de absorção oral e cutânea, respectivamente (AVDEEF et al., 2007; OTTAVIANI et al., 2006, 2007).

Inicialmente, duas metodologias analíticas quantitativas foram desenvolvidas e validadas. As amostras testadas no modelo PAMPA (ambas as modalidades) foram analisadas por espectrofotometria no ultravioleta a 270 nm, possibilitando dessa forma a quantificação de um grande número de amostras simultaneamente, compatibilizando com a natureza rápida e simplista desse ensaio. Já as amostras testadas nos

modelos Caco-2 e com pele de orelha suína foram analisadas com um método simples e rápido por CLAE-UV (isocrático – tempo de retenção ~ 3,8 min) baseado em uma metodologia publicada anteriormente (TAMMELA et al., 2004).

Em relação à predição da absorção oral, tanto no ensaio PAMPA Intestinal quanto no modelo de células Caco-2, o galato de pentila apresentou valores altos de permeabilidade, indicando que esta propriedade não limitaria a absorção *in vivo* desse composto. Adicionalmente, os dados obtidos em ambos os ensaios mostraram boa correlação, que é indicativa de um perfil de permeabilidade passiva, que foi confirmado nos estudos bi-direcionais em Caco-2 (razão BL/AP – AP/BL de 0.73).

Mesmo que tenha sido possível a detecção do composto no compartimento receptor em quantidades expressivas, indicando um perfil de transporte favorável, em ambos os ensaios grande parte do composto adicionado ficou retido (valores baixos de balanço de massas). Essa constatação corrobora os dados da literatura obtidos com compostos estruturalmente relacionados. Tammela e colaboradores (2004) já haviam demonstrado que o tamanho da cadeia lateral dos galatos interfere na sua afinidade por membranas lipídicas, uma vez que os galatos de metila e propila foram capazes de permear células Caco-2, ainda que de forma lenta, enquanto que o galato de octila acumulava extensivamente no interior das células. Os resultados obtidos em nosso estudo mostram que o galato de pentila tem um comportamento ambíguo, apresentando tanto transporte quanto acumulação intracelular (ou na bicamada lipídica no caso do PAMPA), compatível com o seu tamanho de cadeia intermediário em relação aos demais galatos estudados.

Já em relação à predição da absorção cutânea, no modelo clássico *ex vivo* o galato de pentila ficou retido nas camadas da pele, particularmente na epiderme, sendo que essa camada atua como um reservatório, impedindo que o composto permeie para as camadas mais profundas e entre na circulação sistêmica, possivelmente pelo efeito relacionado com a lipofilicidade da molécula e a presença do grupamento galoil. Estudos prévios com o galato de epigalocatequina já haviam demonstrado que compostos polifenólicos, em especial aqueles que possuam o grupamento galoil na molécula, apresentam boas características de penetração e retenção cutânea, embora não atinjam concentrações sistêmicas apreciáveis (DVORAKOVA et al., 1999).

Entretanto, não foi possível estabelecer uma correlação entre os dados *ex vivo* e os resultados obtidos *in vitro* no ensaio PAMPA Pele,

que indicou um bom perfil de permeação. Essa discrepância está muito provavelmente relacionada com a configuração da membrana lipídica, que mimetiza apenas as camadas mais superiores da pele.

Em suma, o galato de pentila apresenta perfis de permeabilidade intestinal e cutânea favoráveis para um composto com ação anti-herpética, ou seja, pela via oral sua biodisponibilidade não seria limitada pela permeabilidade, e pela via tópica ficaria restrito às camadas da pele no local de aplicação. Os dados obtidos nesse estudo fornecem informações valiosas para o desenvolvimento de formas farmacêuticas contendo esse composto e sua utilização em experimentos de avaliação da atividade antiviral *in vivo*. Sua veiculação em nanoemulsões lipídicas já está em andamento (Tese de Doutorado de Regina G. Kelmann, Programa de Pós-Graduação em Ciências Farmacêuticas, UFRGS), com previsão da realização dos estudos *in vivo* para 2012.

CONSIDERAÇÕES FINAIS

- O cultivo de células Caco-2 foi implementado e padronizado no Laboratório de Virologia Aplicada da UFSC e a respectiva linhagem celular foi integrada ao banco de células. As características morfológicas da monocamada celular cultivada sobre insertos de policarbonato foram avaliadas e os resultados demonstraram que as células permaneceram viáveis após 21-25 dias de cultivo, constituindo uma monocamada celular diferenciada, capaz de mimetizar as condições intestinais *in vivo*.

- Foi desenvolvido e validado uma método por CLAE-UV para o doseamento de seis marcadores de permeabilidade (propranolol, carbamazepina, aciclovir, hidroclorotiazida, vinblastina e verapamil) utilizados durante a avaliação da adequação do modelo de permeabilidade intestinal *in vitro*.

- O modelo de permeabilidade intestinal *in vitro* com células Caco-2 foi validado através de experimentos de transporte bi-direcionais. Para os marcadores de permeabilidade passiva, os resultados obtidos demonstraram uma correlação entre perfis de alta e baixa permeabilidade e a fração absorvida desses fármacos em humanos. No transporte ativo, foi demonstrada a funcionalidade da Glicoproteína-P através do efluxo da vimblastina (substrato) e também da inibição desse efeito em presença do inibidor verapamil.

- Foram obtidos complexos de inclusão talidomida:HPβCD pela técnica de kneading. Esses complexos foram caracterizados no estado sólido e os resultados obtidos indicaram a complexação da talidomida.

- A complexação da talidomida com HPβCD aumentou a solubilidade da talidomida, bem como da sua taxa de dissolução, entretanto a complexação não promoveu uma melhora da permeabilidade intestinal *in vitro*.

- Os resultados obtidos no estudo da complexação da talidomida indicaram que a utilização de ciclodextrinas poderia aumentar a biodisponibilidade oral desse fármaco, entretanto estudos *in vivo* são necessários para confirmar essa hipótese.

- Foram estabelecidos os perfis *in vitro* de permeabilidade intestinal e cutânea do composto anti-herpético galato de pentila visando à realização de experimentos *in vivo* e a preparação de formas farmacêuticas.

- Os resultados obtidos tanto no PAMPA quanto no ensaio com células Caco-2 demonstraram um perfil de alta permeabilidade passiva para o galato de pentila, sendo possível predizer que no trato gastrointestinal sua absorção não seria limitada pela permeabilidade.

- Em relação à permeabilidade cutânea do galato de pentila, foi evidenciado que o composto acumula nas camadas da pele, particularmente na epiderme, o que restringe a sua absorção por essa via, sendo essa uma característica desejável para uma possível ação antiviral local *in vivo*.

Finalmente, por meio dos procedimentos realizados e dos resultados obtidos durante a implementação e aplicação do modelo de permeabilidade *in vitro* com células Caco-2 no Laboratório de Virologia Aplicada da UFSC, foi possível assegurar a aplicabilidade e a reprodutibilidade desse ensaio. Estudos futuros visando à estruturação de um banco de dados de permeabilidade intestinal *in vitro* de compostos e fármacos permitirão a realização de estudos colaborativos, sobretudo com o enfoque do Sistema de Classificação Biofarmacêutica, visando ao crescimento da pesquisa dessa área no Brasil.

REFERÊNCIAS

ABE, I.; SEKI, T.; NOGUCHI, H. Potent and selective inhibition of squalene epoxidase by synthetic galloyl esters. **Biochemical and Biophysical Research Communications**, v. 270, p. 137-140, 2000.

ABRAHAM, J. Partial progress? The development of American and British drug regulation. In: ABRAHAM, J. (Ed.) **Science, Politics, and the Pharmaceutical Industry**. New York: St, Martin's, 1995. p. 36-87.

ADIBI, S. The oligopeptide transporter (PEPT-1) in human intestine: biology and function. **Gastroenterology**, v. 113, p. 332–340, 1997.

ALLEN, F.H.; TROTTER, J. Crystal and Molecular Structure of Thalidomide. **Chemical Communications**, v. 12, p. 778-779, 1970.

ALVAREZ, C.; CALERO, J.; MENENDEZ, J.C.; TORRADO, S.; TORRADO, J.J. Effects of hydroxypropyl-beta-cyclodextrin on the chemical stability and the aqueous solubility of thalidomide enantiomers. **Pharmazie**, v. 63, p. 511-513, 2008.

AMIDON, G.L.; LENNERNÄS, H.; SHAH, V.P.; CRISON, J.R. A theoretical basis for a biopharmaceutical drug classification: the correlation of *in vitro* drug product dissolution and *in vivo* bioavailability. **Pharmaceutical Research**, v. 12, p. 413-420, 1995.

ANSEL, H.C.; POPOVICH, N.G.; ALLEN, L.V. **Farmacotécnica**: formas farmacêuticas e sistemas de liberação de fármacos. São Paulo: Premier, 2000.

ARAÚJO, F.A.; KELMANN, R.A.; ARAÚJO, B.V.; FINATTO, R.B.; TEIXEIRA, H.F.; KOESTER, L.S. Development and characterization of parenteral nanoemulsions containing thalidomide. **European Journal of Pharmaceutical Sciences,** v. 42, p. 238-245, 2011.

ARTURSSON, P. Epithelial transport of drugs in cell culture. I: A model for studying the passive diffusion of drugs over intestinal absorptive (Caco-2) cells. **Journal of Pharmaceutical Sciences,** v. 79, p. 476-482, 1990.

ARTURSSON, P.; PALM, K.; LUTHMAN, K. Caco-2 monolayers in experimental and theoretical predictions of drug transport. **Advanced Drug Delivery Reviews**, v. 46, p. 27-43, 2001.

AUGUSTIJNS, P.F.;BRADSHAW, T.P.; GAN, L.-S.L.; HENDREN, R.W.; THAKKER, D.R. Evidence for a polarized efflux system in Caco-2 cells capable of modulating cyclosporin A transport. **Biochemical and Biophysical Research Communications,** v. 197, p. 360-365, 1993.

AVDEEF, A. Physicochemical profiling (solubility, permeability and charge state). **Current Topics in Medicinal Chemistry**, v. 1, p. 277-351, 2001.

AVDEEF, A. The rise of PAMPA. **Expert Opinion on Drug Metabolism and Toxicology**, v. 1, p. 325-342, 2005.

AVDEEF, A.; BENDELS, S.; DI, L.; FALLER, B.; KANSY, M.; SUGANO, K.; YAMAUCHI, Y. PAMPA – Critical factors for better predictions of absorption. **Journal of Pharmaceutical Sciences**, v. 96, p. 2893-2909, 2007.

AZMI, A.S.; BHAT, S.H.; HANIF, S.; HADI, S.M. Plant polyphenols mobilize endogenous copper in human peripheral lymphocytes leading to oxidative DNA breakage: a putative mechanism for anticancer properties. **FEBS Letters**, v. 580, p. 533-538, 2006.

BAER-DUBOWSKA, W.; GNOJKOWSKI, J.; FENRYCH, W. Effect of tannic acid on benzo[a]pyrene-DNA adduct formation in mouse epidermis: comparison with synthetic gallic acid esters. **Nutrition and Cancer**, v. 29, p. 42-47, 1997.

BALIMANE, P.V., HAN, Y.H., CHONG, S. Current industrial practices of assessing permeability and P-glycoprotein interaction. **AAPS Journal**, v. 8, p. E1-13, 2006.

BANSAL, T.; SINGH, M.; MISHRA, G.; TALEGAONKAR, S.; KHAR, R.K.; JAGGI, M.; MUKHERJEE, R. Concurrent determination of topotecan and model permeability markers (atenolol, antipyrine, propranolol and furosemide) by reversed phase liquid chromatography:

Utility in caco-2 intestinal absorption. **Journal of Chromatography B**, v. 859, p. 261-266, 2007.

BARRY, B. Transdermal drug delivery. In: AULTON, M.E. (Ed.) **Pharmaceutics**: the science of dosage form design. New York: Churchill Livingstone, 2002.

BASTIANETTO, S.; YAO, Z.X.; PAPADOPOULOS, V.; QUIRION, R. Neuroprotective effects of green and black teas and their catechin gallate esters against beta-amyloid-induced toxicity. **European Journal of Neuroscience**, v. 23, p. 55-64, 2006.

BATCHELDER, R.J.; CALDER, R.J.; THOMAS, C.P.; HEARD, C.M. *In vitro* transdermal delivery of the major catechins and caffeine from extract of Camellia sinensis. **International Journal of Pharmaceutics**, v. 283, p. 45-51, 2004.

BELO, S.E.; GASPAR, L.R.; MAIA CAMPOS, P.M.B.G.; MARTY, J.P. Skin Penetration of Epigallocatechin-3-Gallate and Quercetin from Green Tea and Ginkgo biloba Extracts Vehiculated in Cosmetic Formulations. **Skin Pharmacology and Physiology**, v. 22, p. 299-304, 2009.

BLEICHER, K.H.; BOHM, H.J.; MULLER, K.; ALANINE, A.I. Hit and lead generation: beyond high-throughput screening. **Nature Reviews Drug Discovery**, v. 2, p. 369-378, 2003.

BOHETS, H.; ANNAERT, P.; MANNENS, G.; VAN BEIJSTERVELDT, L.; ANCIAUS, K.; VERBOVEN, P.; MEULDERMANS, W.; LAVRIJSEN, K. Strategies for absorption screening in drug discovery and development. **Current Topics in Medicinal Chemistry**, v. 1, p. 367-383, 2001.

BOUWSTRA, J.A.; HONEYWELL-NGUYEM, P.L.; GOORIS, G.S.; PONEC, M. Structure of the skin barrier and its modulation by vesicular formulations. **Progress in Lipid Research**, v. 42, p. 1-36, 2003.

BRASIL. Ministério da Saúde, Agência Nacional de Vigilância Sanitária, Portaria 25, 2002. Disponível em < http://e-legis.bvs.br/leisref/public/showAct.php?mode=print_version&id=6205> . Acesso em 20.05.2011.

BRASIL. Ministério da Saúde, Secretaria Nacional de Vigilância Sanitária, Portaria 354, 1997. Disponível em < http://e-legis.bvs.br/leisref/public/showAct.php?mode=print_version&id=7173> . Acesso em 20.05.2011.

BRASIL. Ministério da Saúde, Secretaria Nacional de Vigilância Sanitária, Portaria 344, 1998. Disponível em < http://e-legis.anvisa.gov.br/leisref/public/showAct.php?id=17235&word=>. Acesso em 20.05.2011.

CAIRA, M.R.; BOTHA, S.A.; FLANANGAR, D.R. Polymorphism of N-(2,6-dioxo-3-piperidyl)pthalimide (Thalidomide): Structural characterization of a second monoclinic racemic modification. **Journal of Chemical Crystallography**, v. 24, p. 95-99, 1994.

CAON, T.; COSTA, A.C.O.; OLIVEIRA, M.A.L.; MICKE, G.A.; SIMÕES, C.M.O. Evaluation of the transdermal permeation of different paraben combinations through a pig ear skin model. **International Journal of Pharmaceutics**, v. 391, p. 1-6, 2010.

CARINI, J.P.; PAVEI, C.; SILVA, A.P.; MACHADO, G.; MEXIAS, A.S.; PEREIRA, V.P.; FIALHO, S.L.; MAYORGA, P. Solid state evaluation of some thalidomide raw materials. **International Journal of Pharmaceutics**, v. 372, p. 17-23, 2009.

CHANG, S.K.; WILLIAMS, P.L.; DAUTERMAN, W.C.; RIVIERE, J.E. Percutaneous absorption, dermatopharmacokinetics and related biotransformation studies of carbaryl, lindane, malathion, and parathion in isolated perfused porcine skin. **Toxicology**, v. 91, p. 269-280, 1994.

CHEN, X.; ANTMAN, M.D.; GESENBERG, C.; GUDMUNDSSON, O.S. Discovery pharmaceutics – challenges and opportunities. **The AAPS Journal**, v. 8, p. E402-E408, 2006.

CHEN, H.; GU, Y.; HU, Y. Comparison of two polymeric carrier formulations for controlled release of hydrophilic and hydrophobic drugs. **Journal of Materials Science: Materials in Medicine**, v. 19, p. 651-658, 2008.

CHEN, T.L.; VOLGESANG, G.B.; PETTY, B.G.; BRUNDRETT, R.B.; NOE, D.A.; SANTOS, G.W.; COLVIN, O.M. Plasma pharmacokinetics and urinary excretion of thalidomide after oral dosing in healthy male volunteers. **Drug Metabolism and Disposition**, v. 17, p. 402-405, 1989.

DEFERME, S.; ANNAERT, P.; AUGUSTIJNS, P. *In vitro* screening models to assess intestinal drug absorption and metabolism. In: EHRHARDT, C.; KIM, K.-J. (Eds.) **Drug Absorption Studies**. In situ, *In vitro* and *in silico* models**.** New York: Springer, 2008. Chapter 8. p. 182-215.

DI, L.; KERNS, E.H. Application of pharmaceutical profiling assays for optimization of drug-like properties. **Current Opinion in Drug Discovery and Development**, v. 8, p. 495-504, 2005.

DICKSON, M.; GAGNON, J.P. Key factors in the rising cost of new drug discovery and development. **Nature Reviews in Drug Discovery**, v. 3, p. 417-429, 2004.

DIMASI, J.A.; FELDMAN, L.; SECKLER, A.; WILSON, A. Trends in risks associated with new drug development: success rates for investigational drugs. **Clinical and Pharmacology and Therapeutics**, v. 87, p. 272-277, 2010.

DIMASI, J.A.; HANSEN, R.W.; GRABOWSKI, H.G. The price of innovation: new estimates of drug development costs. **Journal of Health Economics**, v. 22, p. 151-185, 2003.

DUBE, A.; NICOLAZZO, J.A.; LARSON, I. Chitosan nanoparticles enhance the intestinal absorption of the green tea catechins (+)-catechin and (−)-epigallocatechin gallate. **European Journal of Pharmaceutics**, v. 41, p. 219-225, 2010.

DVORAKOVA, K.; DORR, R.T.; VALCIC, S.; TIMMERMANN, B.; ALBERTS, D.S. Pharmacokinetics of the green tea derivative, EGCG, by the topical route of administration in mouse and human skin. **Cancer Chemotherapy and Pharmacology**, v. 43, p. 331-335, 1999.

EHRHARDT, C.; KIM, K.J. (Eds.) **Drug Absorption Studies**. In situ, *In vitro* and *in silico* models. New York: Springer, 2008.

ERIKSSON, T.; BJÖRKMAN, S.; HÖGLUND, P. Clinical pharmacology of thalidomide. **European Journal of Clinical Pharmacology**, v. 57, p. 365-376, 2001.

ERIKSSON, T.; BJÖRKMAN, S.; ROTH, B.; FYGE, A.; HÖGLUND, P. Enantiomers of thalidomide: blood distribution and the influence of serum albumin on chiral inversion and hydrolysis. **Chirality**, v. 10, p. 223-228, 1998.

ERIKSSON, T.; BJÖRKMAN, S.; ROTH, B.; HÖGLUND, P. Pharmacokinetic and initial pharmacodynamic characterization in man. **Journal of Pharmacy and Pharmacology,** v. 52, p. 807-817, 2000.

FALLER, B.; ERTL, P. Computational approaches to determine solubility. **Advanced Drug Delivery Reviews**, v. 59, p. 533-545, 2007.

FALLER, B. Artificial membrane assays to assess permeability. **Current Drug Metabolism**, v. 9, p. 886-892, 2008.

FANG, J.Y.; HUNG, C.F.; HWANG, T.L.; WONG, W.W. Transdermal Delivery of Tea Catechins by Electrically Assisted Methods. **Skin Pharmacology and Physiology**, v. 19, p. 28-37, 2006.

FIUZA, S.M.; GOMES, C.; TEIXEIRA, L.J.; GIRAO DA CRUZ, M.T.; CORDEIRO, M.N.; MILHAZES, N.; BORGES, F.; MARQUES, M.P. Phenolic acid derivatives with potential anticancer properties--a structure-activity relationship study. Part 1: methyl, propyl and octyl esters of caffeic and gallic acids. **Bioorganic and Medicinal Chemistry**, v. 12, p. 3581-3589, 2004.

FOGH, J.; FOGH, J.M.; ORFEO, T. One hundred and twenty seven cultured human tumor cell lines producing tumors in nude mice. **Journal of the National Cancer Institute,** v. 59, p. 221-226, 1977.

FRANKS, M.E.; MACPHERSON, G.R.; FIGG, W.D. Thalidomide. **The Lancet**, v. 363, p. 1802-1811, 2004.

FRANTZ, S.W. Instrumentation and methodology for *in vitro* skin diffusion cells in methodology for skin absorption. In: KEMPPAINEN, B.W. REIFENRATH, W.G. (Eds.). **Methods for Skin Absorption**. Boca Raton:CRC, 1990.

FUJITA, K.; KUBO, I. Antifungal activity of octyl gallate. **Internation Journal of Food Microbiology**, v. 79, p. 193-201, 2002a.

FUJITA, K.; KUBO, I. Plasma membrane injury induced by nonyl gallate in *Saccharomyces cerevisiae*. **Journal of Applied Microbiology**, v. 92, p. 1035-1042, 2002b.

GANESAN, A. The impact of natural products upon the modern drug discovery. **Current Opinion in Chemical Biology**, v. 12, p. 306-317, 2008.

GNOJKOWSKI, J.; KRAJKA-KUZNIAK, V.; BAER-DUBOWSKA, W. Monoclonal antibody-directed analysis of benzo[a]pyrene metabolism in rat liver and extrahepatic tissues: effect of propyl and octyl gallate. **Nutrition and Cancer**, v. 39, p. 117-125, 2001.

HA, T.J.; NIHEI, K.; KUBO, I. Lipoxygenase inhibitory activity of octyl gallate. **Journal of Agricultural and Food Chemistry**, v. 52, p. 3177-3181, 2004.

HAYESHI, R.; HILGENDORF, C.; ARTURSSON, P.; AUGUSTIJNS, P.; BRODIN, B.; DEHERTOGH, P.; FISHER, K.; FOSSATI, L.; HOVENKAMP, E.; KORJAMO, T.; MASUNGI, C.; MAUBON, N.; MOLS, R.; MULLERTZ, A.; MONKKONEN, J.; O'DRISCOLL, C.; OPPERS-TIEMISSEN, H.M.; RAGNARSSON, E.G.E.; ROOSEBOOM, M.; UNGELL, A. Comparison of drug transporter gene expression and functionality in Caco-2 cells from 10 different laboratories. **European Journal of Pharmaceutical Sciences**, v. 35, p. 383-396, 2008.

HERKENNE, C.; NAIK, A.; KALIA, Y.N.; HADGRAFT, J.; GUY, R.H. Pig ear skin *ex vivo* as a model for *in vivo* dermatopharmacokinetic studies in man. **Pharmaceutical Research**, v. 23, p. 1850-1856, 2006.

HIDALGO, I.J. Assessing the absorption of new pharmaceuticals. **Current Topics in Medicinal Chemistry**, v. 1, p. 385-401, 2001

HIDALGO, I.J.; RAUB, T.J.; BORCHARDT, R.T. Characterization of the human colon carcinoma cell line (Caco-2) as a model system for intestinal epithelial permeability. **Gastroenterology,** v. 96, p. 736-749, 1989.

HIIPAKKA, R.A.; ZHANG, H.Z.; DAI, W.; DAI, Q.; LIAO, S. Structure-activity relationships for inhibition of human 5alpha-reductases by polyphenols. **Biochemical Pharmacology**, v. 63, p. 1165-1176, 2002.

HILGERS, A.R.; CONRADI, R.A.; BURTON, P.S. Caco-2 cell monolayers as a model for drug transport across the intestinal mucosa. **Pharmaceutical research,** v. 7, p. 902-910, 1990.

HOUGHTON, P.J. Use of small scale bioassays in the discovery of novel drugs from natural sources. **Phytotherapy Research**, v. 14, p. 419-423, 2000.

HSU, F.L.; CHANG, H.T.; CHANG, S.T. Evaluation of antifungal properties of octyl gallate and its synergy with cinnamaldehyde. **Bioresources Technology**, v. 98, p. 734-738, 2007.

HUBATSCH, I.; RAGNARSSON, E.G.E.; ARTURSSOON, P. Determination of drug permeability and prediction of drug absorption in Caco-2 monolayers. **Nature Protocols**, v. 2, p. 2111-2119, 2007.

HUNTER, J.; JEPSON, M.A.; TSURUO, T.; SIMMONS, N.L.; HIRST, B.H. Functional expression of P-glycoprotein in apical membranes of human intestinal Caco-2 cells. Kinetics of vinblastine secretion and interaction with modulators. **Journal of Biological Chemistry**, v. 268, p. 14991-14997, 1993.

ITO, T.; ANDO, H.; SUZUKI, T.; OGURA, T.; HOTTA, K.; IMAMURA, Y.; YAMAGUCHI, Y.; HANDA, H. Identification of a primary target of thalidomide teratogenicity. **Science**, v. 327, p. 1345-1350, 2010.

KALE, R.; TAYADE, P.; SARAF, M.; JUVEKAR, A. Molecular encapsulation of thalidomide with sulfobutyl ether-7 -beta-cyclodextrin for immediate release property: enhanced *in vivo* antitumor and antiangiogenesis efficacy in mice. **Drug Development and Industrial Pharmacy**, v. 34, p. 149-156, 2008.

KANE, C.J.; MENNA, J.H.; SUNG, C.C.; YEH, Y.C. Methyl gallate, methyl-3,4,5-trihydoxybenzoate, is a potent and highly specific inhibitor

of herpes simplex virus *in vitro*. II. Antiviral activity of methyl gallate and its derivatives. **Bioscience Reports**, v. 8, p. 95-102, 1988.

KANSY, M.; SENNER, F.; GUBERNATOR, K. Physicochemical high throughput screening: parallel artificial membrane permeation assay in the description of passive absorption processes. **Journal of Medicinal Chemistry**, v. 41, p. 1007-1010, 1998.

KARALIS, V.; MACHERAS, P.; PEERS, A.; SHAH, V. Bioavailability and bioequivalence: focus on physiological factors and variability. **Pharmaceutical Research**, v. 25, p. 1956-1962, 2008.

KAITIN, K.I.; DIMASI, J.A. Pharmaceutical innovation in the 21st century: new drugs approvals in the first decade, 2000-2009. **Clinical Pharmacology and Therapeutics**, v. 89, p. 183-188, 2011.

KELSEY, F.O. Thalidomide update: regulatory aspects. **Teratology**, v. 38, p. 221-226, 1988.

KENNEDY, T. Managing the drug discovery/development interface. **Drug Discovery Today**, v. 2, p. 436-444, 1997.

KERNS, E.H.; DI, L.; (Eds.) **Drug-like Properties: Concepts, Structure Design and Methods**. Amsterdam: Elsevier, 2008.

KITAGAWA, S.; NABEKURA, T.; KAMIYAMA, S.; TAKAHASHI, T.; NAKAMURA, Y.; KASHIWADA, Y.; IKESHIRO, Y. Effects of alkyl gallates on P-glycoprotein function. **Biochemical Pharmacology**, v. 70, p. 1262-1266, 2005.

KIMURA, O.; KOTAKI, Y.; HAMAUE, N.; HARAGUCHI, K.; ENDO, T. Transcellular transport of domoic acid across intestinal Caco-2 cell monolayers. **Food Chemistry and Toxicology**, 2011, in press.

KOCH, H.P.; STEINACKER, C. Improvement in solubility and stability of thalidomide by synthesis of inclusion complexes with cyclodextrins. **Archives in Pharmacy** (Weinheim), v. 321, p. 371-373, 1988.

KOLA, I.; LANDIS, J. Can the pharmaceutical industry reduce attrition rates? **Nature Reviews in Drug Discovery**, v. 3, p. 711-715, 2004.

KOLJONEN, M.; ROUSU, K.; CIERNY, J.; KAUKONEN, A.M.; HIRVONEN J. Transport evaluation of salicylic acid and structurally related compounds across Caco-2 cell monolayers and artificial PAMPA membranes. **European Journal of Pharmaceutics and Biopharmaceutics**, v. 70, p. 531-538, 2008.

KONISHI, Y.; KOBAYSHI, S.; SHIMIZU, M. Transepithelial transport of ρ-coumaric acid and gallic acid in Caco-2 cell monolayers. **Biosciences, Biotechnology and Biochemistry**, v. 67, p. 2317-2324, 2003.

KOVACEVIC, I.; PAROJCIC, J.; HOMSEK, I.; TUBIC-GROZDANIS, M.; LANGGUTH, P.; Justification of biowaiver for carbamazepine, a low soluble high permeable compound, in solid dosage forms based on IVIVC and gastrointestinal simulation. **Molecular Pharmaceutics**, v. 6, p. 40-47, 2008.

KRATZ, J.M.; ANDRIGHETTI-FRÖHNER, C.R.; KOLLING, D.J.; LEAL, P.C.; CIRNE-SANTOS, C.C.; YUNES, R.A.; NUNES, R.J.; TRYBALA, E.; BERGSTROM, T.; FRUGULHETTI, I.C.P.; BARARDI, C.R.M.; SIMÕES, C.M.O. Anti-HSV-1 and anti-HIV-1 Activity of Gallic Acid and Pentyl Gallate. **Memórias do Instituto Oswaldo Cruz**, v. 103, p. 437-442, 2008a.

KRATZ, J.M.; ANDRIGHETTI-FRÖHNER, C.R.; LEAL, P.C.; NUNES, R.J.; YUNES, R.A.; TRYBALA, E.; BERGSTROM, T.; BARARDI, C.R.M.; SIMÕES, C.M.O. Evaluation of Anti-HSV-2 Activity of Gallic Acid and Pentyl Gallate. **Biological and Pharmaceutical Bulletin**, v. 31, p. 903-907, 2008b.

KRATZ, J.M.; TEIXEIRA, M.R.; KOESTER, L.S.; SIMÕES, C.M.O. An HPLC-UV method for the measurement of permeability of marker drugs in the Caco-2 cell assay. **Brazilian Journal of Medical and Biological Research**, v. 44, p. 531-537, 2011.

KREANDER, K.; VUORELA, P.; TAMMELA, P. A rapid screening method for detecting active compounds against erythromycin-resistant bacterial strains of Finnish origin. **Folia Microbiologica (Praha)**, v. 50, p. 487-493, 2005.

KRENN, M.; GAMCSIK, M.P.; VOGELSANG, G.B.; COLVIN, O.M.; LEONG, K.W. Improvements in solubility and stability of thalidomide upon complexation with hydroxypropyl-beta-cyclodextrin. **Journal of Pharmaceutical Sciences**, v. 81, p. 685-689, 1992.

KUBO, I.; FUJITA, K.; NIHEI, K.; MASUOKA, N. Non-antibiotic antibacterial activity of dodecyl gallate. **Bioorganic and Medicinal Chemistry**, v. 11, p. 573-580, 2003.

KUBO, I.; FUJITA, K.; NIHEI, K.; NIHEI, A. Antibacterial activity of alkyl gallates against *Bacillus subtilis*. **Journal of Agricultural and Food Chemistry**, v. 52, p. 1072-1076, 2004.

KUBO, I.; MASUOKA, N.; XIAO, P.; HARAGUCHI, H. Antioxidant activity of dodecyl gallate. **Journal of Agricultural and Food Chemistry**, v. 50, p. 3533-3539, 2002a.

KUBO, I.; XIAO, P.; FUJITA, K. Antifungal activity of octyl gallate: structural criteria and mode of action. **Bioorganic and Medicinal Chemistry Letters**, v. 11, p. 347-350, 2001.

KUBO, I.; XIAO, P.; NIHEI, K.; FUJITA, K.; YAMAGIWA, Y.; KAMIKAWA, T. Molecular design of antifungal agents. **Journal of Agricultural and Food Chemistry**, v. 50, p. 3992-3998, 2002b.

LARA-OCHOA, F.; ESPINOSA PÉREZ, G.; MIJANGOS-SANTIAGO, F. Calorimetric determinations and theoretical calculations of polymorphs of thalidomide. **Journal of Molecular Structure**, v. 840, p. 97-106, 2007.

LEAL, P.C.; MASCARELLO, A.; DERITA, M.; ZULJAN, F.; NUNES, R.J.; ZACCHINO, S.; YUNES, R.A. Relation between lipophilicity of alkyl gallates and antifungal activity against yeasts and filamentous fungi. **Bioorganic and Medicinal Chemistry Letters**, v. 19, p. 1793-1796, 2009.

LENNERNÄS, H.; ABRAHAMSSON, B. The use of biopharmaceutic classification of drugs in drug discovery and development: current status and future extension. **Journal of Pharmacy and Pharmacology**, v. 57, p.273-285, 2005.

LI, C.; WAINHAUS, S.; USS, A.S.; CHENG, K.C. High-throughput screening using Caco-2 cell and PAMPA systems. In: EHRHARDT, C.; KIM, K.-J. (Eds.) **Drug Absorption Studies**. In situ, *In vitro* and *in silico* models. New York: Springer, 2008. Chapter 18. p. 418-429.

LIPINSKI, C.A.; LOMBARDO, F.; DOMINY, B.W.; FEENEY, P.J. Experimental and computational approaches to estimate solubility and permeability in drug discovery and development settings. **Advanced Drug Delivery Reviews**, v. 23, p. 3-25, 1997.

LOCATELLI, C.; ROSSO, R.; SANTOS-SILVA, M.C.; SOUZA, C.A.; LICÍNIO, M.A.; LEAL, P.C.; BAZZO, M.L.; YUNES, R.A.; CRECZYNSKI-PASA, T.B. Ester derivatives of gallic acid with potential toxicity toward L1210 leukemia cells. **Bioorganic and Medicinal Chemistry**, v. 16, p. 3791-3799, 2008.

LOCATELLLI, C.; CARVALHO, D.R.; MASCARELLO, A.; CORDOVA, C.A.S.; YUNES, R.A.; NUNES, R.J.; CRECZYNSKI-PASA, T.B. Antimetastatic activity and low systemic toxicity of tetradecyl gallate in a preclinical melanoma mouse model. **Investigational New Drugs**, 2011, in press.

LOFTSSON, T.; DUCHENE, D. Cyclodextrins and their pharmaceutical applications. **International Journal of Pharmaceutics**, v. 329, p. 1-11, 2007.

LOFTSSON, T.; JARHO, P.; MASSON, M.; JARVINEN, T. Cyclodextrins in drug delivery. **Expert Opinion on Drug Delivery**, v. 2, p. 335-351. 2005.

LOMBARDINO, J.G.; LOWE, J.A. The role of the medicinal chemists in drug discovey – then and now. **Nature Reviews in Drug Discovery**, v. 3, p. 853-862, 2004.

MATTHEWS, S.J.; McCOY, C. Thalidomide: A Review of Approved and Investigational Uses. **Clinical Therapeutics**, v. 25, p. 342-395, 2003.

MARTINEZ, M.N.; AMIDON, G.L. A mechanistic approach to understanding the factors affecting drug absorption: a review of

fundamentals. **Journal of Clinical Pharmacology**, v. 42, p. 620-643, 2002.

MELCHERT, M.; LIST, A. The Thalidomide Saga. **The International Journal of Biochemistry and Cell Biology**, v. 39, p. 1489-1499, 2007.

MIRET, S.; ABRAHAMSE, L.; DE GROENE, E.M. Comparison of *in vitro* models for the prediction of compound absorption across the human intestinal mucosa. **Journal of Biomolecular Screening**, v. 9, p. 598-606, 2004.

MUHAMMAD, F.; RIVIERE, J.E. *In vivo* models. In: RIVIERE, J.E. (Ed.). **Dermal absorption models in toxicology and pharmacology**. New York: CRC, 2006.

MULLERTZ, A.; OGBONNA, A.; REN, S.; RADES, T. New perspectives on lipid and surfactant based drug delivery systems for oral delivery of poorly soluble drugs. **Journal of Pharmacy and Pharmacology**, v. 62, p. 1622-1636, 2010.

MUNOZ, D.; AUDICANA, M.; GASTAMINZA, G.; FERNÁNDEZ E. Dermatitis de contacto por galatos. **Journal of Investigational Allergology and Clinical Immunology**, v. 17, p. 173-177, 2002.

MURASE, T.; KUME, N.; HASE, T.; SHIBUYA, Y.; NISHIZAWA, Y.; TOKIMITSU, I.; KITA, T. Gallates inhibit cytokine-induced nuclear translocation of NF-kappaB and expression of leukocyte adhesion molecules in vascular endothelial cells. **Arteriosclerosis, Thrombosis and Vascular Biology**, v. 19, p. 1412-1420, 1999.

NEERVANNAN, S. Preclinical formulations for discovery and toxicology: physicochemical challenges. **Expert Opinion on Drug Metabolism and Toxicology**, v. 2, p. 715-731, 2006.

NEUHOFF, S.; UNGELL, A.; ZAMORA, I.; ARTURSSON, P. pH-Dependent Bidirectional Transport of Weakly Basic Drugs across Caco-2 Monolayers: Implications for Drug–Drug Interactions. **Pharmaceutical Research**, v. 20, p. 1141-1148, 2003.

OLIVEIRA, M.A.; BERMUDEZ, J.A.Z.; SOUZA, A.C.M. Talidomida no Brasil: vigilância com responsabilidade compartilhada? **Cadernos de Saúde Pública**, v. 15, p. 99-112, 1999.

OTTAVIANI, G.; MARTEL, S.; CARRUPT, C.A. Parallel artificial membrane permeability assay: a new membrane for the fast prediction of passive human skin permeability. **Journal of Medicinal Chemistry**, v. 49, p. 3948-3954, 2006.

OTTAVIANI, G.; MARTEL, S.; CARRUPT, C.A. *In silico* and *in vitro* filters for the fast estimation of skin permeation and distribution of new chemical entities. **Journal of Medicinal Chemistry**, v. 50, p. 742-748, 2007.

OW Y.Y.; STUPANS I. Gallic acid and gallic acid derivatives: effects on drug metabolizing enzymes. **Current Drug Metabolism**, v. 4, p. 241-248, 2003.

PANG, K.S.; MAENG, H.; FAN, J. Interplay of transporters and enzymes in drug and metabolite processing. **Molecular Pharmaceutics**, v. 6, p. 1734-1755, 2009.

PAULINO, N.; PIZOLLATTI, M.G.; YUNES, R.A.; FILHO, V.C.; CRECZYNSKI-PASA, T.B.; CALIXTO, J.B. The mechanisms underlying the relaxant effect of methyl and ethyl gallates in the guinea pig trachea *in vitro*: contribution of potassium channels. **Archives of Pharmacology**, v. 360, p. 331-336, 1999.

PINTO, M.; ROBINE LEON, S.; APPAY, M.D. Enterocyte-like differentiation and polarization of the human colon carcinoma cell line Caco-2 in culture. **Biology of the Cell,** v. 47, p. 323-330, 1983.

PRAUSNITZ, M.R.; MITRAGOTRI, S.; LANGER, R. Current status and future potential of transdermal drug delivery. **Nature Reviews**, v. 3, p.115-124, 2004.

PRESS, B.; DI GRANDI, D. Permeability for intestinal absorption: Caco-2 assay and related issues. **Current Drug Metabolism**, v. 9, p. 893-900, 2008.

PREZIOSI, P. Science, pharmacoeconomics and ethics in drug R&D: a sustainable future scenario? **Nature Reviews Drug Discovery**, v. 3, p. 521-526, 2004.

REEPMEYER, J.C.; RHODES, M.O.; COX, D.C.; SILVERTON, J.V. Characterization and crystal structure of two polymorphic forms of racemic thalidomide. **Journal of Chemistry Society**, v. 9, p. 2063-2067, 1994.

ROSSO, R.; VIEIRA, T.O.; LEAL, P.C.; NUNES, R.J.; YUNES, R.A.; CRECZYNSKI-PASA, T.B. Relationship between the lipophilicity of gallic acid n-alquil esters' derivatives and both myeloperoxidase activity and HOCl scavenging. **Bioorganic and Medicinal Chemistry**, v. 14, p. 6409-6413, 2006.

SAEKI, K.; YUO, A.; ISEMURA, M.; ABE, I.; SEKI, T.; NOGUCHI, H. Apoptosis-inducing activity of lipid derivatives of gallic acid. **Biological and Pharmaceutical Bulletin**, v. 23, p. 1391-1394, 2000.

SAMBUY, Y.; DE ANGELIS, I.; RANALDI, G.; SCARINO, M.L.; STAMMATI, A.; ZUCCO, F. The Caco-2 cell line as a model of the intestinal barrier: influence of cell and culture-related factors on Caco-2 cell functional characteristics. **Cell Biology and Toxicology**, v. 21, p. 1-26, 2005.

SAVI, L.A.; LEAL P.C.; VIEIRA T.O.; ROSSO R.; NUNES R.J.; YUNES R.A.; CRECZYNSKI-PASA T.B.; BARARDI C.R.; SIMOES C.M. Evaluation of anti-herpetic and antioxidant activities, and cytotoxic and genotoxic effects of synthetic alkyl-esters of gallic acid. **Arzneimittelforschung**, v. 55, p. 66-75, 2005.

SCHMOOK, F.P.; MEINGASSNER, J.G.; BILLICH, A. Comparison of human skin or epidermis models with human and animal skin in *in vitro* percutaneous absorption. **International Journal of Pharmaceutics**, v. 215, p. 51-56, 2001.

SCHNEIDER, N.F.Z. **Padronização do ensaio PAMPA (parallel artificial membrane permeation assay) e avaliação *in vitro* da permeabilidade intestinal e cutânea de compostos de origem natural e sintética**. 2011. 112p. Dissertação (Mestrado em Farmácia) –

Departamento de Ciências Farmacêuticas, Universidade Federal de Santa Catarina, Florianópolis, 2011.

SHIBATA, H.; KONDO, K.; KATSUYAMA, R.; KAWAZOE, K.; SATO, Y.; MURAKAMI, K.; TAKAISHI, Y.; ARAKAKI, N.; HIGUTI, T. Alkyl gallates, intensifiers of beta-lactam susceptibility in methicillin-resistant *Staphylococcus aureus*. **Antimicrobial Agents and Chemotherapy**, v. 49, p. 549-555, 2005.

SHIRASAKA, Y.; SAKANE, T.; YAMASHITA, S. Effect of P-glycoprotein expression levels on the concentration-dependent permeability of drugs to the cell membrane. **Journal of Pharmaceutical Sciences**, v. 97, p. 553-565 , 2008.

SIEFERT, B.; PLEYER, U.; MULLER, M.; HARTMANN, C.; KEIPERT, S. Influence of cyclodextrins on the *in vitro* corneal permeability and *in vivo* ocular distribution of thalidomide. **Journal of Ocular Pharmacology and Therapeutics**, v. 15, p. 429-438, 1999.

SIISSALO, S.; LAINE, L.; TOLONEN, A.; KAUKONEN, A.M.; FINEL, M.; HIRVONEN, J. Caco-2 cell monolayers as a tool to study simultaneous phase II metabolism and metabolite efflux of indomethacin, paracetamol and 1-naphthol. **International Journal of Pharmaceutics,** v. 383, p. 24-29, 2010.

SOUZA, J.; FREITAS, Z.M.F.; STORPIRTIS, S. Modelos *in vitro* para determinação da absorção de fármacos e previsão da relação dissolução/absorção. **Revista Brasileira de Ciências Farmacêuticas**, v. 43, p. 515-527, 2007.

STAPLETON, P.D.; SHAH, S.; ANDERSON, J.C.; HARA, Y.; HAMILTON-MILLER, J.M.; TAYLOR, P.W. Modulation of beta-lactam resistance in *Staphylococcus aureus* by catechins and gallates. **International Journal of Antimicrobial Agents**, v. 23, p. 462-467, 2004.

STORPIRTIS, S.; GONÇALVEZ, J.E.; CHIANN, C.; GAI, M.N. (Eds.) **Biofarmacotécnica**. Rio de Janeiro: Guanabara Koogan, 2009.

TAMMELA, P.; LAITINEN, L.; GALKIN, A.; WENNBERG, T.O.; HECZKO, R.O.; VUORELA, H.O.; SLOTTE, J.P.; VUORELA, P.

Permeability characteristics and membrane affinity of flavonoids and alkyl gallates in Caco-2 cells and in phospholipids vesicles. **Archives of Biochemistry and Biophysics**, v. 425, p. 193-199, 2004.

TEO, S.K. Properties of thalidomide and its analogs: implications for anticancer therapy. **AAPS Journal**, v. 7, p. E14-E19, 2005.

TEO, S.K.; COLBURN, W.A.; THOMAS, S.D. Single-dose oral pharmacokinetics of three formulations of thalidomide in healthy male volunteers. **Journal of Clinical Pharmacology**, v. 39, p. 1162-1168, 1999.

TEO, S.K.; COLBURN, W.A.; TRACEWELL, W.G.; KOOK, K.A.; STIRLING, D.I.; JAWORSKY, M.S.; SCHEFFLER, M.A.; THOMAS, S.D.; LASKIN, O.L. Clinical Pharmacokinetics of Thalidomide. **Clinical Pharmacokinetics**, v. 43, p. 311-327, 2004.

UOZAKI, M.; YAMASAKI, H.; KATSUYAMA, Y.; HIGUCHI, M.; HIGUTI, T.; KOYAMA, A.H. Antiviral effect of octyl gallate against DNA and RNA viruses. **Antiviral Research**, v. 73, p. 85-91, 2006.

THERAPONTOS, C.; ERSKINE, L.; GARDNER, E.R.; FIGG, W.D.; VARGESSON, N. Thalidomide induces limb defects by preventing angiogenic outgrowth during early limb formation. **PNAS**, v. 106, p. 8573-8578, 2009.

US Food and Drug Administration (FDA). **Draft Guidance for Industry** – Drug interaction studies – Study design, data analysis, and implications for dosing and labeling. Rockville: FDA, 2006.

US Food and Drug Administration (FDA). **Guidance for Industry** – Waiver of *in vivo* bioavailability and bioequivalence studies for immediate-release solid oral dosage forms based on a biopharmaceutics classification system. Rockville: FDA, 2000.

VAIDYANATHAN, J.B.; WALLE, T. Cellular Uptake and Efflux of the Tea Flavonoid (-)-Epicatechin-3-gallate in the Human Intestinal Cell Line Caco-2**. The Journal of Pharmacology and Experimental Therapeutics**, v. 307, p. 745-752, 2003.

VAIDYANATHAN, J.B.; WALLE, T. Transport and Metabolism of the Tea Flavonoid (−)-Epicatechin by the Human Intestinal Cell Line Caco-2. **Pharmaceutical Research**, v. 18, p. 1420-1425, 2001.

VAN DER HEIJDEN, C.A.; JANSSEN, P.J.; STRIK, J.J. Toxicology of gallates: a review and evaluation. **Food and Chemical Toxicology**, v. 24, p. 1067-1070, 1986.

VELURI, R.; SINGH, R.P.; LIU, Z.; THOMPSON, J.A.; AGARWAL, R.; AGARWAL, C. Fractionation of grape seed extract and identification of gallic acid as one of the major active constituents causing growth inhibition and apoptotic death of DU145 human prostate carcinoma cells. **Carcinogenesis**, v. 27, p. 1445-1453, 2006.

VERSCHRAAGEN, M.; KOKS, C.H.; SCHELLENS, J.H.; BEIJNEN, J.H. P-glycoprotein system as a determinant of drug interactions: The case of digoxin-verapamil. **Pharmacology Research**, v. 40, p. 301–306, 1999.

VOLPE, D.A. Variability in Caco-2 and MDCK cell-based intestinal permeability assays. **Journal of Pharmaceutical Sciences**, v. 97, p. 712-725, 2008.

WATERBEEMD, H.V.; GIFFORD, E. ADMET *in silico* modeling: toward prediction paradise? **Nature Reviews Drug Discovery**, v. 2, p. 193-204, 2003.

WILSON, G.; HASSAN, I.F.; DIX, C.J.; WILLIAMSON, I.; SHAH, R.; MACKAY, M.; ARTURSSON, P. Transport and permeability properties of Caco-2 cells: An *in vitro* model of the intestinal epithelial cell barrier. **Journal of Controlled Release,** v. 11, p. 25-40, 1990.

WHITE, R.E. High-throughput screening in drug metabolism and pharmacokinetic support of drug discovery. **Annual Reviews in Pharmacology and Toxicology**, v. 22, p. 133-157, 2000.

YAMASHITA, S.; FURUBAYASHI, T.; KATAOKA, M.; SAKANE, T.; SEZAKI, H.; TOKUDA, H. Optimized conditions for prediction of intestinal drug permeability using Caco-2 cells. **European Journal of Pharmaceutical Sciences**, v. 10, p. 195-204, 2000.

YAMASHITA, S.; KONISHI, K.; YAMAZAKI, Y.; TAKI, Y.; SAKANE, T.; SEZAKI, H.; FURUYAMA, Y. New and better protocols for a short-term Caco-2 cell culture system. **Journal of Pharmaceutical Sciences,** v. 91, p. 669-679, 2002.

YANG, S. Biowaiver extension potential and IVIVC for BCS class II drugs by formulation design: case study for cyclosporine self-microemulsifying formulation. **Archives of Pharmacal Research**, v. 33, p. 1835-1842, 2010.

YOSHINO, M.; HANEDA, M.; NARUSE, M.; HTAY, H.H.; IWATA, S.; TSUBOUCHI, R.; MURAKAMI, K. Prooxidant action of gallic acid compounds: copper-dependent strand breaks and the formation of 8-hydroxy-2'-deoxyguanosine in DNA. **Toxicology *in vitro***, v. 16, p. 705-709, 2002.

ZAKI, N.M.; ARTURSSON, P.; BERGSTRÖM, C.A.S. A modified physiological BCS for prediction of intestinal absorption in drug discovery. **Molecular Pharmaceutics**, v. 7, p. 1478-1487, 2010.

ZERROUK, N.; CORTI, G.; ANCILLOTI, S.; MAESTRELLI, F.; CIRRI, F.; MURA, P. Influence of cyclodextrins and chitosan, separately or in combination, on glyburide solubility and permeability. **European Journal of Pharmaceutics and Biopharmaceutics**, v. 62, p. 241-246, 2006.

ZHANG, L.; ZHENG, Y.; CHOW, M.S.S.; ZUO, Z. Investigation of intestinal absorption and disposition of green tea catechins by Caco-2 monolayer model. **International Journal of Pharmaceutics**, v. 287, p. 1-12, 2004.

ZHOU, S.; LI, Y.; KESTELL, P.; SCHAFER, P.; CHAN, E.; PAXTON, J.W. Transport of thalidomide by the human intestinal Caco-2 monolayers. **European Journal of Drug Metabolism and Pharmacokinetics**, v. 30, p. 49-61, 2005.

ZHOU, S.; LI, Y.; KESTELL, P.; SCHAFER, P.; PAXTON, J.W. Determination of thalidomide in transport buffer for Caco-2 cell monolayers by high-performance liquid chromatography with ultraviolet detection. **Journal of Chromatography B**, v. 785, p. 165-173, 2003.

ZIMMERMANN, C.; GUTMANN, H.; DREWE, J. Thalidomide does not interact with P-glycoprotein. **Cancer Chemotherapy and Pharmacology**, v. 57, p. 599-606, 2006.

ZUO, Z.; KWON, G.; STEVENSON, B.; DIAKUR, J.; WIEBE, L.I. Flutamide-hidroxypropyl-β-cyclodextrin complex: formulation, physical characterization, and absorption studies using the Caco-2 *in vitro* model. **Journal of Pharmacy and Pharmaceutical Sciences**, v. 3, p. 220-227, 2000.

APÊNDICE 1

An HPLC-UV method for the measurement of permeability of marker drugs in the Caco-2 cell assay

J.M. Kratz[1], M.R. Teixeira[1], L.S. Koester[2] and C.M.O. Simões[1]

[1]Departamento de Ciências Farmacêuticas, Universidade Federal de Santa Catarina, Florianópolis, SC, Brasil
[2]Faculdade de Farmácia, Universidade Federal do Rio Grande do Sul, Porto Alegre, RS, Brasil

Abstract

The Caco-2 cell line has been used as a model to predict the *in vitro* permeability of the human intestinal barrier. The predictive potential of the assay relies on an appropriate in-house validation of the method. The objective of the present study was to develop a single HPLC-UV method for the identification and quantitation of marker drugs and to determine the suitability of the Caco-2 cell permeability assay. A simple chromatographic method was developed for the simultaneous determination of both passively (propranolol, carbamazepine, acyclovir, and hydrochlorothiazide) and actively transported drugs (vinblastine and verapamil). Separation was achieved on a C18 column with step-gradient elution (acetonitrile and aqueous solution of ammonium acetate, pH 3.0) at a flow rate of 1.0 mL/min and UV detection at 275 nm during the total run time of 35 min. The method was validated and found to be specific, linear, precise, and accurate. This chromatographic system can be readily used on a routine basis and its utilization can be extended to other permeability models. The results obtained in the Caco-2 bi-directional transport experiments confirmed the validity of the assay, given that high and low permeability profiles were identified, and P-glycoprotein functionality was established.

Key words: Caco-2; HPLC-UV; Marker drugs; Permeability

Introduction

Among the numerous techniques available for the prediction of intestinal permeability, the Caco-2 cell line has been extensively used and characterized as a model of the intestinal barrier (1,2). These human cells are able to fully polarize into differentiated monolayers with well-established tight junctions and brush border membrane as well as to express several membrane transporters and metabolizing enzymes, allowing the measurement of functional permeability (both passive diffusion and active transport) (3). Consequently, this assay is widely accepted by both the pharmaceutical industry and regulatory agencies since the permeability determined using Caco-2 cells correlates well with oral absorption in humans (4-6).

In 2000, the United States Food and Drug Administration (FDA) published guidelines (7) based on the Biopharmaceutical Classification System (BCS) (8), whereby *in vitro* assays can be used to determine permeability class

during the request of biowaivers of *in vivo* bioavailability and/or bioequivalence studies in immediate-release solid oral dosage forms.

More recently, the International Transporter Consortium (ITC), a group of industrial, regulatory and academic scientists with expertise in drug metabolism, transport and pharmacokinetics, presented their recommendations regarding the design of *in vitro* membrane transporter assays (9), particularly in relation to transporters involved in important clinical drug-drug interactions, highlighting the importance of these models in the early stages of the drug development process.

Although the Caco-2 assay presents many advantages, variable culture conditions can lead to inconsistent cell characteristics, poor reproducibility and relatively wide intra- and inter-laboratory variability. Therefore, cell culture techniques and experimental conditions should be specified in detail

Correspondence: C.M.O. Simões, Laboratório de Virologia Aplicada, Departamento de Ciências Farmacêuticas, Universidade Federal de Santa Catarina, Campus Universitário Trindade, 88040-900 Florianópolis, SC, Brasil. Fax: +55-48-3721-9258. E-mail: claudias@reitoria.ufsc.br

(10,11). The assay must be able to discriminate between high and low passive permeability profiles. Bi-directional transport experiments with P-glycoprotein (P-gp) substrates and inhibitors are regarded as the definitive assay for the identification of active transport (7,9). For the continuous assessment of the internal performance, marker drugs should be used during transport experiments (7,12).

The objective of the present study was to develop an HPLC-UV method using a single chromatographic step for the determination of six marker drugs, acyclovir, carbamazepine, hydrochlorothiazide, propranolol, verapamil, and vinblastine, which were employed in the demonstration of the validity of the Caco-2 permeability assay.

Material and Methods

Chemicals and reagents

The physicochemical properties and permeation mechanism of all the marker drugs used in this study are presented in Table 1. Acyclovir (ACV), carbamazepine (CBZ), hydrochlorothiazide (HTZ), and propranolol hydrochloride (PRO) reference standards (≥99%) were obtained from the National Institute of Health Quality Control (INCQS, Brazil). Verapamil hydrochloride (VER, ≥99%), vinblastine sulfate (VIN, ≥96%), Hank's balanced salt solution (HBSS), sodium 4-(2-hydroxyethyl)-1-piperazineethanesulfonate (HEPES), methanesulfonic acid (MES), ethylenediaminetetraacetic acid (EDTA), trypsin, bovine serum albumin (BSA), dimethyl sulfoxide (DMSO), and Lucifer yellow (LY) were obtained from Sigma (USA). Acetonitrile and ammonium acetate (HPLC grade) were obtained from Tedia Co. (USA). Dulbecco's modified Eagle's medium (DMEM) with high glucose, fetal bovine serum (FBS), nonessential amino acids, and antibiotics/antimycotics were purchased from Invitrogen, Ltd. (USA). All other chemicals and reagents used in this study were of the highest commercially available purity.

HPLC and chromatographic conditions

Quantitative determinations of all six marker drugs were performed on a Perkin Elmer Series 200 HPLC instrument (USA), which consisted of a quaternary pump, vacuum degasser, autosampler, and diode-array detector (DAD). Separation was achieved on a C18 column (5 μm, 4.6 mm x 300 mm; Luna, Phenomenex, USA). A step-gradient elution was employed with acetonitrile as solvent A and an aqueous solution of ammonium acetate, pH 3.0 (25 mM), as solvent B, at a flow rate of 1.0 mL/min. Elution started at 3:97 (A:B, v/v) isocratic for 8.0 min and the gradient was then increased to 80:20 (A:B, v/v) for 14 min, before being returned to the initial condition of 3:97 (A:B, v/v) for 8.0 min, followed by 5 min equilibration. Effluent absorbance was measured at 275 nm and 20-μL samples were injected into the column. UV spectra from 200 to 400 nm were recorded with the DAD online during the chromatographic run.

Validation of the chromatographic method

Method validation was performed based on both FDA and International Conference on Harmonization (ICH) guidelines for the validation of analytical methods (13,14). All samples used during validation were freshly prepared in HBSS buffer. Exploration and optimization of several chromatographic parameters, such as selectivity (α), tailing factor (T_f), number of theoretical plates (N) and peak resolution was performed, and the chromatogram showing the optimized separation of all six marker drugs is presented in Figure 1. Specificity was assessed by injecting individual drugs and recording their retention times and UV spectra. Chromatograms were compared to those of blank samples. Linearity was established by the construction of individual seven-point calibration curves over a range of 0.5-100 μM. Precision was established by both intra-day and inter-day precision. The intra-day precision was assessed by nine determinations covering the specified range (3 concentrations/3 replicates each), while the inter-day precision was assessed on different days by nine determinations covering the specified range (3 concentrations/3 replicates each/3 days). The relative standard deviation (RSD) of each drug was calculated as a measure of precision. The accuracy of the method was established by nine determinations covering the specified range (3 concentrations/3 replicates each/3 days). The percent difference of the mean values from the nominal concentrations was the measure of accuracy. The low limit of quantification (LLOQ) was determined as the lowest concentration in the calibration curve with a precision of 20% and accuracy of 80-120%.

Cell culture

Caco-2 cells (HTB-37) were obtained from the American Type Culture Collection (ATCC, USA). Cells were maintained in a humidified 5% CO_2 air atmosphere at 37°C and were cultured in DMEM (4.5 g/L glucose) with 20% FBS, 1% non-essential amino acids, 100 U/mL penicillin, 100 μg/mL streptomycin, and 25 μg/mL amphotericin B. After reaching 80-90% confluence, cells were harvested with 0.25% trypsin/EDTA solution, and counted by the Trypan blue exclusion method on a Countess® automated cell counter (Invitrogen). Only cultures with ≥95% viability were used.

Transport studies

For the intestinal permeability experiments, Caco-2 cells between passages 25 and 31 were seeded on Millicell® polycarbonate inserts (0.6 cm², 0.4 μm pore size; Millipore, USA) at a density of 100,000 cells per insert and cultivated for 21-25 days. Culture medium was replaced three times per week until the time of use.

The transepithelial electrical resistance (TEER) of the monolayers and the permeability to the paracellular marker LY were considered to be indicators of monolayer integrity. TEER was assessed at 37°C using a Millicell® ERS meter (Millipore) connected to a WPI® Endohm tissue resistance

measurement chamber (USA) and reported as Ωcm^2. The permeability of the monolayers to LY (100 µg/mL) was assessed using a Tecan® Infinite 200 microplate reader (Switzerland). Only monolayers with TEER values above 200 Ωcm^2 and LY permeability $\leq 0.2 \times 10^{-6}$ cm/s were used.

The transport experiments were carried out according to the recommendations previously described (15). HBSS at pH 6.0 (10 mM MES) and pH 7.4 (10 mM HEPES) was used as transport buffer in the apical (AP) and basolateral (BL) compartments, respectively, in order to mimic *in vivo* conditions. Before the experiments, monolayers were washed twice with HBSS, pH 7.4, and incubated for 30 min at 37°C for TEER measurement. Next, DMSO stock solutions (1 mM) of all marker drugs were diluted in HBSS and added to the donor compartment, while fresh HBSS was added to the receiver compartment.

The permeability of passive diffusion markers was assessed on isolated drugs (PRO, CBZ, ACV, and HTZ) or on a drug mixture (CBZ and HTZ). The P-gp functionality was evaluated with VIN alone (P-gp substrate) or in the presence of VER (P-gp inhibitor; 100 µM; both compartments). All experiments were performed in both directions, i.e., from AP to BL and from BL to AP, for the period of 2 h, at 37°C in an orbital shaker (100 rpm). At appropriate times, 100-µL aliquots were removed from the receiver compartment and replaced with an equal volume of fresh HBSS. At the end of the experiment, samples were collected from donor compartments in order to perform the mass balance calculation.

Transport experiments were conducted under sink conditions (where less than 10% of the drug was transported across the cell monolayer) and the apparent permeability coefficient (P_{app}) (cm/s) values were calculated as follows (15):

$$P_{app} = \frac{(\Delta Q)}{(\Delta t)} \times \frac{1}{A \times C_0 \times 60}$$

Eq. 1

where ($\Delta Q/\Delta t$) is the steady-state flux (mol/s), A is the surface area of the filter (cm²), and C_0 is the initial concentration in the donor compartment (mol/mL) (16). For
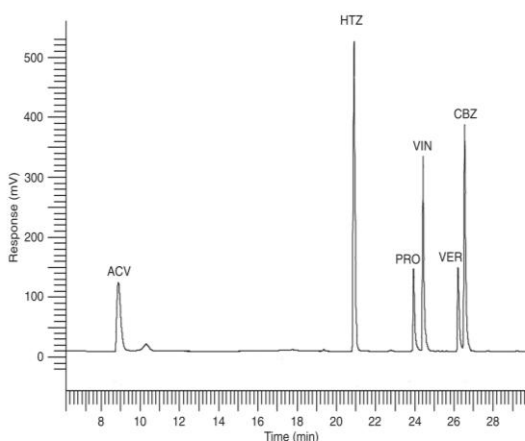
Figure 1. Representative chromatogram of marker drugs (50 µM) in HBSS buffer. Marker drugs: acyclovir (ACV), hydrochlorothiazide (HTZ), propranolol (PRO), vinblastine (VIN), verapamil (VER), and carbamazepine (CBZ). Separation was achieved on a C18 column (5 µm, 4.6 mm x 300 mm) with step-gradient elution. Acetonitrile (A) and an aqueous solution of ammonium acetate (B), pH 3.0 (25 mM) were used as mobile phase components. Flow rate was 1.0 mL/min. Elution started at 3:97 (A:B, v/v) isocratic for 8.0 min followed by gradient to 80:20 (A:B, v/v) for 14 min and return to the initial condition of 8.0 min. Equilibration time of 5 min. UV detection at 275 nm. UV spectra from 200 to 400 nm were recorded with the DAD online during the chromatographic run.

rapidly transported drugs, where sink conditions could not be maintained for the full duration of the experiments, permeability coefficient (P_{app}) values (cm/s) were calculated as follows:

$$C_R(t) = \frac{M}{V_D + V_R} + \left(C_{R,0} - \frac{M}{V_D + V_R} \right) e^{-P_{app}A(1/V_D + V_R)t}$$

Eq. 2

where $C_R(t)$ is the time-dependent drug concentration in the receiver compartment, M is the amount of drug in the system, V_D and V_R are the volumes of the donor and receiver compartments, respectively, and t is the time from the start of the interval. P_{app} values were obtained from nonlinear regression minimizing the sum of squared residuals ($\sum(C_{R,i,obs} - C_{R,i,calc})^2$), where $C_{R,i,obs}$ is the observed receiver concentration at the end of the interval and $C_{R,i,calc}$ is the corresponding concentration calculated according to Equation 2 (16,17).

Statistical analysis

Data are reported as the mean ± SD of three independent experiments. For transport experiments, triplicate

124

534   J.M. Kratz et al.

inserts were used in each experiment repetition. Microsoft Excel 2007® (USA) was used for the linear and non-linear regression analyses.

Results and Discussion

The Caco-2 cell model is the most frequently used method for *in vitro* gastrointestinal permeability assessment. The experience collected with this cell line over the last two decades has shown both successes and failures in its predictive capability (18). From this standpoint, the appropriate validation of the assay within research laboratories is mandatory for the suitable application of the assay to drug profiling projects in order to avoid the intrinsic variability of cell culture techniques. Therefore, the main purpose of the present study was to determine the suitability of a Caco-2 assay through the determination of marker drugs.

Marker drug set assembly

Six marker drugs with known fraction absorbed in humans (FA%) and a broad range of physicochemical properties were selected based on published data (Table 1) (17,19-23). Drugs were divided into two experimental groups: one for the determination of passive permeability, and the other for the demonstration of P-gp functionality. In agreement with FDA recommendations (7), these drugs encompass a wide range of FA% (17-100%) covering all four BCS classes. For the measurement of functional efflux mediated by P-gp, VIN and VER were selected as substrate and inhibitor, respectively, since both drugs have already been described as model drugs for cellular P-gp interaction studies (9).

HPLC

The optimum wavelength for the detection of all analytes with adequate sensitivity and specificity was found to be 275 nm. A fixed UV wavelength was used in order to allow equipment interchangeability, even though DAD was available. The next step was the selection of the mobile phase components and composition. Acetonitrile (solvent A) and ammonium acetate (25 mM; solvent B) were selected for

the initial studies. In order to achieve a balance between adequate peak resolution and total run time, a gradient elution was programmed. Best peak shapes were obtained with pH 3.0 in the aqueous phase with a flow rate of 1.0 mL/min, since lower flows improved tailing, while a higher flow generated elevated backpressure.

ACV was initially challenging, since this analyte required a high aqueous content (3:97, v/v) for adequate peak shape and retention time. The remaining drugs were eluted by a gradual shift to a high organic content (80:20, v/v). With these conditions, only PRO and VIN presented low peak resolution (≤2.0). To improve this feature, a 300-mm C18 column was employed in place of the standard 150-mm column initially used. With these optimized chromatographic conditions, the average retention times were 8.88, 20.90, 23.95, 24.43, 26.22, and 26.58 min, for ACV, HTZ, PRO, VIN, VER, and CBZ, respectively (Figure 1).

Table 2 summarizes linearity, range, precision, and accuracy data. VER was not included in Table 2 since it was used exclusively for inhibition of P-gp. Although a baseline alteration due to gradient shift was detected at about 10 min, no interference was observed in the retention time windows of each analyte, and specificity was confirmed by comparison of UV spectra to previously published data (24). The LLOQs were determined as 0.5 µM for all drugs (lowest concentration in the calibration curve), since the RSDs at this concentration were ≤1.84%. The data in Table 2 show that the method presented here is appropriate for the determination of these markers (13,14).

This method can be readily employed for the suitability demonstration and in-house validation of Caco-2 permeability assays. In addition, the applicability of this method can be extended to other *in vitro/in situ/ex vivo* permeability assays. Although several studies have reported the simultaneous determination of permeability of marker drugs by HPLC (25-29), to our knowledge, this is the first report of an HPLC-UV method for the determination of the P-gp substrate VIN concomitantly with the corresponding inhibitor VER, and the four passive permeability markers used in this study.

Table 1. Physicochemical properties of marker drugs used in this study.

Marker drug	Permeability class	BCS class	Transport mechanism	FA%	pK_a	log P
Propranolol	High	I	Transcellular	90%	9.52	3.43
Carbamazepine	High	II	Transcellular	100%	-	2.45
Acyclovir	Low	III	Paracellular	17%	2.34, 9.23	-2.42
Hydrochlorothiazide	Low	IV	Paracellular	55%	8.77, 9.79	-0.17
Vinblastine	-	-	P-gp substrate	-	7.4	4.32
Verapamil	High	I	P-gp inhibitor	98%	8.66	3.96

BCS = Biopharmaceutical Classification System (8); FA% = fraction absorbed in humans; log P = partition coefficient; P-gp = P-glycoprotein. The data presented in this table were obtained from Refs. 17,19-23.

Braz J Med Biol Res 44(6) 2011   www.bjournal.com.br

Caco-2 permeability assay - suitability demonstration

The formation of a functional single monolayer on polycarbonate inserts is an important feature regarding the mimicking of *in vivo* conditions in the Caco-2 permeability assay. As small changes in the culture conditions can lead to significant differences in cell phenotype (10), the integrity of the monolayers and the formation of a robust tight junction (TJ) network were monitored by TEER measurement and LY transport.

TEER profiles were obtained throughout the period of culture (21-25 days). Detectable values emerged from the 4th day of culture (values around 100 Ωcm^2) and continued to increase, until reaching a plateau on the 11th day of culture. The average TEER value obtained before the transport experiments was 297 ± 21 Ωcm^2. Additional information regarding the integrity and tightness of monolayers was obtained by LY permeability assays. LY is a fluorescent paracellular marker with very low permeability and has been used as a marker of TJ maturation (30). The average LY P_{app} value obtained after 21 days of culture was ≤0.2 x 10^{-6} cm/s, in agreement with previously published data (31). For cut-off purposes, only monolayers with TEER values above 200 Ωcm^2 and LY permeability ≤0.2 x 10^{-6} cm/s were considered to be appropriate for the experiments.

Through bi-directional transport experiments, P_{app} values were determined for each marker drug across Caco-2 cell monolayers and the summary of the permeability data is shown in Table 3. Four marker drugs were employed for passive permeability evaluation, i.e., PRO and CBZ as high permeability standards, along with ACV and HTZ as

low permeability standards. All drugs presented adequate P_{app} values, which correlated well with the FA% of these drugs, allowing the establishment of a rank order relationship as intended.

Another important aspect considered was the efflux ratios ($P_{app \ BL-AP}/P_{app \ AP-BL}$) obtained. Passively transported drugs should produce efflux ratios close to 1.00 in order to demonstrate independence from active transport mechanisms (9). In the present study, only CBZ, ACV and HTZ presented proper values, while PRO showed an efflux ratio of 2.81, which could lead to a false interpretation toward an active transport pathway. However, since a pH gradient setup was employed in the transport experiments, and PRO is a basic drug with pK_a around 9.5, data analysis revealed that PRO permeability was pH-sensitive due to ionization effects, as already described (30).

Moreover, the permeability of CBZ and HTZ was assessed via a cocktail approach. The results obtained with this strategy were very similar, and maintained the rank order agreement. CBZ presented AP-BL and BL-AP P_{app} (cm/s) values of 110.61 ± 3.41 and 116.6 ± 5.50, while HTZ presented values of 1.81 ± 0.22 and 2.36 ± 0.34, respectively. Therefore, CBZ and HTZ were selected to be used as a single mixture control for the continuous evaluation of the internal performance of the Caco-2 permeability assay.

The permeability profile of VIN, a P-gp substrate, was also determined in order to demonstrate the suitability of the method regarding active transport mechanisms. Special attention was given to the selection of drug concentration in order to avoid transporter saturation (9,32). As shown

Table 2. Chromatographic validation data for the determination of marker drugs used in the Caco-2 permeability assay.

Marker drug	Range (µM)	Equation (r^2)	Theoretical concentration (µM)	Intra-day		Inter-day	
				Accuracy (%)	%RSD	Accuracy (%)	%RSD
Propranolol	0.5-100	y = 7652x - 7957 (0.9996)	50	103.61	0.56	97.24	3.55
			25	105.13	0.71	89.06	3.38
			10	111.68	0.40	96.50	0.23
Carbamazepine	0.5-100	y = 24003x - 16365 (0.9997)	50	99.48	0.68	91.48	1.22
			25	101.30	0.31	92.20	3.72
			10	103.75	0.35	98.31	1.50
Acyclovir	0.5-100	y = 15244x - 7135 (0.9999)	50	109.40	1.96	93.03	9.55
			25	113.22	2.86	93.34	10.41
			10	115.37	1.42	95.46	10.53
Hydrochlorothiazide	0.5-100	y = 36301x - 7957 (0.9998)	50	96.23	0.21	92.82	1.05
			25	97.52	0.60	96.58	3.49
			10	98.48	0.10	90.99	0.95
Vinblastine	0.5-100	y = 16664x - 13615 (0.9991)	50	111.12	0.86	100.11	1.78
			25	104.55	1.27	96.57	3.54
			10	92.23	1.26	97.62	5.30

Intra-day and inter-day accuracy and precision were determined in triplicate for each concentration. Accuracy was defined as percent difference from the nominal concentration. Precision is reported as the relative standard deviation (RSD).

in Table 3, an efflux ratio of 17.75 was obtained. An acceptable system produces a minimum efflux ratio of 2.00 (9). Moreover, the permeability of VIN was evaluated in the presence of VER, a known P-gp inhibitor. In this setup, the $P_{app\ AP\text{-}BL}$ value obtained was 4.5-fold higher than that of VIN alone, and the efflux ratio observed was much lower (4.28). These findings agree with recommendations that the efflux ratio should be significantly reduced by the addition of a known inhibitor (more than 50%) (9,32), as observed in the present study, thereby corroborating the adequacy of the Caco-2 permeability assay in relation to P-gp functionality.

Table 3. *In vitro* intestinal permeability data of the marker drugs across Caco-2 cell monolayers.

Marker drug	Donor concentration (μM)	P_{app} (10^{-6}; cm/s)		Efflux ratio	R (%)
		AP-BL	BL-AP		
Propranolol	25	9.00 ± 0.15	25.28 ± 3.72	2.81	87
Carbamazepine	25	144.31 ± 4.04	121.5 ± 5.56	0.84	91
Acyclovir	50	1.32 ± 0.15	1.53 ± 0.30	1.16	92
Hydrochlorothiazide	50	1.46 ± 0.21	1.79 ± 0.08	1.23	100
Vinblastine (-)	40	4.41 ± 0.65	78.26 ± 9.37	17.75	93
Vinblastine (+)	40	20.08 ± 1.12	85.94 ± 3.44	4.28	92

Transport experiments were performed at an apical pH of 6.0 and a basolateral pH of 7.4. Apparent permeability coefficients (P_{app}) were calculated according to equations 1 and 2 and data are reported as means ± SD (N = 3). AP-BL = apical to basolateral direction; BL-AP = basolateral to apical direction; efflux ratio = $P_{app\ BL\text{-}AP}/P_{app\ AP\text{-}BL}$; R = mass balance recuperation; (-) and (+) indicate the absence and the presence of Verapamil (100 μM), respectively.

A simple, accurate and precise HPLC method using UV detection was developed and validated for the simultaneous determination of marker drugs directly in the transport buffer. This method was successfully employed in the Caco-2 permeability assay during the in-house validation of the technique within our research laboratory, and can be readily employed on a routine basis with other permeability models. The results obtained in the present study confirmed the suitability of the Caco-2 permeability assay for the assessment of high and low permeability profiles, and for the establishment of P-gp functionality. To our knowledge, this is the first report of an HPLC-UV method developed for the determination of vinblastine concomitantly with verapamil, and four other passive permeability markers - propranolol, carbamazepine, acyclovir, and hydrochlorothiazide.

Acknowledgments

References

1. Balimane PV, Han YH, Chong S. Current industrial practices of assessing permeability and P-glycoprotein interaction. *AAPS J* 2006; 8: E1-13.
2. Press B, Di Grandi D. Permeability for intestinal absorption: Caco-2 assay and related issues. *Curr Drug Metab* 2008; 9: 893-900.
3. Hidalgo IJ, Raub TJ, Borchardt RT. Characterization of the human colon carcinoma cell line (Caco-2) as a model system for intestinal epithelial permeability. *Gastroenterology* 1989; 96: 736-749.
4. Artursson P, Karlsson J. Correlation between oral drug absorption in humans and apparent drug permeability coefficients in human intestinal epithelial (Caco-2) cells. *Biochem Biophys Res Commun* 1991; 175: 880-885.
5. Elsby R, Surry DD, Smith VN, Gray AJ. Validation and application of Caco-2 assays for the *in vitro* evaluation of development candidate drugs as substrates or inhibitors of P-glycoprotein to support regulatory submissions. *Xenobiotica* 2008; 38: 1140-1164.
6. Matsson P, Bergstrom CA, Nagahara N, Tavelin S, Norinder U, Artursson P. Exploring the role of different drug transport routes in permeability screening. *J Med Chem* 2005; 48: 604-613.
7. FDA (Food and Drug Administration). *Guidance for industry - Waiver of in vivo bioavailability and bioequivalence studies for immediate-release solid oral dosage forms based on a biopharmaceutics classification system*. 2000.
8. Amidon GL, Lennernas H, Shah VP, Crison JR. A theoretical basis for a biopharmaceutic drug classification: the correlation of *in vitro* drug product dissolution and *in vivo* bioavailability. *Pharm Res* 1995; 12: 413-420.
9. Giacomini KM, Huang SM, Tweedie DJ, Benet LZ, Brouwer KL, Chu X, et al. Membrane transporters in drug development. *Nat Rev Drug Discov* 2010; 9: 215-236.
10. Volpe DA. Variability in Caco-2 and MDCK cell-based intestinal permeability assays. *J Pharm Sci* 2008; 97: 712-725.
11. Corti G, Maestrelli F, Cirri M, Zerrouk N, Mura P. Development and evaluation of an *in vitro* method for prediction of human drug absorption II. Demonstration of the method suitability. *Eur J Pharm Sci* 2006; 27: 354-362.
12. Polli JE, Yu LX, Cook JA, Amidon GL, Borchardt RT, Burnside BA, et al. Summary workshop report: biopharmaceutics classification system - implementation challenges and extension opportunities. *J Pharm Sci* 2004; 93: 1375-1381.

13. FDA (Food and Drug Administration). *Guidance for industry - Bioanalytical method validation.* 2001.

14. ICH (International Conference on Harmonization). *Validation of analytical procedures: text and methodology, Q2(R1).* 2005.

15. Hubatsch I, Ragnarsson EG, Artursson P. Determination of drug permeability and prediction of drug absorption in Caco-2 monolayers. *Nat Protoc* 2007; 2: 2111-2119.

16. Grasjo J, Taipalensuu J, Ocklind G, Artursson P. Applications of epithelial cell culture in studies of drug transport. In: Wise C (Editor), *Epithelial cell culture protocols.* Totowa: Humana Press Inc.; 2002. p 233-272.

17. Bergstrom CA, Strafford M, Lazorova L, Avdeef A, Luthman K, Artursson P. Absorption classification of oral drugs based on molecular surface properties. *J Med Chem* 2003; 46: 558-570.

18. Ungell AL. Caco-2 replace or refine? *Drug Discovery Today* 2004; 1: 423-430.

19. Winiwarter S, Bonham NM, Ax F, Hallberg A, Lennernas H, Karlen A. Correlation of human jejunal permeability (*in vivo*) of drugs with experimentally and theoretically derived parameters. A multivariate data analysis approach. *J Med Chem* 1998; 41: 4939-4949.

20. Lee KJ, Johnson N, Castelo J, Sinko PJ, Grass G, Holme K, et al. Effect of experimental pH on the *in vitro* permeability in intact rabbit intestines and Caco-2 monolayer. *Eur J Pharm Sci* 2005; 25: 193-200.

21. Wu CY, Benet LZ. Predicting drug disposition via application of BCS: transport/absorption/elimination interplay and development of a biopharmaceutics drug disposition classification system. *Pharm Res* 2005; 22: 11-23.

22. Skold C, Winiwarter S, Wernevik J, Bergstrom F, Engstrom L, Allen R, et al. Presentation of a structurally diverse and commercially available drug data set for correlation and benchmarking studies. *J Med Chem* 2006; 49: 6660-6671.

23. Ahlin G, Karlsson J, Pedersen JM, Gustavsson L, Larsson R, Matsson P, et al. Structural requirements for drug inhibition of the liver specific human organic cation transport protein 1. *J Med Chem* 2008; 51: 5932-5942.

24. Moffat AC, Osselton MD, Widdop B (Editors). *Clarke's analysis of drugs and poisons.* Chicago: Pharmaceutical Press; 2003.

25. Bansal T, Singh M, Mishra G, Talegaonkar S, Khar RK, Jaggi M, et al. Concurrent determination of topotecan and model permeability markers (atenolol, antipyrine, propranolol and furosemide) by reversed phase liquid chromatography: utility in Caco-2 intestinal absorption studies. *J Chromatogr B Analyt Technol Biomed Life Sci* 2007; 859: 261-266.

26. Venkatesh G, Ramanathan S, Mansor SM, Nair NK, Sattar MA, Croft SL, et al. Development and validation of RP-HPLC-UV method for simultaneous determination of buparvaquone, atenolol, propranolol, quinidine and verapamil: a tool for the standardization of rat *in situ* intestinal permeability studies. *J Pharm Biomed Anal* 2007; 43: 1546-1551.

27. Chawla S, Ghosh S, Sihorkar V, Nellore R, Kumar TR, Srinivas NR. High-performance liquid chromatography method development and validation for simultaneous determination of five model compounds, antipyrine, metoprolol, ketoprofen, furosemide and phenol red, as a tool for the standardization of rat *in situ* intestinal permeability studies using timed wavelength detection. *Biomed Chromatogr* 2006; 20: 349-357.

28. Augustijns P, Mols R. HPLC with programmed wavelength fluorescence detection for the simultaneous determination of marker compounds of integrity and P-gp functionality in the Caco-2 intestinal absorption model. *J Pharm Biomed Anal* 2004; 34: 971-978.

29. Palmgren JJ, Monkkonen J, Jukkola E, Niva S, Auriola S. Characterization of Caco-2 cell monolayer drug transport properties by cassette dosing using UV/fluorescence HPLC. *Eur J Pharm Biopharm* 2004; 57: 319-328.

30. Thiel-Demby VE, Humphreys JE, St John Williams LA, Ellens HM, Shah N, Ayrton AD, et al. Biopharmaceutics classification system: validation and learnings of an *in vitro* permeability assay. *Mol Pharm* 2009; 6: 11-18.

31. Uchida M, Fukazawa T, Yamazaki Y, Hashimoto H, Miyamoto Y. A modified fast (4 day) 96-well plate Caco-2 permeability assay. *J Pharmacol Toxicol Methods* 2009; 59: 39-43.

32. Shirasaka Y, Sakane T, Yamashita S. Effect of P-glycoprotein expression levels on the concentration-dependent permeability of drugs to the cell membrane. *J Pharm Sci* 2008; 97: 553-565.

APÊNDICES 2 E 3

No ano de 2010, durante a realização do estágio (Bolsa PDEE, CAPES) no Laboratório de Pesquisas Avançadas em Absorção de Fármacos, coordenado pelo Prof. Dr. Per Artursson, da Universidade de Uppsala, Suécia, estive engajado em diversos estudos colaborativos que, embora não estejam relacionados diretamente com o conteúdo desta tese de doutorado, contribuíram para a minha formação e geraram publicações. Os manuscritos que até o momento da redação desta tese já se encontravam em fase final de submissão estão disponíveis para apreciação na forma de apêndices.

O Departamento de Farmácia da Universidade de Uppsala faz parte de uma plataforma de desenvolvimento pré-clínico de fármacos conhecida como UDOPP – *The Uppsala University Drug Optimization and Pharmaceutical Profiling Plataform* (http://www.farmfak.uu.se/farm/UDOPP/) – cujo objetivo principal é fornecer às instituições acadêmicas e também às indústrias farmacêuticas uma base para a otimização racional das propriedades farmacocinéticas e toxicológicas (ADMET) de candidatos a fármacos. Essa plataforma é um dos pilares de uma rede de pesquisa e desenvolvimento maior, o *Chemical Biology Consortium Sweden* (CBCS – http://www.cbcs.se). A lógica consiste em prover os interessados com moléculas da mais alta qualidade e que possuam grande probabilidade de sucesso em estudos clínicos futuros, e, ao mesmo tempo, os projetos contribuírem para a atualização e melhoramento contínuo do pessoal envolvido e das competências singulares presentes nessa plataforma, que compreende diversos grupos de pesquisa.

Nesse âmbito, em uma parceria com o Departamento de Química Medicinal, coordenado pela Profa. Dra. Anja Sandström, foram estudadas duas séries de compostos peptidomiméticos. Esse grupo tem trabalhado com o neurotransmissor conhecido como Substância P e seu metabólito ativo SP1-7. Em estudos anteriores foram identificaram peptídeos menores com grande afinidade pelo receptor desse metabólito, com potencial analgésico, antiinflamatório e no tratamento da dependência de opióides. Dessa forma, o grande objetivo dos estudos era a identificação e o desenvolvimento de candidatos com ótimas propriedades biofarmacêuticas para serem utilizados em um estudo clínico posterior. Meu papel consistiu na avaliação da permeabilidade intestinal desses compostos, com foco na interação com transportadores de membrana, tanto de absorção quanto de efluxo, e também na avaliação da estabilidade metabólica.

Esses estudos culminaram na seleção de um candidato modificado que possui importante atividade farmacológica, bem como um bom perfil de permeabilidade e estabilidade frente às enzimas hepáticas. Adicionalmente, também foi identificada uma nova série de compostos ativos e estáveis metabolicamente, cujo esqueleto estrutural não é susceptível ao efluxo na barreira hemato-encefálica, característica essa de suma importância uma vez que o alvo farmacológico encontra-se no sistema nervoso central.

Constrained H-Phe-Phe-NH2 Analogues with High Affinity to the Substance P 1-7 Binding Site and with Improved Metabolic Stability and Cell Permeability

Rebecca Fransson,[a] Milad Botros,[b] Christian Sköld,[a] Jadel M. Kratz,[c,d] Richard Svensson,[c,e] Per Artursson,[c,e] Fred Nyberg,[b] Mathias Hallberg,[b] and Anja Sandström[a*]

[a] Department of Medicinal Chemistry, Uppsala University, Box 574, SE-751 23 Uppsala, Sweden
[b] Department of Pharmaceutical Biosciences, Uppsala University, Box 591, SE-751 24 Uppsala, Sweden.
[c] Department of Pharmacy, Uppsala University, Box 580, SE-751 23 Uppsala, Sweden.
[d] Programa de Pós-Graduação em Farmácia, Centro de Ciências da Saúde, Departamento de Ciências Farmacêuticas, Universidade Federal de Santa Catarina, 88.040-900, Florianópolis, SC, Brasil.
[e] The Uppsala University Drug Optimization and Pharmaceutical Profiling Platform, Uppsala University, Box 580, SE-751 23 Uppsala, Sweden.

Abstract

The N-terminal fragment of substance P (SP), the heptapeptide substance P 1-7 (SP1−7, H-Arg-Pro-Lys-Pro-Gln-Gln-Phe-OH), is a bioactive metabolite that has been shown to oppose several effects of SP. Specific binding sites for SP1−7 that differ from the NK1 receptor have been identified in both mouse and rat. To fully characterize the binding site for SP1−7 and to reveal the role of the heptapeptide in complex animal models, there is a need for drug-like low molecular weight SP1−7 mimetics. Recently, we reported the discovery of the small peptide H-Phe-Phe-NH2 as a high affinity ligand of the specific binding site for SP1−7. With the overall aim to develop stable and cell permeable SP1−7 mimetics for in-depth mechanistic studies, the dipeptide H-Phe-Phe-NH2 was chosen as a lead compound. Herein, we report the synthesis and SAR of a set of constrained and modified H-Phe-Phe-NH2 analogues evaluated in a binding assay displacing [3H]-SP1−7. Local constraints as methylation along the peptide backbone and rigidification by cyclization of the dipeptide were performed. The SAR obtained from the binding study was further rationalized using a pharmacophore search providing us with a plausible binding

conformation. Additionally, the potential active uptake by PepT1 transporter, intestinal permeability and metabolic stability of the dipeptides were evaluated. Taken together, we herein report on the identification of compound 8a, a C-terminal rigidified HPhe-Phe-NH2 analogue comprising a cis-3-phenyl-pyrrolidine moiety, with high affinity, improved stability and better cell-permeability.

Introduction

The undecapeptide substance P (SP, H-Arg-Pro-Lys-Pro-Gln-Gln-Phe-Phe-Gly-Leu-Met-NH2)[1] is a well known neurotransmitter and a neuromodulator in the central and peripheral nervous system. This neuropeptide is a member of the tachykinin family and is the endogenous ligand for the neurokinin-1 (NK-1) receptor.[2, 3] SP is degraded into several bioactive fragments of which the N-terminal metabolite SP 1–7 (SP1–7, H-Arg-Pro-Lys-Pro-Gln-Gln-Phe-OH) is the major one.[4-6]

SP1–7 has been shown to counteract the expression of naloxone provoked opioid tolerance and withdrawal, in contrast to SP and its C-terminal fragments that increase the opioid withdrawal signs.[7, 8] It has also been demonstrated that SP1–7 attenuates the inflammatory[9] and the nociceptive[10] effects exerted by SP. Additionally, it was recently observed that SP1–7 induces antihyperalgesia in diabetic mice which indicates a conceivable effect on neuropathic pain.[11] We find this observation particularly interesting since no satisfactory treatment of neuropathic pain is available today.[12] The effect seems to be mediated through an indirect activation of the naloxone-sensitive sigma receptor (σ1) system. However, SP1–7 itself is not an active ligand for the σ1 receptor.[11] Although most studies on SP1–7 have been done on rodents we believe in its relevance in humans due to firstly, the known presence of SP and SP degrading enzymes in human and secondly due to the presence of the heptapeptide fragment in human cerebrospinal fluid (CSF).[13,14] The biological effects observed for SP1–7 seem not to be mediated through any of the known tachykinin- or opioid receptors.

Even though the inhibitory effect of SP1–7 on SP induced behavior can be reversed by the non-selective opioid ligand naloxone, none of the specific antagonist for the opioid receptors (μ, δ and κ) can inhibit the effect.[15, 16] More likely, the effects of SP1–7 are generated via the specific binding sites that have been identified for this heptapeptide in rat and mouse spinal cord and brain, but of which the exact nature still is unknown.[17-19] We previously reported a structure–activity

relationship study (SAR) of the heptapeptide towards the specific binding site that revealed that the first four N-terminal amino acids in SP1–7 are not essential for binding since these could be substituted with an alanine or removed without significantly affecting the affinity.20 Interestingly, amidation of the C-terminal of SP1–7 resulted in a peptide with greater binding affinity towards the SP1–7 binding site as compared to the native heptapeptide (Ki = 0.3 nM and Ki = 1.6 nM, respectively). In analogy with the binding studies it was found that the amidated analogue of SP1–7 was more potent than SP1–7 in reducing abstinence symptoms in morphine dependent rats.[8]

In parallel with the SAR investigation of SP1–7 similar studies were performed on the endogenous μ-receptor agonist, endomorphin-2 (EM-2, H-Tyr-Pro-Phe-Phe-NH2).[21] The interest in this tetrapeptide originates from the observations by Botros et al.[18] where they have found that endomorphin-1 (EM-1, H-Tyr-Pro-Trp-Phe NH2) and EM-2 interact with the SP1–7 binding site. However, a significant difference in binding affinity between the two tetrapeptides was observed. EM-1 and EM-2 displayed a 1000-fold and a 10-fold lower affinity, respectively, compared to that of SP1–7. From the alanine scan and truncation study of EM-2 the same SAR trend as for SP1–7 was observed. The C-terminal was shown to be crucial for binding affinity to the SP1–7 binding site and substitution of the two amino acids in the N-terminal with an alanine resulted in only small differences in affinity. Truncation of EM-2 resulted in identification of the dipeptide H-Phe-Phe-NH2 (**1**) possessing a Ki value of 1.5 nM.

With the overall aim to develop stable and cell permeable SP1–7 mimetics for in-depth mechanistic studies, the dipeptide H-Phe-Phe-NH2 was chosen as a lead compound. Herein, we report the synthesis and SAR of a set of constrained H-Phe-Phe-NH2 analogues evaluated in a binding assay displacing [³H]-SP1–7. The compound series was further used to derive a pharmacophore model in order to generate a potential bioactive conformation. Additionally, the potential active uptake by PepT1 transporter, intestinal permeability and metabolic stability of the dipeptides were investigated.
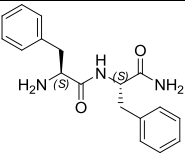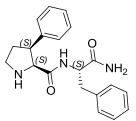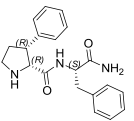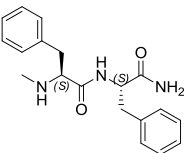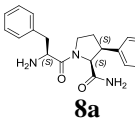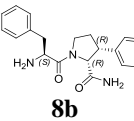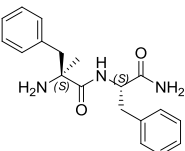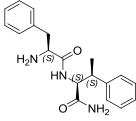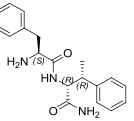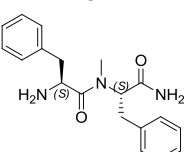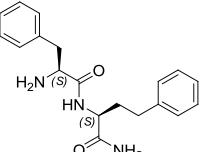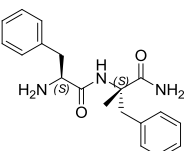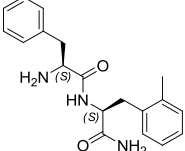
Results

Biological evaluation

The dipeptides **1–12** in Table 1 were prepared using solid-phase peptide synthesis. The compounds were evaluated in a binding assay

using spinal cord membrane from Sprague-Dawley rats and radioactive [^{3}H]-SP1–7 as tracer.[18] The binding affinities of compounds **1–12** for the SP1–7 binding site are summarized in Table 1.

Table 1. Binding affinity of H-Phe-Phe-NH$_2$ analogues to the SP1-7 binding site.

Compound	$K_i \pm S.E.M$	Compound	$K_i \pm S.E.M$
1	8.4 ± 0.4^a $(1.5 \pm 0.1)^b$	**7a** **7b**	33.9 ± 2.5^d 50.5 ± 1.5^d
2	189 ± 3	**8a** **8b**	$2.4 \pm 0.6^{d,e}$ 93.1 ± 0.2^d
3	70.4 ± 3.0	**9a** **9b**	17.5 ± 0.8^d 68.0 ± 1.2^d
4	9.4 ± 0.1^c	**10**	6.2 ± 0.2
5	26.0 ± 1.2	**11**	11.5 ± 0.1

6	136 ± 2
12	3.3 ± 0.2

[a] K_i-value determined at the same occasion as for **2–12**.
[b] Previously reported and determined K_i-value.[21]
[c] Tested in a mixture (92:8) of the opened and the ring closed diketopiperazine.
[d] Correspondence to each diastereomers undetermined.
[e] Tested once, at six different concentration, in triplicate.

Methylation of the peptide backbone giving analogues **2**, **3**, **5** and **6** resulted in lower affinity in general (K_i = 26–189 nM) except for compound **4** that maintained similar affinity as the original compound H-Phe-Phe-NH2 **1** (K_i = 9.4 nM and 8.4 nM, respectively). Rigidification of the N-terminal phenylalanine using a proline-based analogue resulted in reduced binding affinities (**7a** and **7b**, K_i = 33.9–50.5 nM). However, corresponding rigidification in the C-terminal phenylalanine gave **8a** and **8b**, of which one diastereomer showed improved binding affinity (IC_{50} = 2.4 nM) and one diastereomer lower binding affinity (K_i = 93.1 nM). A methyl group on the β-carbon in the C-terminal side chain as in compounds **9a** and **9b** reduced the binding affinity 2–8 times. Elongation of the side chain with one carbon gave compound **10**, which showed similar affinity as compound **1**. Furthermore, small modifications on the aromatic part of the C-terminal phenylalanine were well tolerated (cf. **1** with **11** and **12**).

Metabolic stability

The metabolic stability was determined by incubating the compounds with pooled human liver microsomes. *In vitro* half-life (t½) and *in vitro* intrinsic clearance (Clint) were calculated using previously published models and the results are presented in Table 2.[22, 23] The Clint can be of value to rank compounds and to give an estimation of the risk of first pass metabolism *in vivo*. A general classification is, Clint < 47 (µl/min/mg) no risk for high first metabolism *in vivo*, 47 < Clint < 92 moderate risk, and Clint > 92 high risk.

Table 2. Metabolic stability data of compounds **1–12**.[a]

Compound	Metabolic Stability Clint[b] (µl/min/mg)	Metabolic Stability t½[c] (min)
1	121 ± 39	12 ± 4
2	2.7 ± 1.5	597 ± 40
3	64 ± 11	22 ± 4
4	92 ± 0	15 ± 1
5	38 ± 15	40 ± 16
6	175 ± 5	7.9 ± 0.2
7a	28 ± 3	50 ± 6
7b	16 ± 9	103 ± 6
8a	16 ± 3	88 ± 15
8b	7.6 ± 1.9	187 ± 5
9a	39 ± 4	36 ± 3
9b	16 ± 7	98 ± 4
10	44 ± 6	32 ± 5
11	99 ± 5	14 ± 1
12	107 ± 12	13 ± 1

[a] Results are expressed as mean ± SD. All compounds were analysed at 100 µM. See experimental section for experimental conditions.
[b] Clint = *in vitro* intrinsic clearance.
[c] t½ = *in vitro* half-life.

In the methylated series, analogues **2**, **3**, and **5** resulted in more metabolic stable compounds with low or moderate risk for high first pass metabolism and increased half-life up to 50 times (cf. **1** with **2**). However, internal or C terminal methylation (**4** and **6**, respectively) did not improve the metabolic stability. In all the rigidified analogues the metabolic stability increased and the half-life became 4-16 times longer (cf. **1** with **7a–8b**). Furthermore, methylation at the β-carbon (compound **9a** and **9b**) or elongation of the phenylalanine (see compound **10**) also improved the metabolic stability while decoration of the aromatic ring of the C-terminal phenylalanine did not significantly influence the stability (cf. **1** with **11** and **12**).

Permeability and Uptake Experiments

The intestinal epithelial permeability, expressed as apparent permeability coefficients (P_{app}), was determined from transport rates across Caco-2 cell monolayers, as described previously.[24] The experiments were run in both apical to basolateral (a-b) and basolateral to apical (b-a) directions (Table 3). A P_{app} value below 0.2×10^{-6} cm/s indicates low permeability, a P_{app} value ranging from 0.2×10^{-6} cm/s to 1.6×10^{-6} cm/s moderate permeability and a P_{app} value above 1.6×10^{-6} cm/s indicates high permeability.[25]

Uptake studies with CHO-K1 and CHO-PepT1 cells (control and PepT1 stably transfected cells, respectively) were performed and the results are expressed as pmol/mg of protein/min. If the compounds are substrates for the peptide transporter PepT1 and actively transported into the cell the PepT1/K1 ratio should be greater than one.

The PepT1/K1 ratios for the synthesized compounds ranged from 0.6 (**11**) to 1.4 (**7a** and **7b**), which indicates that these compounds are not actively transported. However, the permeability data in the a–b direction showed that the methylated analogues **2–5** had high permeability (ranging from 9×10^{-6} cm/s to 20×10^{-6} cm/s) while the C-terminal methylated analogue (**6**) possessed moderate permeability. Thus, the cell permeability was significantly increased compared to H-Phe-Phe-NH2 (**1**, 0.02×10^{-6} cm/s). Furthermore, the cyclized analogues **7a**, **7b** and **8b** together with compound **9a** were classified to have moderate permeability (ranging from 0.5×10^{-6} cm/s to 0.8×10^{-6} cm/s) and the analogues **8a** and **9b** to have high permeability (3.6×10^{-6} cm/s and 4.4×10^{-6} cm/s, respectively). In contrast, the C-terminal modified analogues **10–12** showed only low permeability with P_{app} values ranging from 0.02×10^{-6} cm/s to 0.1×10^{-6} cm/s. Unfortunately, all the compounds displayed efflux, with a 3–95-fold higher transport rate in the b-a direction than the a-b direction.

Table 3. Uptake and permeability data of compounds **1–12**.[a]

Cmp.	Uptake (pmol/mg protein/min)			Caco-2 Permeability P_{app}[b] (10^{-6} cm/s)			
	CHO-PepT1	CHO-K1	Ratio	AB[c]	BA[d]	Ratio AB/BA	Ratio BA/AB
1	0.3±0.0	0.3±0.0	1.0	0.02±0.00	0.2±0.0	0.1	11
2	2.2±0.7	2.4±0.5	0.9	13.9±0.5	124±21	0.1	8.9
3	1.1±0.2	1.5±0.2	0.7	18.4±0.1	86.5±0.2	0.2	4.7

4	18.8±0.3	23.0±2.5	0.8	9.0±2.2	124±19	0.1	14
5	32.7±1.8	32.1±8.6	1.0	20.4±2.0	224±5	0.1	11
6	0.3±0.1	0.4±0.1	0.7	0.3±0.1	0.9±0.2	0.3	3.0
7a	30.9±4.1	22.3±2.2	1.4	0.5±0.0	26.3±1.0	0.0	53
7b	14.9±2.2	10.9±1.2	1.4	0.8±0.1	76.2±1.1	0.0	95
8a	13.1±2.3	11.2±1.3	1.2	3.6±0.4	75.1±2.1	0.1	21
8b	11.4±1.0	8.7±0.8	1.3	0.6±0.0	51.4±1.8	0.0	86
9a	0.6±0.1	0.7±0.0	0.9	0.7±0.0	5.4±0.4	0.1	8.4
9b	24.8±3.8	22.2±3.1	1.1	4.4±0.1	171±6	0.0	39
10	0.6±0.0	0.9±0.2	0.7	0.1±0.0	0.9±0.3	0.1	9.0
11	0.8±0.1	1.3±0.3	0.6	0.02±0.00	0.3±0.0	0.1	15
12	0.2±0.0	0.3±0.0	0.7	0.1±0.0	0.8±0.1	0.1	8.0

[a] Results are expressed as mean ± SD. All compounds were analysed at 100 μM. See experimental section for experimental conditions. [b] Paap = apparent permeability coefficient. [c] AB = apical to basolateral. [d] BA = basolateral to apical.

Pharmacophore search

In order to further investigate the SAR in the compound series and to derive a binding conformation we carried out a pharmacophore search in the compound series using Phase.[26] The dipeptides with Ki values of 10 nM or lower and known stereochemistry were defined as actives (**1**, **4**, **10**, and **12**). No compounds in the series were devoid of affinity but the three dipeptides with lowest affinity (Ki values of 70–190 nM) and known stereochemistry were defined as inactives (**2**, **3**, and **6**). With the requirement that all four active ligands should match the pharmacophore the maximum number of pharmacophore features in each compound that gave pharmacophore hypotheses was six. These hypotheses were further evaluated. Two sets of pharmacophore features were found among the hypotheses. One set which resulted in 242 hypotheses consisted of two hydrogen bond acceptors, one donor, one

positively charged group, and two aromatic rings. The other set was very similar with the difference that two hydrogen bond donors were included, one replacing the positively charged group. This set of pharmacophore features resulted in 2145 hypotheses. The hypotheses were scored by matching the actives to the pharmacophore hypotheses. The score formula used was the sum of the vector-, site-, and volume scores plus a score for rewarding a high number of matches. Because the number of actives matching the pharmacophore hypotheses was four in all cases the latter term was set to a constant 1. The other terms in the formula have the range 0–1, which gives a matching score range of 1–4. With the default filter and complete clustering 39 hypotheses with scores of 3.42–3.65 remained after scoring. A final score for each hypothesis was derived by subtracting the matching scores of the inactives from the score obtained matching the actives, resulting in scores of 0.77–1.57. The ten pharmacophore hypothesis clusters with the highest final scores where visually inspected and the dipeptides excluded from the set of actives were aligned to the hypotheses, required to match all six pharmacophore features. The analysis showed that the top hypothesis indeed represented a plausible pharmacophore in the active dipeptides and is shown in Figure 1 with fitness scores for the compounds presented in Table 4.

The other pharmacophore hypotheses inspected had either problem explaining the affinity of the rigidified analogues (e.g. neither **8a** nor **8b** could match the hypothesis although one of them has the highest affinity in the series) or some of the inactive compounds had a high fitness score. Although the top scoring hypothesis also suffered from a rather high fitness score of the inactive compounds **2** and **6**, their scores could be rationalized by a good alignment of all but one pharmacophore feature in each compound, resulting in a fairly low penalty to their scores.
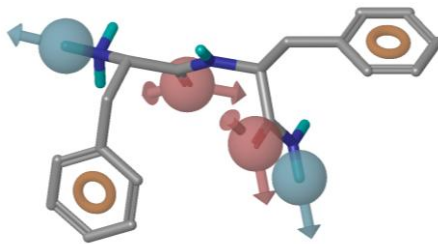
Figure 1. The top score pharmacophore shown with **1** aligned.

Table 4. Fitness score for the alignment to the pharmacophore for compounds **1–12** and their set membership.

Compound	Fitness[a]	Set
1	3	Active
2	2.19	Inactive
3	1.7	Inactive
4	2.58	Active
5	2.27	Test
6	2.07	Inactive
7a	1.38	Test
7b	0.38	Test
8a	2.65	Test
8b	1.13	Test
9a	2.7	Test
9b	0.69	Test
10	2.14	Active
11	2.92	Test
12	2.96	Active

[a] The sum of the vector-, site-, and volume scores (range 0–3).
[b] Active = compounds used for generating pharmacophore hypotheses, Inactive = compounds used to penalize questionable hypotheses that match inactives, Test = compounds used for validating the hypotheses.

Discussion

A potential specific receptor for the N-terminal partial sequences of SP in mouse spinal cord was discussed already in the beginning of the 1980s[27] but it was not until 1990, when it was found that the binding was specific, saturable, and reversible, that the hypothesis of a specific SP1–7 receptor was proposed.[17] During the 1990s the biological roles of the N-terminal fragment of SP were investigated by several groups[7, 15, 28, 29] More recently the SAR of SP1–7 and other ligands (e.g. EM-2) have been investigated by our group leading to the discovery of dipeptides with high affinity to the SP1–7 binding site.[20, 21]

In the present study we are currently addressing the challenging task to transform these dipeptides into compounds with more drug-like features. One way to achieve this is to introduce local constrains in the peptide backbone by incorporation of N-methyl amino acids. The advantage of incorporating a single methyl group is that it provides a

balance between decreasing conformational entropy sufficient to change the binding affinity whilst still allowing sufficient conformational flexibility for the ligand to adopt the conformation required for molecular recognition to the target. Furthermore, the incorporation of a methyl group often provides metabolic stability due to resistance to proteolytic degradation.[30, 31] In the dipeptides series presented herein we introduced a methyl group in each position along the backbone of the dipeptide H-Phe-Phe-NH2. Highest influence on binding affinity is seen when substituting the N-terminal amine or the C-terminal amide with a methyl group (**2** and **6**, respectively), resulting in reduced binding affinities by 17–23 times. A possible explanation for this can be seen when looking at the proposed pharmacophore in the series (Figure 2). The pharmacophore presented proposes six important interactions features that all high affinity compounds can present to the target protein, namely two hydrogen bond acceptors, two hydrogen bond donors and two aromatic rings. In **2** the methyl group on the N-terminus is positioned in the direction of the hydrogen bond donor vector from the amine to the protein in the pharmacophore.

The hydrogen bond donor feature assigned to the amine would also be compatible with a positively charged feature in the series and this was also found in other pharmacophore hypotheses. However, if that was the case the directional property of the feature would be lost and **2** would have a higher fitness to the pharmacophore. The reduced affinity observed for **6,** in which the primary amide was methylated to a secondary amide, is also accounted for in the pharmacophore. This is because the hydrogen bond pattern for the C-terminal amide is optimal for a primary amide as can be seen in Figure 2 where **6** is aligned to the pharmacophore, unable to match this hydrogen bond donor feature. When **1** was methylated on the internal nitrogen no influence on the affinity potency could be observed (see compound **4**). It is well known that internal methylated dipeptides often undergo ring closure to the corresponding diketopiperazine.[32] Since the opened analogue equilibrated with the diketopiperazine formation, was compound **4** tested in a mixture of the opened and the ring closed formation.

To investigate the spatial arrangement of the phenylalanine side chain and the effect of a more strongly rigidified HPhe-Phe-NH2 analogues the compounds with side chain constrains **7a**–**8b** were synthesized. This modification showed to be stereochemically depending, which is expected in a defined receptor pocket. When introducing the cis-3-phenyl-pyrrolidine moiety in the N-terminal (**7a** and **7b**) the affinity dropped 4–6 times. Both these diastereomers show

low fitness scores to the proposed pharmacophore, which indicates that the compounds have problems obtaining an optimal binding conformation. Interestingly however, when the cis-3-phenyl-pyrrolidine moiety was incorporated in the C-terminal the phenyl group seems to be positioned well in the active binding site in one of the diastereomers, resulting in almost four times higher binding affinity. Comparing **8a** and **8b,** a clear difference in fitness to the pharmacophore is seen, supporting the (*S,S*) configuration of the cis-3-phenyl-pyrrolidine in the high affinity analogue **8a**.

Compound **2**

Compound **6**

Figure 2. Compounds **2** and **6** aligned to the pharmacophore.

A β-methylation of the phenylalanine side chain can have an effect on how the side chain interacts with the binding site.[33] When a methyl group was introduced on the β-carbon in the C-terminal phenylalanine in **1** a 4-fold difference between the (*S,S*)- and the (*R,R*)-configuration could be observed (cf. **9a** with **9b**).

Compound **8a**

Compound **8b**

Figure 3. Compounds **8a** and **8b** aligned to the pharmacophore.

Inspecting the fitness scores of the two diastereomers when matched to the pharmacophore supports **9a** with the (*S*,*S*) configuration of the β-methylphenylalanine as the analogue with highest binding affinity. Furthermore, a β-methylation reduces the conformational flexibility of the phenylalanine side chain by imposing a steric rotational constraint, which can be advantageous by reducing entropic penalty upon binding. However, this was not advantageous for the binding since **1** possessed 2 times higher binding affinity compared to **9a**.

Elongation of the C-terminal phenylalanine side chain was well tolerated (cf. **1** with **10**) which indicates that there is room for modification in this part of the molecule. Interestingly, in the previous SAR investigation that led to identification of H-Phe-Phe-NH2 the replacement of the C-terminal phenylalanine for a phenylglycine resulted in a completely inactive compound and even replacing the

phenyl ring with thiophene resulted in significantly lower affinity.[21] Moreover, the binding pocket seems to tolerate substituents on the aromatic moiety since both compound **11** and compound **12** showed great binding affinities, especially compound **12** (Ki = 3.3 nM) in which a hydrogen in meta position has been exchanged by a fluorine atom. This is somewhat contradictory to the result of the previous SAR investigation where the same C-terminal amino acids as in **11** and **12** in combination with O-methylated tyrosin and cyclohexylalanine as the N-terminal amino acids, respectively, was devoid of affinity to the SP1–7 binding site. However, in the latter case the main problem might be that the change in both terminal parts was done concurrently, which gave a negative synergistic effect upon binding. Altogether, it seems that C-terminal changes are allowed if the N-terminal is preserved.

The *in vitro* pharmacokinetic properties of the compounds were studied, i.e. uptake, permeability and metabolic stability. The metabolic stability study was concentrated to the liver since this tissue constitutes the major site of metabolism for most drugs.[22] By using the *in vitro* parameter intrinsic clearance (CLint) we can describe the rate of metabolism of the compounds under *in vivo* conditions, which gives an indication of which compounds to choose for further development.[23] Methyl groups along the peptide backbone can increase the metabolic stability. Indeed, the stability increased for all the methylated analogues of H-Phe-Phe-NH2 except for the internal (**4**) and the C-terminal (**6**) N-methylated analogues. However, the apparent instability of the internal N-methylated compound is partly explained by the fact that the opened analogue was in equilibrium with the diketopiperazine form as mentioned earlier. To our satisfaction, the rigidified analogues of H-Phe-Phe-NH2 not only resulted in metabolically more stable compounds (**7a–8b**) but also in the most potent binder **8a**. In fact, **8a** turned out to be 7 times more stable than H-Phe-Phe-NH2, which makes this analogue a good candidate for replacing **1** in further animal studies. Modifications of the C-terminal phenylalanine in form of elongation as in compound **10** or β-methylation also improved the stability. However, *ortho*-methyl and *meta*-fluoro substitutions on the aromatic part of the phenylalanine do not seem to have any effect on the metabolism as compared to H-Phe-Phe-NH2 (**1**) itself.

Furthermore, the membrane permeability and the transport mechanism of the analogues in this series were investigated. The di/tri-peptide transporter PepT1 is expressed in the intestine and ensures efficient absorption of small peptides from digestion of dietary proteins. PepT1 is also important for absorption of a variety of peptidomimetic

drugs, such as β-lactam antibiotics and angiotensin converting enzyme (ACE) inhibitors.[34, 35] In order to achieve efficient binding and activation of the transporter some important structural features of dipeptides need to be fulfilled: 1) No substitution at the N-terminal amine, 2) A negatively charged C-terminus, 3) A amide carbonyl oxygen and 4) the interaction of the N-and C-terminal amino acids side chain with a proposed hydrophobic pocket, preferably aromatic groups.[36-38] Thus, an efficient transport with PepT1 was not expected for the synthesized dipeptides herein, all with primary amides in the C-terminal. However, the aromaticity, the dipeptides character and the fact that dipeptides with C-terminal amides have been shown to be PepT1 substrates motivated us to investigate if the dipeptides in this series, could be actively transported over the membrane. The uptake studies using CHO cells transfected with the transporter PepT1 however indicated that the compounds are no good substrates for this transport system (see PepT1/K1 ratio in Table 3; all around 1). A very weak increase of PepT1 activation could be seen for the dipeptides incorporating the cis-3-phenyl-pyrrolidine moiety (**7a–8b)**, and this might be explained by the study of Vig et al.[39] were they demonstrated that dipeptides with a proline at the C- or N-terminal with the proper attendant amino acid exhibits both high affinity and activation of the PepT1 transporter. Although the compounds were not actively transported, the permeability data in the a–b direction generally indicated that the analogues had moderate or high permeability, which in contrast to H-Phe-Phe-NH2 (**1**) indicates that these compounds indeed are cell permeable. Satisfyingly, compound **8a** with highest binding affinity (IC_{50} = 2.4 nM) also possessed high permeability (3.6 x 10^{-6} cm/s).

The efflux transporter P-glycoprotein (PgP) has an important role in limiting entry of various drugs in to the central nervous system which makes it an important factor to consider when working with CNS active compounds.[40] All of the analogues studied in here displayed a large efflux (the ba/ab ratio ranging from 3-95), which might be explained by interactions with PgP. Nevertheless, in the Caco-2 cells other efflux transporters are present and could be involved in the secretion of the compounds. To be noticed though is that the efflux was substantially lower for the methylated analogues (**2–6**) compared to the rigidified ones (**7a–8b**). Thus, an important molecular feature for PgP substrates is the ability to form hydrogen bonds with PgP which might be the explanation for the lowered efflux of the methylated series.[41] Also the stereochemistry seemed to influence the efflux since there were big

differences in the ba/ab ratios between all the diastereomeres (cf. **7a** and **7b**, **8a** and **8b**, **9a** and **9b**).

Conclusion

A series of constrained and modified dipeptides analogues of H-Phe-Phe-NH2 has been synthesized and evaluated regarding their binding affinity, uptake, permeability and metabolic stability. Local constraints as methylation along the peptide backbone and rigidification by cyclization delivered compounds with increased metabolic stability and generally improved cell-permeability. Unfortunately, the propensity for efflux was not reduced. Compound **8a**, a C-terminal rigidified H-Phe-Phe-NH2 analogue comprising a cis-3-phenyl-pyrrolidine moiety with *S*,*S* configuration as supported by pharmacophore analysis, was the only compound with both improved stability and cell permeability and that also retained high affinity to the SP1–7 binding site. Moreover, in this study it seems like it is allowed to make changes in the C-terminal, e.g. substitution with *ortho*-methyl or *meta*-fluoro in the aromatic part or elongation of the phenylalanine side chain without any loss in binding affinity. Taken together, we herein report the identification of optimized H-Phe-Phe-NH2 analogues with not only better binding affinity but also better stability and cell permeability. The stable and cell permeable compound **8a** will serve as a good starting point in future development of novel SP1–7 analogues that can be used as a research tools in animal models to clarify the physiological role of SP1–7 and its specific binding site.

Experimental

General Methods

Preparative RP-HPLC was performed on a system equipped with a Zorbax SB-C8 column (150 × 21.2 mm) or a 10 μm Vydac C18 column (250 × 22 mm), in both cases with UV detection at 230 nm. Analytical RP-HPLC-MS was performed on a Gilson-Finnigan ThermoQuest AQA system (Onyx monolithic C18 column, 50 × 4.6 mm; MeCN/H$_2$O gradient with 0.05% HCOOH) in ESI mode, using UV (214 and 254 nm) and MS detection. The purity of each of the peptides was determined by RP-HPLC using the columns: ACE 5 C18 (50 × 4.6 mm) and ACE 5 Phenyl (50 x 4.6 mm) or Thermo Hypersil Fluophase

RP (50 x 4.6 mm) with a H_2O/MeCN gradient with 0.1% TFA and UV detection at 220 nm. All peptides showed purity above 95%.

NMR spectra were recorded on a Varian Mercury plus spectrometer (^{1}H at 399.8 MHz and ^{13}C at 100.5 MHz or ^{1}H at 399.9 MHz and ^{13}C at 100.6 MHz) at ambient temperature. Chemical shifts (δ) are reported in ppm referenced indirectly to TMS via the solvent residual signal. Exact molecular masses were determined on a Micromass Q-Tof2 mass spectrometer equipped with an electrospray ion source at the Department of Pharmaceutical Biosciences, Uppsala University, Sweden. All other chemicals and solvents were of analytical grade from commercial sources.

General synthesis of peptides **1-12**

Coupling

The peptides **1-12** were synthesized manually from Rink Amide MBHA resin (0.66 mmol/g) or Methyl Indole AM resin (0.63 mmol/g) in 2 mL disposable syringes fitted with porous polyethylene filter. Standard Fmoc conditions were used and the Fmoc protecting group was removed by treatment with 20% piperidine in DMF (2×1.5 mL, 2 + 10 min) and the polymer was washed with DMF (6×1.5 mL, 6×1 min). Coupling of the appropriate amino acid, Fmoc-AA-OH (1.5 or 4 equiv) was performed in DMF (1.5 mL) using *N*-[(1*H*-benzotriazole-1-yl)-(dimethylamino)methylene]-*N*-methylmethanaminium hexafluorophosphate *N*-oxide (HBTU, 1.5 or 4 equiv.) in the presence of DIEA (3 or 8 equiv). The resin was washed with DMF (5×1.5 mL, 5×1 min) and subsequently deprotected and washed as described above. After completion of the coupling cycle the resin was also washed with several portions of DMF, CH_2Cl_2 and MeOH before it was dried in a vacuum overnight.

Cleavage

The final peptide was cleaved from the resin by treatment with triethylsilane (100 µL) and 95% aqueous trifluoroacetic acid (TFA, 1.5 mL) followed by agitation for 2 h in room temperature. The resin was filtered off and washed with TFA (2×0.3-0.5 mL). The filtrate was collected in a centrifuge tube and concentrated in a stream of nitrogen. Cold diethyl ether (≤ 7 mL) was used to precipitate the product, which

was collected by centrifugation, washed with cold diethyl ether ($\leq 3 \times 7$ mL) and dried.

Purification

The crude peptide was dissolved in MeCN/0.1% aqueous TFA, filtered through a 0.45 µm nylon membrane and purified in 1-2 runs by RP-HPLC. Selected fractions were analyzed by RP-HPLC and RP-HPLC-MS, and those containing pure product were pooled and lyophilized. The reported yields are based on the loading of the starting resin.

Peptide 1 (H-Phe-Phe-NH2)

The crude peptide was purified to yield 23 mg (37%). HPLC purity: C18-column > 99%, Fluophase > 98%. Spectral data was in agreement with previous reports.[21]

Peptide 2 (N-Me-Phe-Phe-NH2)

The crude peptide was purified to yield 14.8 mg (45%). HPLC purity: C18-column > 99%, Fluophase > 98%. ^{1}H-NMR (MeOD) δ 2.11 (s 3H), 2.79 (dd, *J* = 10.4, 13.9 Hz, 1H), 3.05-3.15 (m, 2H), 3.21 (dd, *J* = 5.0, 13.9 Hz, 1H), 3.86-3.93 (m, 1H), 4.77 (dd, *J* = 5.0, 10.4 Hz, 1H), 7.18-7.36 (m, 10H). ^{13}C-NMR (MeOD) δ 32.1, 37.9, 39.3, 55.5, 64.1, 127.9, 129.0, 129.5, 130.2, 130.5, 130.51, 135.0, 138.4, 167.7, 174.8. HRMS (M + H$^+$): 326.1870, $C_{19}H_{23}N_3O_2$ requires 326.1869.

Peptide 3 (α-Me-Phe-Phe-NH2)

The crude peptide was purified to yield 3.6 mg (11.2%). HPLC purity: C18-column > 98%, Fluophase > 99%. ^{1}H-NMR (MeOD) δ 1.38 (s, 3H), 2.98 (dd, *J* = 10.1, 13.9 Hz, 1H), 3.30 (d, *J* = 14.4 Hz, 1 H), 3.23 (dd, *J* = 5.2, 13.9 Hz, 1H), 3.31 (d, *J* = 14.4 Hz, 1H), 4.78 (dd, *J* = 5.2, 10.1 Hz, 1H), 7.2-7.36 (m, 10H). ^{13}C-NMR (MeOD) δ 22.8, 39.2, 43.7, 55.7, 61.8, 127.9, 129.1, 129.5, 130.0, 130.4, 131.4, 134.2, 138.4, 171.5, 175.5. HRMS (M + H$^+$): 326.1866, $C_{19}H_{23}N_3O_2$ requires 326.1869.

Peptide 4 (Phe-N-Me-Phe-NH2)

The crude peptide was purified to yield 9.8 mg (30.1%). HPLC purity: C18-column 94.6%, Fluophase > 92.1. ^{1}H-NMR (MeOD) δ 2.82 (s, 3H), 2.95-3.15 (m, 4H), 4.51 (dd, J = 6.5, 7.6 Hz, 1H), 5.21 (dd, J = 7.4, 8.6 Hz, 1H), 7.13-7.39 (m, 10H). ^{13}C-NMR (MeOD) δ 32.69, 35.51, 37.98, 53.31, 60.31, 127.89, 129.03, 129.66, 130.09, 130.25, 130.59, 135.18, 138.41, 170.28, 173.66. HRMS (M + H$^+$): 326.1866, $C_{19}H_{23}N_3O_2$ requires 326.1869.

Peptide 5 (Phe-α-Me-Phe-NH2)

The crude peptide was purified to yield 17.3 mg (53.2%). HPLC purity: C18-column > 99%, Fluophase > 99%. ^{1}H-NMR (MeOD) δ 1.46 (s, 3H), 2.97 (dd, J = 9.5, 14.2 Hz, 1H), 3.14 (dd, J = 5.6, 14.2 Hz, 1H), 3.25 (d, J = 13.4 Hz, 1H), 3.37 (d, J = 13.4 Hz, 1H), 4.10 (dd, J = 5.6, 9.5 Hz, 1H), 7.1-7.4 (m, 10H). ^{13}C-NMR (MeOD) δ 23.9, 38.6, 41.5, 55.9, 61.8, 127.99, 128.9, 129.2, 130.2, 130.4, 131.7, 135.9, 137.5, 168.9, 178.2. HRMS (M + H$^+$): 326.1866, $C_{19}H_{23}N_3O_2$ requires 326.1869.

Peptide 6 (Phe-Phe-NHMe)

The crude peptide was purified to yield 25.7 mg (79.1%). HPLC purity: C18-column > 99%, Fluophase > 99%. ^{1}H-NMR (MeOD) δ 2.65 (bs, 3H), 2.95 (dd, J = 7.6, 13.7 Hz, 1H), 3.03 (dd, J = 8.2, 14.2 Hz, 1H), 3.07 (dd, J = 7.4, 13.7 Hz, 1H), 3.23 (dd, J = 5.7, 14.2 Hz, 1H), 4.09 (dd, J = 5.7, 8.2 Hz, 1H), 4.55 (dd, J = 7.4, 7.6 Hz, 1H), 7.16-7.38 (m, 10H). ^{13}C-NMR (MeOD) δ 26.2, 38.5, 39.2, 55.5, 56.6, 127.9, 128.8, 129.5, 130.1, 130.2, 130.5, 135.5, 138.1, 169.4, 173.1. HRMS (M + H$^+$): 326.1870, $C_{19}H_{23}N_3O_2$ requires 326.1869.

Peptide 7a (Cis-3-phenyl-pyrrolidine-Phe-NH2)

The crude peptide was purified to yield 5.4 mg (32%). HPLC purity: C18-column > 99%, Fluophase > 99%. ^{1}H-NMR (MeOD) δ 2.35-2.50 (m, 2H), 2.77 (dd, J = 7.5, 13.7 Hz, 1H), 3.00 (dd, J = 6.5, 13.7 Hz, 1H), 3.38 (m, J = 7.4, 9.7, 11.4 Hz, 1H), 3.73 (m, J = 3.6, 7.8, 11.4 Hz, 1H), 3.88 (ddm, J = 7.4, 9.3 Hz, 1H) 4.33 (dd, J = 6.5, 7.5 Hz, 1H), 4.48 (d, J = 9.3 Hz, 1H) 7.15-7.40 (m, 10H). ^{13}C-NMR (MeOD) δ 31.63, 39.41, 46.62, 48.23, 55.53, 64.82, 127.82, 129.21, 129.41 (2C),

129.93, 130.34, 137.60, 137.99, 167.12, 173.84. HRMS (M + H$^+$): 338.1875, $C_{20}H_{23}N_3O_2$ requires 338.1869.

Peptide 7b (Cis-3-phenyl-pyrrolidine-Phe-NH2)

The crude peptide was purified to yield 9.3 mg (55%). HPLC purity: C18-column > 99%, Fluophase > 99%. ^{1}H-NMR (MeOD) δ 2.20 (dd, J = 5.9, 13.6 Hz, 1H), 2.41-2.49 (m, 2H), 2.50 (dd, J = 8.6 13.6 Hz 1H), 3.42 (ddm, J = 8.7, 11.2 Hz, 1H), 3.75 (dd, J = 5.4, 11.2 Hz 1H), 3.89 (dm, J = 8.8 Hz, 1H) 4.11 (dd, J = 5.9, 8.6 Hz, 1H), 4.55 (d, J = 9.3 Hz, 1H) 6.94-6.99 (m, 2H), 7.16-7.36 (m, 8H). ^{13}C-NMR (MeOD) δ 31.50, 38.58, 46.76, 48.38, 56.02, 64.65, 127.88, 129.19, 129.51, 129.64, 129.84, 130.18, 137.57, 137.70, 167.44, 178.22. HRMS (M + H$^+$): 338.1870, $C_{20}H_{23}N_3O_2$ requires 338.1869.

Peptide 8a (Phe-Cis-3-phenyl-pyrrolidine-NH2)

The crude peptide was purified to yield 14.2 mg (42%) in a 2:1 ratio (8a:8b) calculated from NMR. HPLC purity: C18-column 70%, Fluophase 70%, due to presence of 8b. ^{1}H-NMR (MeOD) δ 2.18 (m, J = 1.03, 6.3, 12,3 Hz, 1H), 2.67 (m, J = 8.6 10.6, 12.3 Hz, 1H), 3.04 (dd, J = 7.7, 14.4 Hz, 1H), 3.35 (dd, J = 6.0, 14.4 Hz, 1H), 3.59-3.74 (m, 3H), 4.38 (dd, J = 6.0, 7.7 Hz, 1H), 4.75 (d, J = 8.7 Hz, 1H), 7.11 (m, 1H), 7.21-7.53 (m, 9H). ^{13}C-NMR (MeOD) δ 29.56, 38.30, 47.75, 47.95, 54.06, 65.61, 128.59, 129.17, 129.43, 129.44, 130.13, 130.71, 135.51, 137.49, 168.40, 174.46. HRMS (M + H$^+$): 338.1865, $C_{20}H_{23}N_3O_2$ requires 338.1869.

Peptide 8b (Phe-Cis-3-phenyl-pyrrolidine-NH2)

The crude peptide was purified to yield 11.2 mg (33%). HPLC purity: C18-column > 99%, Fluophase > 99%. ^{1}H-NMR (MeOD) δ 1.92 (m, J = 1.2, 6.2, 13,2 Hz, 1H), 2.58 (m, J = 8.5, 10.7, 11.8, 13.2 Hz, 1H), 2.73 (m, J = 6.2, 9.6, 10.9 Hz, 1H), 3.17 (d, J = 7.6 Hz, 2H), 3.31 (m, J = 8.6 Hz, 1H), 3.84 (m, J = 1.2, 8.5, 9.7 Hz, 1H), 4.42 (t, J = 7.6 Hz, 1H), 4.53 (d, J = 8.6 Hz, 1H), 7.11 (m, 1H), 7.21-7.45 (m, 10H). ^{13}C-NMR (MeOD) δ 30.07, 37.70, 47.64, 47.72, 54.16, 65.54, 128.94, 129.25, 129.42, 129.49, 130.31, 130.85, 135.36, 137.79, 168.49, 173.78. HRMS (M + H$^+$): 338.1865, $C_{20}H_{23}N_3O_2$ requires 338.1869.

Peptide 9a (Phe-β-Me-Phe-NH2)

The crude peptide was purified to yield 4.7 mg (29%). HPLC purity: C18-column > 98.4%, Fluophase > 97.8%. ^{1}H-NMR (MeOD) δ 1.31 (dd, J = 1.6, 7.1 Hz, 3H), 2.95 (dd, J = 8.4, 14.3 Hz, 1H), 3.13-3.21 (m, 2H), 3.93 (ddd, J = 1.6, 5.0, 8.4 Hz, 1H), 4.65 (dd, J = 1.6, 9.7 Hz, 1H) 7.16-7.40 (m, 10H). ^{13}C-NMR (MeOD) δ 19.9, 38.4, 42.9, 55.2, 59.6, 128.0, 128.8, 128.9, 129.6, 130.2, 130.5, 135.3, 144.0, 169.1, 175.2. HRMS (M + H$^+$): 326.1863, $C_{19}H_{23}N_3O_2$ requires 326.1869.

Peptide 9b (Phe-β-Me-Phe-NH2)

The crude peptide was purified to yield 4.5 mg (28%). HPLC purity: C18-column > 99%, Fluophase > 99%. ^{1}H-NMR (MeOD) δ 1.29 (dd, J = 0.9, 7.0 Hz, 3H), 2.42 (dd, J = 8.9, 14.5 Hz, 1H), 2.57 (dd, J = 5.0, 14.5 Hz, 1H), 3.13 (ddm, J = 6.7, 9.9 Hz, 1H), 3.95 (dd, J = 5.0, 8.9 Hz, 1H) 4.66 (dd, J = 0.9, 9.9 Hz, 1H), 6.96-7.01 (m, 2H), 7.17-7.33 (m, 8H). ^{13}C-NMR (MeOD) δ 19.6, 38.3, 43.4, 55.4, 59.4, 128.1, 128.8, 128.9, 129.7, 130.1, 130.3, 135.3, 144.1, 169.1, 175.5. HRMS (M + H$^+$): 326.1868, $C_{19}H_{23}N_3O_2$ requires 326.1869.

Peptide 10 (Phe-homoPhe-NH2)

The crude peptide was purified to yield 21.8 mg (67%). HPLC purity: C18-column > 99%, Fluophase > 99%. ^{1}H-NMR (MeOD) δ 1.91-2.15 (m, 2H), 2.60-2.77 (m, 2H), 3.06 (dd, J = 8.5, 14.2 Hz, 1H), 3.31 (dd, J = 5.9, 14.3 Hz, 1H), 3.19 (dd, J = 5.9, 8.5 Hz, 1H) 4.41 (dd, J = 5.4, 8.5 Hz, 1H), 7.14-7.40 (m, 10H). ^{13}C-NMR (MeOD) 33.0, 35.4, 38.6, 54.4, 55.6, 127.2, 128.9, 129.4, 129.5, 130.2, 130.6, 135.6, 142.4, 169.6, 175.8. HRMS (M + H$^+$): 326.1873, $C_{19}H_{23}N_3O_2$ requires 326.1869.

Peptide 11 (Phe-Phe(3-F)-NH2)

The crude peptide was purified to yield 12.9 mg (40%). HPLC purity: C18-column 98.9%, Fluophase 98.7%. ^{1}H-NMR (MeOD) δ 2.98 (s, 3H), 3.00 (dd, J = 7.6, 14.0 Hz, 1H), 3.02 (dd, J = 8.4, 14.3 Hz, 1H), 3.12 (dd, J = 7.6, 14.0 Hz, 1H), 3.25 (dd, J = 5.7, 14.3 Hz, 1H), 4.09 (dd, J = 5.7, 8.4 Hz, 1H) 4.66 (dd, J = 7.6, 7.6 Hz, 1H), 7.07-7.21 (m, 4H), 7.26-7.41 (m, 5H). ^{13}C-NMR (MeOD) 19.6, 36.5, 38.6, 54.7, 55.5,

127.0, 128.0, 128.9, 130.2, 130.5, 130.8, 131.4, 135.5, 136.1, 137.9, 169.3, 175.3. HRMS (M + H$^+$): 326.1866, $C_{19}H_{23}N_3O_2$ requires 326.1869.

Peptide 12 (Phe-Phe(2-Me)-NH2)

The crude peptide was purified to yield 12.4 mg (38%). HPLC purity: C18-column > 99%, Fluophase > 99%. ^{1}H-NMR (MeOD) δ 2.98 (dd, J = 8.4, 13.9 Hz, 1H), 3.01 (dd, J = 8.5, 14.3 Hz, 1H), 3.15 (dd, J = 6.3, 13.9 Hz, 1H), 3.26 (dd, J = 5.4, 14.3 Hz, 1H) 4.08 (dd, J = 5.4, 8.5 Hz, 1H) 4.66 (dd, J = 6.3, 8.4 Hz, 1H), 6.92-7.00 (m, 1H), 7.01-7.13 (m, 2H), 7.26-7.40 (m, 6H). ^{13}C-NMR (MeOD) 38.6, 38.7, 55.5, 55.7, 114.6 (J= 21.4 Hz), 117.0 (J = 21.7 Hz), 126.2 (J = 2.77 Hz), 128.9, 130.2, 130.5, 131.2 (J = 8.29 Hz), 135.4, 141.0 (J = 7.56 Hz), 164.3 (J = 244.4 Hz), 169.5, 174.9. HRMS (M + H$^+$): 330.1621, $C_{18}H_{20}N_3O_2F$ requires 330.1618.

[2,4-DehydroPro]SP1-7

The precursor peptide for tritium-labeling [2,4-DehydroPro]SP$_{1-7}$ was prepared by standard solid-phase peptide synthesis techniques using Fmoc/t-butyl protection and purified as described above. Tritium labeling of the precursor was performed by Amersham Biosciences (Cardiff, UK) and resulted in 370 MBq (10 mCi) of [^{3}H]-SP1-7 with a specific activity of 3.11 TBq/mmol (84 Ci/mmol).

Animal experiment and membrane preparation

The preparations of receptor membranes were conducted using spinal cords from male Sprague–Dawley rats. The rats (Alab AB, Sollentuna, Sweden), weighing 200–250 g, were housed in groups of four in air-conditioned rooms (22–23 °C and a humidity of 50–60%) under an artificial light–dark cycle and had free access to food and water. Prior to tissue sampling the rats were allowed to adapt to the laboratory environment for 1 week. The animals (n=15) were killed by decapitation and the spinal cords were rapidly removed and quickly frozen. Tissues were then kept at −80 °C until analyzed. The animal experiment was approved by the local ethical committee in Uppsala, Sweden.

The frozen spinal cords weighing approximately 250–300 mg/animal, were thawed and placed on ice before being homogenized

for 30 s in 30 volumes of ice-cold 50 mM Tris–HCl buffer (pH 7.4), containing 5 mM KCl and 120 mM NaCl, using a Polytron homogenizer. The homogenate was then centrifuged at $40,000 \times$ g for 20 min at 4°C and the supernatant was discarded. The resulting pellet was re-suspended in 30 volumes of ice-cold 50 mM Tris–HCl buffer (pH 7.4), containing 300 mM KCl and 10 mM EDTA. Following incubation on ice for 30 min the sample was centrifuged at $40,000 \times$ g for 20 min at 4°C. The pellet obtained was diluted and homogenized in 30 volumes of ice-cold 50 mM Tris–HCl, containing 0.02% BSA, 5 mM, EDTA, 3 mM $MnCl_2$ and 40 µg bacitracin and re-centrifuged twice as described above. The final pellet was re-suspended and homogenized in 5 volumes of ice-cold 50 mM Tris–HCl buffer (pH 7.4) and immediately frozen at −80°C until used in binding studies. The protein concentration of the membrane suspension was determined according to the method of Lowry[41] using bovine serum albumin as protein standard.

Radioligand Binding assay

Assessment of the binding affinity for the various compounds analyzed in this study was carried out using the analogue [³H]-SP1–7 as tracer. Assays were performed in tubes containing 50 µl of spinal cord membrane suspension (200 µg protein) and 0.9 nM of [³H]-SP1–7 (specific activity: 3.11 TBq/mmol (84 Ci/mmol)) in a final volume of 0.5 ml 50 mM Tris binding buffer (pH 7.4), containing, 3 mM $MnCl_2$, 0.2% BSA and peptidase inhibitors (40 µg/ml bacitracin, 4 µg/ml leupeptin, 2 µg/ml aprotinin and 4 µg/ml phosphoramidon). The amount of total and unspecific binding in percent of the total radioactivity added were approximately 7% and 1.7%, respectively. The competition experiments were determined at six different concentrations varying between 0.01 nM and 1 µM of unlabeled compounds. Non-specific binding was determined in the presence of 1 µM SP1–7. Samples were incubated for 60 min at 4°C before being terminated by rapid filtration under vacuum with a Brandel 24-sample cell harvester through Whatman GF/C glass fiber filters treated with a solution containing 50 mM Tris (pH 7.4), 0.3% polyethylenimine (PEI) and 0.5% Triton X-100 at 4°C overnight. Filters were washed twice with 3 ml of cold 50 mM Tris–HCl (pH 7.4) complemented with 0.1 mg/ml BSA and 3 mM $MnCl_2$. The filters were air dried for about 60 min before the bound radioactivity was determined using a liquid scintillation counter (Beckman LS 6000IC) at 63% efficiency in 5 ml of counting scintillant. The specific binding was determined as the difference between total and

unspecific binding. All assays were run in triplicates and each assay was repeated at least three times at different days. Data and statistics from the competition experiments were analyzed in the GraFit program (Erithacus Software, UK).

Pharmacophore search

Compounds **1–12** were built in Maestro[42] and imported to Phase.[22] The structures were ionized at pH 7.0 (i.e. protonation of the N-terminus). Conformations were generated in Phase using 200 search steps per rotatable bond of mixed MCMM/LMOD with sampling set to Thorough. Energy minimization was performed using maximum 100 steps of Truncated Newton Conjugate Gradient minimization with convergence criterion set to $0.05 \text{ kJ mol}^{-1} \text{ Å}^{-1}$. The force field OPLS 2005[43] and the generalized-Born/surface area (GB/SA) model for water[44] as solvation model were used. Conformations within 5 kcal mol^{-1} of the lowest found energy minimum were saved and redundant conformations were removed based on maximum atom pair distance of 0.5 Å after superposition. The pharmacophore features found and assigned in the active compounds were hydrogen bond acceptors and donors, aromatic rings, and positively charged groups.

Metabolic Stability

Compounds (1 µM) were pre-incubated for 15 min at 37°C with pooled human liver microsomes (0.5 mg/mL; Xenotech, Kansas, KS) in 0.1M potassium phosphate buffer pH 7.4 prior to the addition of NADPH (1 mM) to initiate the reaction. Reactions were then incubated for 0, 5, 20 and 40 min and at each time point the reaction was stopped by the addition of acetonitrile. Plates were centrifuged at 3,500 rpm for 20 min at 4°C, and the supernatants were subjected to liquid chromatography/mass spectrometry analysis. The natural logarithm of the analytical peak area ratio (relative to 0 min sample which was considered as 100%) was plotted against time and analyzed by linear regression. *In vitro* half-life (t½) and *in vitro* intrinsic clearance (Clint) were calculated on the basis of first-order reaction kinetics of the percentage of remaining compound. Dextromethorphan (3 µM) and midazolam (5 µM) were used as positive controls for cytochrome P450 enzymes (CYP) isoforms CYP2D6 and CYP3A4, respectively.

Cell Culture

Caco-2 cells (obtained from American Tissue Collection, Rockville, MD) were maintained in an atmosphere of 90% air and 10% CO_2 as described previously.[25] For transport experiments, 3.0×10^5 cells (passages 98 to 102) were seeded on polycarbonate filter inserts (12 mm diameter; pore size 0.4 µm; Costar, Cambridge, MA) and allowed to grow and differentiate for 21–24 days. The monolayers integrity was assessed by measuring the paracellular marker [^{14}C]-Mannitol (1.0 µCi/mL 57.3 mCi/mmol; Perkin-Elmer Life Sciences, Boston, MA) transport and the transepithelial electrical resistance (TEER) before and after the experiments.

CHO-K1 and CHO-PepT1 cells (control and stably transfected cells, respectively, were kind gifts from Dr. Anna-Lena Ungell, AstraZeneca Mölndal) and were maintained at 37°C in an atmosphere of 90% air and 10% CO_2, with DMEM containing 4.5 g/L glucose, 10 % fetal bovine serum, 1% non essential amino acids and 50 µg/mL of gentamicin sulphate (Invitrogen, Carlsbad, CA). For the uptake experiments, 1.0×10^5 cells/well were seeded in 24-well plates and allowed to grow in antibiotic-free media for 2 days.

Transcellular Transport and Uptake Experiments

Stock solutions (10 mM) of the peptides were prepared in dimethylsulfoxide (DMSO) and diluted to 100 µM (final DMSO concentration of 1%) in Hank's balanced salt solution (HBSS) containing 10 mM MES at pH 6.0 (HBSS pH 6.0) or containing 10 mM HEPES at pH 7.4 (HBSS pH 7.4). In all experiments, [^{14}C]-Glycyl-sarcosine ([^{14}C]-GlySar; 1.82 µM, 0.1 µCi/mL; 55 mCi/mmol; ARC, St. Louis, MO) was used as a PepT1 substrate control. For inhibition controls, an excess of unlabeled competitor (10mM; Sigma-Aldrich, St. Louis, MO) was used.

The intestinal epithelial permeability was determined from transport rates across Caco-2 cell monolayers. The cell monolayers were gently rinsed with HBSS pH 6.0 and left to equilibrate in the same solution for 30 min at 37°C. The transport experiments were run for 2 h at 37°C, and were started by the application of the compound solution to the donor side, which was the apical chamber in the apical to basolateral (a–b) experiments, and the basolateral chamber in the basolateral to apical (b–a) experiments. Filter inserts were continuously stirred at 500

rpm on IKA-Schüttler MTS4 to obtain data that were unbiased by the aqueous boundary layer. The receiver chambers were sampled in suitable time points and the samples were replaced with equal volumes of pre-heated receiver solution. For transport studies performed under sink conditions, where less than 10% of the compound was transported across the Caco-2 cell monolayers, the apparent permeability coefficients (P_{app}) were calculated from the equation

$$P_{app} = \frac{(\Delta Q)}{(\Delta t)} \times \frac{1}{A \times C_0}$$

where $\Delta Q/\Delta t$ is the steady-state flux (mol/s), C_0 is the initial concentration in the donor chamber at each time interval (mol/mL), and A is the surface area of the filter (cm^2). If the fraction transported exceeded 10% the P_{app} coefficients were calculated applying non-sink conditions from the equation:

$$C_R(t) = \frac{M}{V_D + V_R} + \left(C_{R,0} - \frac{M}{V_D + V_R} \right) e^{-P_{app}A(1/V_D + V_R)t}$$

where $C_R(t)$ is the time-dependent drug concentration in the receiver compartment (μM), M is the amount of drug in the system (nmol), V_D and V_R are the volumes of the donor and receiver compartment (mL), respectively, and t is the time that has elapsed from the start of the interval (s).[45] P_{app} was obtained from nonlinear regression of the accumulated dose in the receiver compartment over time, minimizing the sum of squared residuals in the equation.

Uptake studies with CHO cells were performed at 37°C in HBSS pH 6.0. Initially, cells were gently rinsed and left to equilibrate for 30min at 37°C. After the equilibration period, buffer was removed and replaced by compound diluted in HBSS pH 6.0 and cells were incubated for 15 min at 37°C. Uptake was terminated by buffer removal followed by two washes with ice-cold phosphate buffer saline (PBS). Cells were then lysed with acetonitrile/water (60:40, v/v) and centrifuged at 3,500 rpm and 4°C for 20min. In the case of experiments with [^{14}C]-GlySar, sodium hydroxide 1M solution was used for cell lysis. The results were expressed as pmol/mg of protein/min.

Data Analysis

All experiments were performed in, at least, triplicates, and samples were subjected to liquid chromatography/mass spectrometry analysis with a ThermoFinnigan TSQ Quantum Discovery triple-quadrupole (electrospray ionization, ESI; Thermo Electron Corp. Waltham, USA) coupled to an Acquity Ultra High Performance LC system (Waters, Milford, MA). For chromatographic separation, an Acquity UPLC C18 column (1.7 µm; Waters, Milford, MA) and a flow rate of 600 µL/min were used. During the analysis 10 µL of the samples were injected with a gradient with 0.1% formic acid in acetonitrile and 0.1% formic acid in water. Electrospray ionization was used in positive mode, and the daughter ions of m/z 120.1 (**1**, **6**, and **12**), 134.1 (**2**, **3**, **4**, **5**, **9**, and **11**), 146.1 (**7** and **8**) and 281.2 (**10**) were used for quantification of the respective compounds. The internal standard warfarin (20 nM) was used throughout the analysis.
Radioactive samples ([^{14}C]-GlySar and [^{14}C]-Mannitol) were analyzed with a liquid scintillation counter (TopCount NXT, Perkin-Elmer Life Sciences, Boston, MA). Cellular protein content was determined using a protein assay kit with bovine serum albumin (BSA) as standard (Thermo Scientific, Rockford, IL).

Acknowledgment

References

1. Von Euler, U. S.; Gaddum, J. H. An unidentified depressor substance in certain tissue extracts. *J. Physiol.* **1931,** 72, 74-87.
2. Nakanishi, S. Mammalian Tachykinin Receptors. *Annu. Rev. Neurosci.* **1991,** 14, 123-136.
3. Hökfelt, T.; Pernow, B.; Wahren, J. Substance P: a pioneer amongst neuropeptides. *J. Intern. Med.* **2001,** 249, 27-40.
4. Lee, C.-M.; Sandberg, B. E. B.; Hanley, M. R.; Iversen, L. L. Purification and characterization of a membrane-bound substance P-degrading enzyme from human brain. *Eur. J. Biochem.* **1981,** 114, 315-327.
5. Sakurada, T.; Le Greves, P.; Stewart, J.; Terenius, L. Measurement of substance P metabolites in rat CNS. *J. Neurochem.* **1985,** 44, 718-722.

6. Hallberg, M.; Nyberg, F. Neuropeptide conversion to bioactive fragments--an important pathway in neuromodulation. *Curr. Protein Peptide Sci.* **2003,** 4, 31-44.

7. Kreeger, J. S.; Larson, A. A. Substance P-(1-7), a substance P metabolite, inhibits withdrawal jumping in morphine-dependent mice. *Eur. J. Pharmacol.* **1993,** 238, 111-115.

8. Zhou, Q.; Carlsson, A.; Botros, M.; Fransson, R.; Sandstrom, A.; Gordh, T.; Hallberg, M.; Nyberg, F. The C-terminal amidated analogue of the Substance P (SP) fragment SP1-7 attenuates the expression of naloxone-precipitated withdrawal in morphine dependent rats. *Peptides* **2009,** 30, 2418-2422.

9. Wiktelius, D.; Khalil, Z.; Nyberg, F. Modulation of peripheral inflammation by the substance P N-terminal metabolite substance P1-7. *Peptides* **2006,** 27, 1490-1497.

10. Sakurada, C.; Watanabe, C.; Sakurada, T. Occurrence of substance P(1-7) in the metabolism of substance P and its antinociceptive activity at the mouse spinal cord level. *Methods Find. Exp. Clin. Pharmacol.* **2004,** 26, 171-176.

11. Carlsson, A.; Ohsawa, M.; Hallberg, M.; Nyberg, F.; Kamei, J. Substance P1-7 induces antihyperalgesia in diabetic mice through a mechanism involving the naloxone-sensitive sigma receptors. *Eur. J. Pharmacol.* **2010,** 626, 250-255.

12. Dyck, P. J.; Dyck, P. J. B.; Velosa, J. A.; Larson, T. S.; O'Brien, P. C.; Grp, N. G. F. S. Patterns of quantitative sensation testing of hypoesthesia and hyperalgesia are predictive of diabetic polyneuropathy - A study of three cohorts. *Diabetes Care* **2000,** 23, 510-517.

13. Rimon, R.; Legreves, P.; Nyberg, F.; Heikkila, L.; Salmela, L.; Terenius, L. Elevation of Substance P-Like Peptides in the CSF of Psychiatric-Patients. *Biol. Psychiat.* **1984,** 19, 509-516.

14. Nyberg, F.; Le Greves, P.; Sundqvist, C.; Terenius, L. Characterization of substance P(1-7) and (1-8) generating enzyme in human cerebrospinal fluid. *Biochem. Biophys. Res. Commun.* **1984,** 125, 244-50.

15. Skilling, S. R.; Smullin, D. H.; Larson, A. A. Differential-Effects of C-Terminal and N-Terminal Substance-P Metabolites on the Release of Amino-Acid Neurotransmitters from the Spinal-Cord - Potential Role in Nociception. *J. Neurosci.* **1990,** 10, 1309-1318.

16. Mousseau, D. D.; Sun, X. F.; Larson, A. A. Identification of a Novel Receptor Mediating Substance-P-Induced Behavior in the Mouse. *Eur. J. Pharmacol.* **1992,** 217, 197-201.

17. Igwe, O. J.; Kim, D. C.; Seybold, V. S.; Larson, A. A. Specific binding of substance P aminoterminal heptapeptide [SP(1-7)] to mouse brain and spinal cord membranes. *J. Neurosci.* **1990,** 10, 3653-3663.

18. Botros, M.; Hallberg, M.; Johansson, T.; Zhou, Q.; Lindeberg, G.; Frändberg, P.-A.; Toemboely, C.; Toth, G.; Le Greves, P.; Nyberg, F. Endomorphin-1 and endomorphin-2 differentially interact with specific binding sites for substance P (SP) aminoterminal SP1-7 in the rat spinal cord. *Peptides* **2006,** 27, 753-759.

19. Botros, M.; Johansson, T.; Zhou, Q.; Lindeberg, G.; Tomboly, C.; Toth, G.; Le Greves, P.; Nyberg, F.; Hallberg, M. Endomorphins interact with the substance P (SP) aminoterminal SP1-7 binding in the ventral tegmental area of the rat brain. *Peptides* **2008,** 29, 1820-1824.

20. Fransson, R.; Botros, M.; Nyberg, F.; Lindeberg, G.; Sandström, A.; Hallberg, M. Small peptides mimicking substance P (1-7) and encompassing a C-terminal amide functionality. *Neuropeptides* **2008,** 42, 31-37.

21. Fransson, R.; Botros, M.; Skold, C.; Nyberg, F.; Lindeberg, G.; Hallberg, M.; Sandstrom, A. Discovery of Dipeptides with High Affinity to the Specific Binding Site for Substance P1-7. *J. Med. Chem.* **2010,** 53, 2383-2389.

22. Houston, J. B. Utility of in-Vitro Drug-Metabolism Data in Predicting in-Vivo Metabolic-Clearance. *Biochem. Pharmacol.* **1994,** 47, 1469-1479.

23. Obach, R. S. Prediction of human clearance of twenty-nine drugs from hepatic microsomal intrinsic clearance data: An examination of *in vitro* half-life approach and nonspecific binding to microsomes. *Drug Metab. Disposition* **1999,** 27, 1350-1359.

24. Hubatsch, I.; Ragnarsson, E. G. E.; Artursson, P. Determination of drug permeability and prediction of drug absorption in Caco-2 monolayers. *Nature Protocols* **2007,** 2, 2111-2119.

25. Bergström, C. A. S.; Strafford, M.; Lazorova, L.; Avdeef, A.; Luthman, K.; Artursson, P. Absorption classification of oral drugs based on molecular surface properties. *J. Med. Chem.* **2003,** 46, 558-570.

26. *Phase*, 3.1; Schrödinger, LLC: New York, NY, 2009.

27. Piercey, M. F.; Dobry, P. J. K.; Einspahr, F. J.; Schroeder, L. A.; Masiques, N. Use of Substance-P Fragments to Differentiate Substance-P Receptors of Different Tissues. *Regulatory Peptides* **1982,** 3, 337-349.

28. Huston, J. P.; Hasenoehrl, R. U.; Boix, F.; Gerhardt, P.; Schwarting, R. K. W. Sequence-specific effects of neurokinin substance P on memory, reinforcement, and brain dopamine activity. *Psychopharmacology* **1993,** 112, 147-62.

29. Tomaz, C.; Silva, A. C.; Nogueira, P. J. Long-lasting mnemotropic effect of substance P and its N-terminal fragment (SP1-7) on avoidance learning. *Braz. J. Med. Biol. Res.* **1997,** 30, 231-233.

30. Turk, J.; Panse, G. T.; Marshall, G. R. alpha -Methyl amino acids. Resolution and amino protection. *J. Org. Chem.* **1975,** 40, 953-5.

31. Boyle, S.; Guard, S.; Higginbottom, M.; Horwell, D. C.; Howson, W.; McKnight, A.; Martin, K.; Pritchard, M. C.; O'Toole, J.; et al. Rational design of high affinity tachykinin NK1 receptor antagonists. *Bioorg. Med. Chem.* **1994,** 2, 357-70.

32. Teixido, M.; Albericio, F.; Giralt, E. Solid-phase synthesis and characterization of N-methyl-rich peptides. *J Pept Res* **2005,** 65, 153-166.

33. HaskellLuevano, C.; Toth, K.; Boteju, L.; Job, C.; Castrucci, A. M. D.; Hadley, M. E.; Hruby, V. J. beta-methylation of the Phe(7) and Trp(9) melanotropin side chain pharmacophores affects ligand-receptor interactions and prolonged biological activity. *J. Med. Chem.* **1997,** 40, 2740-2749.

34. Brandsch, M. Transport of drugs by proton-coupled peptide transporters: pearls and pitfalls. *Expert Opin Drug Met* **2009,** 5, 887-905.

35. Brodin, B.; Nielsen, C. U.; Steffansen, B.; Frokjaer, S. Transport of peptidomimetic drugs by the intestinal di/tri-peptide transporter, PepT1. *Pharmacol. Toxicol.* **2002,** 90, 285-296.

36. Bailey, P. D.; Boyd, C. A. R.; Bronk, J. R.; Collier, I. D.; Meredith, D.; Morgan, K. M.; Temple, C. S. How to make drugs orally active: A substrate template for peptide transporter PepT1. *Angew Chem Int Edit* **2000,** 39, 505-508.

37. Rubio-Aliaga, I.; Daniel, H. Mammalian peptide transporters as targets for drug delivery. *Trends Pharmacol. Sci.* **2002,** 23, 434-440.

38. Våbenö, J.; Lejon, T.; Nielsen, C. U.; Steffansen, B.; Chen, W. Q.; Hui, O. Y.; Borchardt, R. T.; Luthman, K. Phe-Gly dipeptidomimetics designed for the di-/tripeptide transporters PEPT1 and PEPT2: Synthesis and biological investigations. *J. Med. Chem.* **2004,** 47, 1060-1069.

39. Vig, B. S.; Stouch, T. R.; Timoszyk, J. K.; Quan, Y.; Wall, D. A.; Smith, R. L.; Faria, T. N. Human PEPT1 pharmacophore distinguishes between dipeptide transport and binding. *J. Med. Chem.* **2006,** 49, 3636-3644.

40. Giacomini, K. M.; Huang, S. M.; Tweedie, D. J.; Benet, L. Z.; Brouwer, K. L. R.; Chu, X. Y.; Dahlin, A.; Evers, R.; Fischer, V.; Hillgren, K. M.; Hoffmaster, K. A.; Ishikawa, T.; Keppler, D.; Kim, R. B.; Lee, C. A.; Niemi, M.; Polli, J. W.; Sugiyama, Y.; Swaan, P. W.;

Ware, J. A.; Wright, S. H.; Yee, S. W.; Zamek-Gliszczynski, M. J.; Zhang, L.; Transporter, I. Membrane transporters in drug development. *Nature Reviews Drug Discovery* **2010,** 9, 215-236.

41. Seelig, A.; Landwojtowicz, E. Structure-activity relationship of P-glycoprotein substrates and modifiers. *Eur. J. Pharm. Sci.* **2000,** 12, 31-40.

42. Lowry, O. H.; Rosebrough, N. J.; Farr, A. L.; Randall, R. J. Protein measurement with the Folin phenol reagent. *J. Biol. Chem.* **1951,** 193, 265-275.

43. *Maestro*, 9.0; Schrödinger, LLC: New York, NY, 2009.

44. Kaminski, G. A.; Friesner, R. A.; Tirado-Rives, J.; Jorgensen, W. L. Evaluation and reparametrization of the OPLS-AA force field for proteins via comparison with accurate quantum chemical calculations on peptides. *J. Phys. Chem. B* **2001,** 105, 6474-6487.

45. Still, W. C.; Tempczyk, A.; Hawley, R. C.; Hendrickson, T. Semianalytical Treatment of Solvation for Molecular Mechanics and Dynamics. *J. Am. Chem. Soc.* **1990,** 112, 6127-6129.

46. Tavelin, S.; Grasjo, J.; Taipalensuu, J.; Ocklind, G.; Artursson, P. Applications of epithelial cell culture in studies of drug transport. *Methods Mol. Biol.* **2002,** 188, 233-272.

Discovery and Pharmacokinetic Profiling of Phenylalanine Based Carbamates as Novel Substance P 1-7 Analogues

Rebecca Fransson,[a] Gunnar Nordvall,[b] Milad Botros,[c] Anna Carlsson,[c] Jadel M. Kratz,[d,e] Richard Svensson,[e,f] Per Artursson,[e,f] Fred Nyberg,[c] Mathias Hallberg,[c] and Anja Sandström.[a*]

[a] Department of Medicinal Chemistry, Uppsala University, Box 574, SE-751 23 Uppsala, Sweden
[b] AstraZeneca, Research & Development, Södertälje SE-151 85 Södertälje, Sweden
[c] Department of Pharmaceutical Biosciences, Uppsala University, Box 591, SE-751 24 Uppsala, Sweden.
[d] Department of Pharmacy, Uppsala University, Box 580, SE-751 23 Uppsala, Sweden.
[e] Programa de Pós-Graduação em Farmácia, Centro de Ciências da Saúde, Departamento de Ciências Farmacêuticas, Universidade Federal de Santa Catarina, 88.040-900, Florianópolis, SC, Brasil;
[f] The Uppsala University Drug Optimization and Pharmaceutical Profiling Platform, Uppsala University, Box 580, SE-751 23 Uppsala, Sweden

Abstract

The N-terminal fragment of Substance P, the heptapeptide SP1-7 (H-Arg-Pro-Lys-Pro-Gln-Gln-Phe-OH), is a bioactive metabolite that has been shown to be associated with several pharmacologically interesting effects. For instance, SP1-7 analogues have been shown to attenuate hyperalgesia in diabetic mice, which indicate a possible use of compounds targeting the SP1-7 binding site as analgesic for neuropathic pain. Aiming at the development of drug-like SP1-7 peptidomimetics we have previously reported on the discovery of H-Phe-Phe-NH2 as a high affinity lead compound. Unfortunately, the pharmacophore of this compound has also been shown to be correlated with low metabolic stability, low cell-permeability and efflux. Herein, we report of the optimization of H-Phe-Phe-NH2 by substituting the N-terminal phenylalanine for a benzylcarbamate group giving a new class of SP1-7 analogues with good binding affinity and improved *in vitro* PK data. Furthermore, evaluation of different C-terminal functional groups, i.e. hydroxamic acid, acyl sulfonamide, acyl cyanamide, hydrazine based

and an oxadiazole, led to the identification of a hydroxamic acid as a preferred C-terminal group.

Introduction

Substance P (SP, H-Arg-Pro-Lys-Pro-Gln-Gln-Phe-Phe-Gly-Leu-Met-NH2)[1] is the endogenous ligand to the neurokinin-1 (NK-1) receptor and acts as a neurotransmitter and neuromodulator in the central and as well in the peripheral nervous system.[2] SP is degraded into several bioactive fragments. In particular, the major N-terminal metabolite substance P 1-7 (SP1-7, H-Arg-Pro-Lys-Pro-Gln-Gln-Phe-OH, **1**) has been extensively studied.[3-5] This heptapeptide is found in the cerebrospinal fluid (CSF) in man and rodants[6] and exhibits high affinity to specific binding sites in the spinal cord and in the brain.[7-9] Several reports suggest that SP1-7 has its own putative receptor, but no receptor has yet been cloned.

This SP metabolite SP1-7 attracted our attention of several reasons; firstly, SP1-7 counteracts the expression of opiate tolerance and withdrawal, in contrast to SP and its C-terminal fragments that instead augment the opioid withdrawal signs,[10, 11] secondly, SP1-7 attenuates the inflammatory[12] and nociceptive[13] effects exerted by SP and thirdly, our group recently demonstrated that SP1-7 could induce a pronounced antihyperalgesia in diabetic mice.[14] The latter finding suggested to us that low molecular weight SP1-7 peptide mimetics are not only desirable as research tools but might in addition have the potential to serve as future therapeutic agents in the treatment of neuropathic pain.

We have commenced a medicinal chemistry program aimed at transforming SP1-7 into drug-like peptide mimetics. An alanine scan and subsequent N- and C-terminal modifications of SP1-7 and endomorphin-2 followed by truncation afforded the lead compound H-Phe-Phe-NH2 (compound **2,** see Chart 1).[15, 16] Notably, SAR studies of dipeptide analogues and by a series of rigid analogues of H-Phe-Phe-NH2 (exemplified by compound **3** in Chart 1) suggested that two aromatic rings with (S,S) configuration, a primary amine in the N-terminal in combination with a primary amide function in the C-terminal seemed optimal for high binding affinity. Unfortunately this pharmacophore was correlated with efflux of the compounds. In order to improve the pharmacokinetic properties and more specifically, to reduce the efflux and to increase the lipophilicity aiming at compounds that not only have good cell-permeability but also eventually can pass the blood-

brain barrier (BBB), we felt prompted to investigate compounds of the prototype structure **A** (Chart 1).

Chart 1.
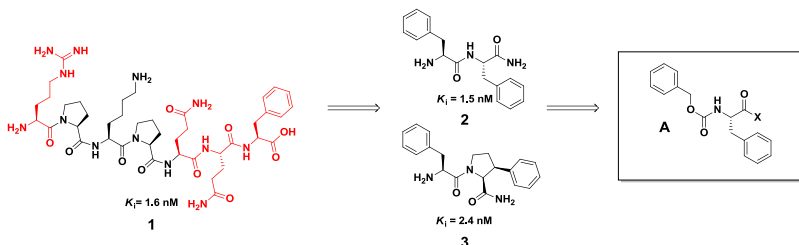
Thus, starting with the prototype compound with a primary amide in the C-terminal we decided to evaluate its binding affinity towards the SP1-7 binding site and thereafter compare its *in vitro* PK data to the previously developed lead compounds **2** and **3**.

We herein report that replacement with a neutral moiety of the basic N-terminal amine group can deliver a new class of more drug-like ligands with retained binding affinity and more favorable *in vitro* PK data. In addition, in this new compound class, the C-terminal requirement for optimal binding affinity has been elucidated by evaluation of a set of C-terminal modifications.
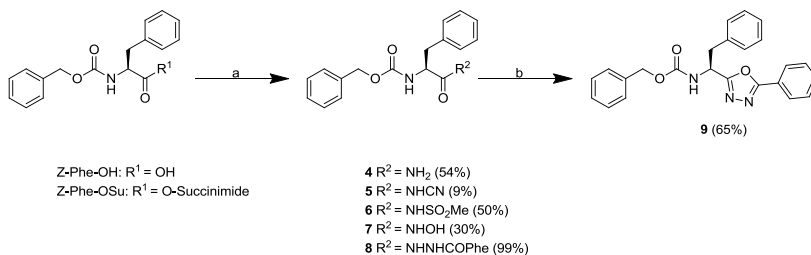
Results

Chemistry

The general synthesis towards the carbamate based derivatives is outlined in Scheme 1. The primary amide **4** was prepared through the reaction of C-terminal activated benzyloxycarbonyl protected phenylalanine (Z-Phe-OSu) with ammonia. The acyl cyanamide **5** was obtained by activation of Z-Phe-OH by *N*-[(dimethylamino)-1*H*-1,2,3-triazolo-[4,5-*b*]pyridine-1-ylmethylene]-*N*-methylmethanaminium hexafluorophosphate *N*-oxide (HATU). Although, the reaction was allowed to run for 3 days at 40 °C, the acyl cyanamide was obtained in low yield. The synthesis of acyl sulfonamide **6** was done by preactivation of Z-Phe-OH with 1,1'-carbonyldiimidazole (CDI) at 60 °C before the methylsulfonamide was added. The reaction was run in 3 h at room temperature, giving the desired compound in 50% yield.

Activation of Z-Phe-OH with isobutylchloroformate at low temperature and coupling with hydroxylamine hydrochloride gave the hydroxamic acid **7** in reasonable yield. The synthesis of the 1,3,4-oxadiazole **9** was prepared via the diacylhydrazine compound **8**, which was further dehydrated using Burgess reagent in order to give the heterocyclic compound **9**.[17]

Scheme 1.

Z-Phe-OH: R^1 = OH
Z-Phe-OSu: R^1 = O-Succinimide

4 R^2 = NH$_2$ (54%)
5 R^2 = NHCN (9%)
6 R^2 = NHSO$_2$Me (50%)
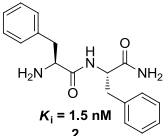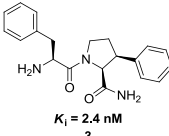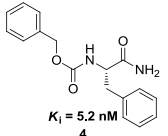**7** R^2 = NHOH (30%)
8 R^2 = NHNHCOPhe (99%)

9 (65%)

Reagents: (*a*) (i) Z-Phe-Osu, NH3, THF, 0°C to r.t. or (ii) Z-Phe-OH, Cyanamide, HATU, DIEA, DMF, 3 days at 40°C, or (iii) Z-Phe-OH, Methylsulfonamide, CDI, DBU, THF, 3h or (iv) Z-Phe-OH, Hydroxylamine hydrochloride, N-methylmorpholine, Isobutylchloroformate, Et3N, THF, DMF, 2h or (v) Z-Phe-OH, Benzhydrazide, HATU, DIEA, DCM, r.t. (*b*) **8**, Burgess reagent, THF, 75°C.

Biological evaluation

Initial investigation of the prototype compound where the N-terminal phenylalanine in lead compound **2** was exchanged to the more lipophilic bensyloxycarbonyl moiety, generating compound **4**, was performed. Firstly, compound **4** was evaluated in the SP1-7 binding assay. Despite discarding the basic N-terminal amine the new carbamate based derivative possessed good binding affinity (Ki = 5.2 nM), demonstrating that this new ligand still maintains significant binding interactions with the target. Together with the other two lead compounds (**2** and **3**), discovered in previous optimization studies, compound **4** were evaluated in an extensive *in vitro* profile program (Table 1).[18-20] Several important parameters were screened, such as solubility, plasma protein binding, permeability including efflux, metabolic stability and their influence on the CYP enzymes, in order to obtain a profound PK profile of each compound.

Table 1. *In vitro* profile of the lead compounds **2**, **3** and **4**.

Compound structure / In vitro profile	K_i = 1.5 nM **2**	K_i = 2.4 nM **3**	K_i = 5.2 nM **4**
ClogP	1.02	1.67	2.15
PSA	107	94	88
Solubility (µM)	> 400	257	97
Human PPB Fu % 10 µM	NV	60	19
Rat PPB Fu % 10 µM	NV	67	18[a]
P_{app} (10^{-6} cm/s)	NV[b]	2.8	31
Efflux ratio	NV[b]	4.2	1
Cl_{int} (Rat Mic)	102.8	8.3	21.2
Cl_{int} (Human Mic)	97.3	13.9	22.6
Cl_{int} (Rat Hep)		7.1	39.4
CYP2D6	Weak	Weak	Weak
CYP3A4	Weak	Moderate	Weak
CYP1A2	Weak	Weak	Weak
CYP2C9	Weak	Weak	Weak

[a] Using protease inhibitors. [b] Below level of quantification. [c] PSA= Polar surface area. [d] PPB = Plasma protein binding. [e] Fu = Fraction unbound. [f] Mic = Microsomes. [g] Clint = Clearance intrinsic (µl/min/mg). [h] Hep = Hepatocytes. [i] Weak: IC_{50} >20uM, Moderate: IC_{50} 2-20uM.

The three first parameters in Table 1 clearly demonstrates, as one might expect, that with reduced peptide character the lipophilicity increases (**4 > 3 > 2**). The decreased polar surface area (PSA) and increased C Log P of compound **4** thus promotes good permeability across the blood-brain barrier. Looking at our first lead compound H-
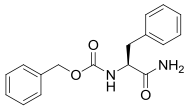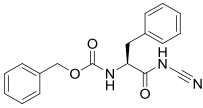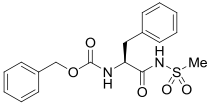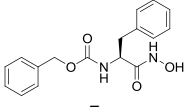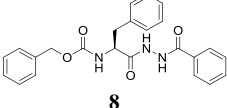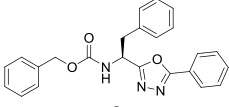
Phe-Phe-NH2 (**2**) it is clear that this dipeptide is not a good drug candidate due to low membrane permeability (below level of quantification). Furthermore, the high clearance and no measurable PPB (fraction unbound), probably due to rapid degradation in plasma, can be problematic in further development. The rigidification of the C-terminal phenylalanine, as in compound **3**, resulted in improved permeability but still with an efflux ration of 4. This two carbon cyclization of the side chain with the peptide backbone also turned out to give a significant reduction in clearance in comparison to compound **2**, human Clint 13.9 μl/min/mg (**3**) and Clint 97 μl/min/mg (**2**), respectively. In fact, in comparison to both **2** and **4**, compound **3** was accompanied with lowest clearance. Replacing the N-terminal basic amine with the carbamate function (**4**) resulted in significant improvement of the permeability (31 x 10^{-6} cm/s) and also notably in less efflux propensity (efflux ratio 1). In order to find a successful candidate drug, with a satisfied free drug concentration, increased membrane permeability and reduced clearance (by enhanced metabolic stability and by decreased efflux) are important. The constrained analogue **3** showed to be very metabolic stable and had only 40 % plasma protein binding while the carbamate based compound **4** demonstrated promising membrane permeability and a low efflux. Moreover, all three compounds showed no or very week inhibition of the tested cytochrome P450 isoenzymes (CYP2D6, CYP3A, CYP1A2, CYP2C9). Taken together, two new analogues have been identified with better PK profile compared to H-Phe-Phe-NH2 (**2**).

Encouraged by the promising binding and PK data of the prototype compound **4** we wanted to further explore this type of compounds by incorporation of different C-terminal groups. The use of bioisosteres is a common strategy in drug discovery in order to optimize a lead structure. A successful isosteric replacement can result in improved potency, selectivity or PK profile.[21, 22] Properties such as acidity and hydrogen bonding and donating capacity were considered when choosing the functional groups. The target compounds **5-9** were evaluated in the binding assay displacing the [^{3}H]-SP1–7 analogue (Table 2).

The benzyl carbamate based compounds showed moderate to good binding affinities towards the SP1-7 binding site (IC_{50} ranging from 4-60 nM, Table 2). When the primary amide in compound **4** was exchanged to an acyl cyanamide (**5**) or to an acyl sulfonamide (**6**) the affinity decreased 3 and 11 times, respectively.

This reduced affinity can be assigned the acidity of these compounds, which are in the same range as a carboxylic acid. This is in agreement with earlier studies on peptide based SP1-7 analogues, which proved carboxylic acids to be far less potent, than the primary amide.[16] Possibly the negative charge of compound **5** and **6** will not be compatible with a good binding since a hydrogen bond interaction will be lost.

Table 2. Binding affinity (IC_{50} values) of the compounds comprising different C-terminal groups.

Compound	$IC_{50} \pm S.E.M$
4	6.2 ± 0.3^a
5	16.5
6	60.6
7	4.2
8	6.5
9	9.0

[a] IC_{50} value of compound **4**, corresponds to the Ki value = 5.2 nM.

In compound **7** where the primary amide was substituted for a hydroxamic acid the binding affinity was slightly improved and resulted

in the most potent compound concerning binding affinity. This can be due to its more neutral character, thus maintaining the possibilities for two hydrogen bonding interactions. The hydrazine-based C-terminal group in **8** and the 1,3,4-oxadiazole in **9** retained good binding affinites (cf. **4** with **8** and **9**) towards the SP1-7 binding site. The diacyl hydrazine **8** still contains both H-bond donating and H-bond accepting atoms which might pick up important interactions in the binding site. Furthermore, the 1,3,4-oxadiazole ring in **9** results in extension of the C-terminal part which might result in additional interaction possibilities of the aromatic group within the binding site.

The synthesized compounds were evaluated with regard to their uptake, permeability and metabolic stability (see Table 3 and Table 4) in order to study the influence of the isosteric replacement on the PK properties. *In vitro* half-life (t½, min) and *in vitro* intrinsic clearance (Clint, μl/min/mg) were calculated using previous published models.[23, 24]

Table 3. Metabolic Stability data[a] of compounds comprising different C-terminal groups.

Compound	Metabolic Stability $Cl_{int}{}^{a}$ (μl/min/mg)	Metabolic Stability t½ [b] (min)
5	10.9 ± 3.7	136 ± 46
6	16.9 ± 3.8	84.2 ± 18.9
7	23.3 ± 1.0	59.6 ± 2.5
8	64.7 ± 12.7	21.9 ± 4.3
9	287 ± 4	4.8 ± 0.1

[a] Results are expressed as mean ± SD. [b] Clint = *in vitro* intrinsic clearance. [c] t½ = *in vitro* half-life.

Three out of the five benzyl carbamate based derivatives (**5**, **6** and **7**) showed significantly reduced Clint in comparison to H-Phe-Phe-NH2 (**1**) itself and comparable with the prototype compound **4**. In this series, the acyl cyanamide (**5**) turned out to be the most stable C-terminal group. In contrast, a C-terminal hydrazine (**8**) and in particular a C-terminal oxadiazole (**9**) significantly decreased the metabolic stability. The increased clearance of these derivatives might be attributed the incorporation of an aromatic group in the C-terminal, susceptible for additional metabolism together with the significantly higher Log P.

The intestinal epithelial permeability, expressed as apparent permeability coefficients (P_{app}), was determined from transport rates across Caco-2 cell monolayers, as described previously.[25] A P_{app} value

below 0.2×10^{-6} cm/s indicates low permeability, a P_{app} value ranging from 0.2×10^{-6} cm/s to 1.6×10^{-6} cm/s indicates moderate permeability and a P_{app} value above 1.6×10^{-6} cm/s indicates high permeability.[26]

Table 4. Uptake and permeability data[a] of compounds comprising different C-terminal groups.

Cpd.	Uptake (pmol/mg protein/min)			Caco-2 Permeability P_{app}[b] $(10^{-6}$ cm/s)			
	CHO-PepT1	CHO-K1	Ratio	AB[c]	BA[d]	Ratio AB/BA	Ratio BA/AB
5	4.1±0.9	4.0 ± 1.5	1.0	52.1±2.3	61.6±1.2	0.9	1.2
6	89.5±0.8	76.5±4.1	1.2	6.2±0.4	3.3±0.1	1.9	0.5
7	5.2 ± 0.2	4.4 ± 0.9	1.2	60.2±2.2	44.8±0.1	1.3	0.7
8	127.1±6.9	155.6±9.9	0.8	10.7±0.1	13.7±0.6	0.8	1.3
9	1081.7±52.7	1128.4±73.5	1.0	13.3±0.1	7.4±0.6	1.8	0.6

[a] Results are expressed as mean ± SD. For uptake and permeability experiments, compound **6** was analysed at 100 μM and **5** and **7-9** were further diluted to 25 μM due to poor aqueous solubility. See supporting information for experimental conditions. [b] Paap = apparent permeability coefficient. [c] AB = apical to basolateral. [d] BA = basolateral to apical.

Uptake studies with CHO-K1 and CHO-PepT1 cells (control and PepT1 stably transfected cells, respectively) were performed and the results were expressed as pmol/mg of protein/min. In order to be classified as a substrate for the peptide transporter PepT1 and be actively transported in to the cell the PepT1/K1 ratio should be above 1. The ratio for the compounds in this series (**5-9**) ranged from 0.8 (**8**) to 1.2 (**6** and **7**), which indicates that these compounds are not actively transported. However, the permeability data in the a-b direction ranged from 6×10^{-6} cm/s (**6**) to 60×10^{-6} cm/s (**7**) and the efflux ratios were close to 1, which in contrast to H-Phe-Phe-NH2 (**2**) indicates that these compounds indeed are cell permeable and can cross the BBB. Satisfyingly compound **7**, with highest binding affinity (IC_{50} = 4.2 nM), also turned out to have the highest permeability (60×10^{-6} cm/s) and low efflux (ratio = 0.7).

Conclusion

A new class of SP1-7 analogues with good binding affinity and improved *in vitro* PK profile has been developed by substituting the N-

terminal phenylalanine of H-Phe-Phe-NH2 (**2**) with a benzylcarbamate group as in prototype compound **4**. The small investigation regarding a potential bioisosteric replacement in the C-terminal further highlights the gain that can be achieved by a successful C-terminal substitution regarding potency and PK properties, in this case a substitution of a primary amide to a hydroxamic acid. The data obtained in here will guide further optimization. Thus, a combination of the complementary profiles of the rigidified H-Phe-Phe-NH2 analog **3** and the prototype compound **4** can generate compounds with increased permeability, metabolic stability and reduced efflux.

References

(1) Von Euler, U. S.; Gaddum, J. H. *J. Physiol.* **1931**, *72*, 74.

(2) Hökfelt, T.; Pernow, B.; Wahren, J. *J. Intern. Med.* **2001**, *249*, 27.

(3) Lee, C.-M.; Sandberg, B. E. B.; Hanley, M. R.; Iversen, L. L. *Eur. J. Biochem.* **1981**, *114*, 315.

(4) Sakurada, T.; Le Greves, P.; Stewart, J.; Terenius, L. *J. Neurochem.* **1985**, *44*, 718.

(5) Hallberg, M.; Nyberg, F. *Curr. Protein Peptide Sci.* **2003**, *4*, 31.

(6) Rimon, R.; Legreves, P.; Nyberg, F.; Heikkila, L.; Salmela, L.; Terenius, L. *Biol. Psychiat.* **1984**, *19*, 509.

(7) Igwe, O. J.; Kim, D. C.; Seybold, V. S.; Larson, A. A. *J. Neurosci.* **1990**, *10*, 3653.

(8) Botros, M.; Hallberg, M.; Johansson, T.; Zhou, Q.; Lindeberg, G.; Frändberg, P.-A.; Toemboely, C.; Toth, G.; Le Greves, P.; Nyberg, F. *Peptides* **2006**, *27*, 753.

(9) Botros, M.; Johansson, T.; Zhou, Q.; Lindeberg, G.; Tomboly, C.; Toth, G.; Le Greves, P.; Nyberg, F.; Hallberg, M. *Peptides* **2008**, *29*, 1820.

(10) Kreeger, J. S.; Larson, A. A. *Eur. J. Pharmacol.* **1993**, *238*, 111.

(11) Zhou, Q.; Carlsson, A.; Botros, M.; Fransson, R.; Sandstrom, A.; Gordh, T.; Hallberg, M.; Nyberg, F. *Peptides* **2009**, *30*, 2418.

(12) Wiktelius, D.; Khalil, Z.; Nyberg, F. *Peptides* **2006**, *27*, 1490.

(13) Sakurada, C.; Watanabe, C.; Sakurada, T. *Methods Find. Exp. Clin. Pharmacol.* **2004**, *26*, 171.

(14) Carlsson, A.; Ohsawa, M.; Hallberg, M.; Nyberg, F.; Kamei, J. *Eur. J. Pharmacol.* **2010**, *626*, 250.

(15) Fransson, R.; Botros, M.; Nyberg, F.; Lindeberg, G.; Sandström, A.; Hallberg, M. *Neuropeptides* **2008**, *42*, 31.

(16) Fransson, R.; Botros, M.; Skold, C.; Nyberg, F.; Lindeberg, G.; Hallberg, M.; Sandstrom, A. *J. Med. Chem.* **2010**, *53*, 2383.

(17) Brain, C. T.; Paul, J. M.; Loong, Y.; Oakley, P. J. *Tetrahedron Lett.* **1999**, *40*, 3275.

(18) Alelyunas, Y. W.; Liu, R. F.; Pelosi-Kilby, L.; Shen, C. *Eur. J. Pharm. Sci.* **2009**, *37*, 172.

(19) Sohlenius-Sternbeck, A. K. *Toxicol. In Vitro* **2006**, *20*, 1582.

(20) Sohlenius-Sternbeck, A. K.; Afzelius, L.; Prusis, P.; Neelissen, J.; Hoogstraate, J.; Johansson, J.; Floby, E.; Bengtsson, A.; Gissberg, O.; Sternbeck, J.; Petersson, C. *Xenobiotica* **2010**, *40*, 637.

(21) Chen, X.; Wang, W. *Annu. Rep. Med. Chem.* **2003**, *38*, 333.

(22) Thornber, C. W. *Chem. Soc. Rev.* **1979**, *8*, 563.

(23) Houston, J. B. *Biochem. Pharmacol.* **1994**, *47*, 1469.

(24) Obach, R. S. *Drug Metab. Disposition* **1999**, *27*, 1350.

(25) Hubatsch, I.; Ragnarsson, E. G. E.; Artursson, P. *Nature Protocols* **2007**, *2*, 2111.

(26) Bergström, C. A. S.; Strafford, M.; Lazorova, L.; Avdeef, A.; Luthman, K.; Artursson, P. *J. Med. Chem.* **2003**, *46*, 558.

Supporting Information

Chemistry

Preparative RP-HPLC was performed on a system equipped with a Zorbax SB-C8 column (150 × 21.2 mm) or a 10 μm Vydac C18 column (250 × 22 mm), in both cases with UV detection at 230 nm. Analytical RP-HPLC-MS was performed on a Gilson-Finnigan ThermoQuest AQA system (Onyx monolithic C18 column, 50 × 4.6 mm; MeCN/H2O gradient with 0.05% HCOOH) in ESI mode, using UV (214 and 254 nm) and MS detection. The purity of each of the peptides was determined by RPHPLC using the columns: ACE 5 C18 (50 × 4.6 mm) and ACE 5 Phenyl (50 x 4.6 mm) or Thermo Hypersil Fluophase RP (50 x 4.6 mm) with a H2O/MeCN gradient with 0.1% TFA and UV detection at 220 nm.

NMR spectra were recorded on a Varian Mercury plus spectrometer (^{1}H at 399.8 MHz and ^{13}C at 100.5 MHz or ^{1}H at 399.9 MHz and ^{13}C at 100.6 MHz) at ambient temperature. Chemical shifts (δ) are reported in ppm referenced indirectly to TMS via the solvent residual signal. Exact molecular masses were determined on a Micromass Q-Tof2 mass spectrometer equipped with an electrospray ion

source at the Department of Pharmaceutical Biosciences, Uppsala University, Sweden. Amino acid analyses were performed at the Department of Biochemistry and Organic Chemistry, Uppsala University, Sweden. All other chemicals and solvents were of analytical grade from commercial sources.

Compound 4

Z-Phe-OSu (450 mg, 1.135 mmol) was weight into a rund bottle flask and flushed with N2. THF (20 mL) was added and the solution was cooled to -0 ºC. NH3 (g) was bubbled into the flask which resulted in precipitation of a white solid. After 50 minutes the NH3 (g) was turned off and the reaction was stirred at room temperature over night. The precipitate was filtered of and dried under vacuum. The filtrate was evaporated to yield a white solid. An aliquot of the crude compound was purified on RP-HPLC to give **13** (15 mg, 54%) as a white solid. HPLC purity: C18-column > 99%, Phenyl > 99%. ^{1}H NMR (CD3CN) δ 2.83 (dd, J = 9.4, 14.0 Hz, 1H), 3.14 (dd, J = 4.9, 14.0 Hz, 1H) 4.31 (ddd, J = 4.9, 8.4, 9.4 Hz, 1H), 4.97 (d, J = 12.7 Hz, 1H), 5.03 (d, J = 12.7 Hz, 1H) 5.84 (br s, 1H) 5.89 (d, J = 8.4 Hz, 1H) 6.42 (br s, 1H) 7.29 (m, 10H). ^{13}C NMR (CD3CN) δ 38.7, 57.0, 67.0, 127.6, 128.6, 128.9, 129.3, 129.4, 130.3, 138.2, 138.7, 156.9, 174.3. Anal. Calcd for (C17H18N2O3): C, 68.44; H, 6.08; N, 9.39. Found: C, 68.35; H, 6.11; N, 9.17.

Compound 5

A mixture of Z-Phe-OH (150 mg, 0.5 mmol), cyanamide (79.8 mg, 1.9 mmol) and HATU (237 mg, 0.625 mmol) was weight into a reaction tube, evacuated and then flushed with N2. DIEA (435 μL, 2.5 mmol) and dry DMF(14 mL) was added and the reaction mixture was stirred at 40 ºC under N2 atmosphere for three days. The reaction mixture was diluted with EtOAc and washed with NaOAc buffer (pH 4), 10 % aqueous NaHCO3 and brine. The organic layer was evaporated and purified on RPHPLC to give **14** (15 mg, 15%) as a white solid. HPLC purity: C18 94.4%, Fluophase 93.7%. ^{1}H-NMR (MeOD) δ 3.18 (dd, J = 2.4, 14.0, 1H), 3.31 (dd, J = 5.7, 14.0, 1H), 4.63 (dd, J = 2.4, 5.7, 1H), 5.32 (d, J = 11.7, 1H), 5.52 (d, J = 11.7, 1H), 6.78-6.84 (m, 2H), 7.07-7.18 (m, 3H), 7.40-7.50 (m, 3H), 7.55-7.60 (m, 2H). ^{13}C-NMR (MeOD) δ 36.2, 64.3, 70.5, 116.9, 128.3, 129.4, 130.0, 130.3,

130.5, 130.6, 135.4, 136.1, 152.4, 185.5. HRMS (M + H+): 324.1351, C18H18N3O3 requires: 324.1348

Compound 6

The equipment and the solid chemicals were dried over night before use. The Z-Phe-OH (150 mg, 0.5 mmol) and CDI (162 mg, 1 mmol) were weight into a round bottom flask, sealed with a septum and flushed with N2. Dry THF (8 mL) was added and the mixture was heated in an oil bath at 60 ºC for 1.5 h. The methylsulfonamide, dissolved in dry THF (3 mL), and 1.8-diazabicyclo[5.5.0]undec-7ene (DBU) (224 µL, 1.5 mmol) were added to the reaction mixture whereafter it was stirred at room temperature for 3 h. The reaction mixture was evaporated and the crude was dissolved in DCM and washed with 5 % citric acid and brine. The organic layer was evaporated and a aliqoute (24 mg (10%) of the crude) was purified on RP-HPLC to give **15** (9.6 mg, 50%) as a white solid. HPLC purity: C18 > 99%, Fluophase > 99%. ^{1}H-NMR (MeOD) δ 2.91 (dd, *J* = 8.9, 13.7, 1H), 3.10 (dd, *J* = 6.1, 13.7, 1H), 3.15 (s, 3H), 4.37 (dd, *J* = 6.1, 8.9, 1H), 5.02 (d, *J* = 12.5, 1H), 5.06 (d, *J* = 12.5, 1H), 7.20-7.35 (m, 10H). ^{13}C-NMR (MeOD) δ 38.6, 41.2, 58.0, 67.7, 128.0, 128.7, 129.0, 129.5, 129.6, 130.5, 137.6, 138.1, 158.3, 173.6. HRMS (M + H+): 377.1173, C18H21N2O5S requires 377.1171.

Compound 7

The Z-Phe-OH (150 mg, 0.5 mmol) was dissolved in dry THF (6 mL) and flushed with N2. N-methylmorpholine (56 µL, 0.5 mmol) was added and the reaction mixture was cooled to -15 ºC before the addition of isobutylchloroformate (69 µL, 0.54 mmol). Hydroxylamine hydrochloride (42 mg, 0.6 mmol) in dry DMF (3mL) and triethylamine (84 69 µL, 0.6 mmol) were thereafter added and the mixture was stirred for 2 h at -15 ºC. The mixture was diluted with H2O and extracted with EtOAc. The organic layer was washed with brine, evaporated and a aliqoute (29 mg (20%) of the crude) was purified on RP-HPLC to give **16** (9.5 mg, 30 %) as a white solid. HPLC purity: C18 97.4%, Fluophase 97.1%. ^{1}H-NMR (MeOD) δ 2.88 (dd, *J* = 8.5, 13.6, 1H), 3.07 (dd, *J* = 6.5, 13.6, 1H), 4.26 (dd, *J* = 6.5, 8.5, 1H), 4.99 (d, *J* = 12.5, 1H), 5.04 (d, *J* = 12.5, 1H), 7.14-7.35 (m, 10H). ^{13}C-NMR (MeOD) δ 39.3, 55.7, 67.6, 127.8, 128.7, 128.9, 129.4, 129.5, 130.4, 138.2, 138.3, 158.1, 170.6. HRMS (M + H+): 315.1348, C17H19N2O4 requires 315.1345.

Compound 8

A mixture of Z-Phe-OH (171 mg, 0.572 mmol), benzhydrazide (117 mg, 0.859 mmol), HATU (261 mg, 0.686 mmol), DCM (6 mL) and DIEA (399 µL, 2.29 mmol) was stirred at room temperature over night. The mixture was diluted with EtOAc and washed with NaOAc buffer (pH 4), 5% aq. NaHCO3 and brine. The organic layer was evaporated and a aliquote (20 mg (6%) of the crude) was purified on RPHPLC to give **17** (14 mg, 99%) as a white solid. HPLC purity: C18 > 99%, Fluophase > 99%. ^{1}H-NMR (MeOD) δ 2.94 (dd, *J* = 9.8, 14.0, 1H), 3.31 (dd, *J* = 4.7, 14.0, 1H), 4.55 (dd, *J* = 4.7, 9.8, 1H), 4.97 (d, *J* = 12.5, 1H), 5.04 (d, *J* = 12.5, 1H), 7.18-7.33 (m, 10H), 7.45-7.51 (m, 2H), 7.54-7.60 (m, 1H), 7.86-7.90 (m, 2H). ^{13}C-NMR (MeOD) δ 39.2, 56.5, 67.5, 127.7, 128.61, 128.64, 128.9 129.39, 129.40, 129.6, 130.4, 133.3, 133.6, 138.1, 138.4, 158.2, 169.0, 173.3. HRMS (M + H+): 418.1771, C24H24N3O4 requires 418.1767.

Compound 9

Compound **17** was used without any further purification. All the equipment was dried before use. A mixture of **17** (83 mg, 0.247 mmol), (methoxycarbonylsulfamoyl)-triethylammonium hydroxide inner salt (Buregess reagent) (145 mg, 0.608 mmol) and dry THF (4 mL) was stirred at 70 ºC under N2 atmosphere in a sealed reaction tube for 3 h. The reaction mixture was evaporated and a aliquote (100 mg (47%) of the crude) was purified on RP-HPLC to give **18** (30 mg, 65%) as a white solid. HPLC purity: C18 89.6 %, Fluophase 89.4%. ^{1}H-NMR (MeOD) δ 3.25 (dd, *J* = 9.2, 13.8, 1H) 3.39 (dd, *J* = 6.4, 13.8, 1H), 5.05-5.06 (m, 2H), 5.28 (dd, *J* = 6.4, 9.2, 1H), 7.17-7.34 (m, 10H), 7.51-7.63 (m, 3H), 7.93-7.98 (m, 2H). 13C-NMR (MeOD) δ 39.6, 50.6, 67.7, 124.6, 127.9, 128.1, 128.7, 129.0, 129.5, 129.6, 130.37, 130.38, 133.3, 137.7, 138.1, 158.1, 166.5, 168.1. HRMS (M + H+): 400.1660, C24H22N3O3 requires 400.1661.

[2,4-DehydroPro]SP1-7

The precursor peptide for tritium-labeling [2,4-DehydroPro]SP1-7 was prepared by standard solid-phase peptide synthesis techniques using Fmoc/*t*-butyl protection and purified as described above. Tritium labeling of the precursor was performed by Amersham Biosciences

(Cardiff, UK) and resulted in 370 MBq (10 mCi) of [³H]-SP1-7 with a specific activity of 3.11 TBq/mmol (84 Ci/mmol).

Animal experiment and membrane preparation

The preparations of receptor membranes were conducted using spinal cords from male Sprague–Dawley rats. The rats (Alab AB, Sollentuna, Sweden), weighing 200–250 g, were housed in groups of four in air-conditioned rooms (22–23 °C and a humidity of 50–60%) under an artificial light–dark cycle and had free access to food and water. Prior to tissue sampling the rats were allowed to adapt to the laboratory environment for 1 week. The animals (n=15) were killed by decapitation and the spinal cords were rapidly removed and quickly frozen. Tissues were then kept at −80 °C until analyzed. The animal experiment was approved by the local ethical committee in Uppsala, Sweden.

The frozen spinal cords weighing approximately 250 - 300 mg/animal, were thawed and placed on ice before being homogenized for 30 s in 30 volumes of ice-cold 50 mM Tris–HCl buffer (pH 7.4), containing 5 mM KCl and 120 mM NaCl, using a Polytron homogenizer. The homogenate was then centrifuged at $40,000 \times g$ for 20 min at 4 °C and the supernatant was discarded. The resulting pellet was re-suspended in 30 volumes of ice-cold 50 mM Tris–HCl buffer (pH 7.4), containing 300 mM KCl and 10 mM EDTA. Following incubation on ice for 30 min the sample was centrifuged at $40,000 \times g$ for 20 min at 4 °C. The pellet obtained was diluted and homogenized in 30 volumes of ice-cold 50 mM Tris–HCl, containing 0.02% BSA, 5 mM, EDTA, 3 mM $MnCl_2$ and 40 μg bacitracin and re-centrifuged twice as described above. The final pellet was re-suspended and homogenized in 5 volumes of ice-cold 50 mM Tris–HCl buffer (pH 7.4) and immediately frozen at −80 °C until used in binding studies. The protein concentration of the membrane suspension was determined according to the method of Lowry[1] using bovine serum albumin as protein standard.

Radioligand Binding assay (Compounds 2–9)

Assessment of the binding affinity for the various compounds analyzed in this study was carried out using the analogue [³H]-SP1–7 as tracer. Assays were performed in tubes containing 50 μl of spinal cord membrane suspension (200 μg protein) and 0.9 nM of [3H]-SP1–7

(specific activity: 3.11 TBq/mmol (84 Ci/mmol)) in a final volume of 0.5 ml 50 mM Tris binding buffer (pH 7.4), containing, 3 mM MnCl2, 0.2% BSA and peptidase inhibitors (40 µg/ml bacitracin, 4 µg/ml leupeptin, 2 µg/ml aprotinin and 4 µg/ml phosphoramidon). The amount of total and unspecific binding in percent of the total radioactivity added were approximately 7% and 1.7%, respectively. The competition experiments were determined at six different concentrations varying between 0.01 nM and 1 µM of unlabeled compounds. Non-specific binding was determined in the presence of 1 µM SP1–7. Samples were incubated for 60 min at 4 °C before being terminated by rapid filtration under vacuum with a Brandel 24-sample cell harvester through Whatman GF/C glass fiber filters treated with a solution containing 50 mM Tris (pH 7.4), 0.3% polyethylenimine (PEI) and 0.5% Triton X-100 at 4 °C overnight. Filters were washed twice with 3 ml of cold 50 mM Tris–HCl (pH 7.4) complemented with 0.1 mg/ml BSA and 3 mM MnCl2. The filters were air dried for about 60 min before the bound radioactivity was determined using a liquid scintillation counter (Beckman LS 6000IC) at 63% efficiency in 5 ml of counting scintillant. The specific binding was determined as the difference between total and unspecific binding. All assays were run in triplicates and each assay was repeated at least three times at different days. Data and statistics from the competition experiments were analyzed in the GraFit program (Erithacus Software, UK).

In vitro Pharmacokinetic Profiling (Compounds 2–4)

This study was performed at AstraZeneca, Södertälje according to literature.[2-4] A brief description of the permeability and the solubility studies performed are presented below:

Cell culture

Caco2 cells (ATCC, American Type Culture Collection, ATCC No. HTB-37) were maintained with DMEM and passed weekly at a confluence at 80-90%. After trypsinization, the cells are seeded on polycarbonate filter inserts in the apical well to obtain the desired cell concentration of 227 000 cells/cm2 and maintained at culture conditions (37°C with 5% CO2 and 95% humidity). The medium is changed every second day. Cells with passage between 25-50 and grown for 14-25 days on filter inserts are used for permeability experiments.

Permeability experiment

The permeability experiment are carried out in transport buffer (HBSS with 25 mM HEPES, pH 7.4). Compounds dissolved in DMSO were diluted to 10 μM in transport buffer to give a final DMSO concentration of less than 1%. Each compound is assayed in duplicates for both directions. The experiment is performed using a Tecan Genesis RSP 200 robot. In short, the filter-grown cell monolayers are equilibrated in transport buffer and 37 °C for 10 minutes in a shaking incubator. The basolateral wells contain 0.80 mL and the apical wells contain 0,20 ml. Transport buffer is then removed from both sides. Test compounds are added to the donor side and fresh buffer to the receiver side before returning to the incubator. The assay is run for 60 min for the AB direction and 30 min for the BA direction. Aliquots of sample are taken from the donor side in the beginning and at the end of experiment. Receiver samples are taken from the basolateral side at the end of experiment. The integrity of the epithelial cell monolayer is monitored by measuring the passive transmembrane diffusion of radiolabeled [^{14}C]mannitol. Concentrations of compounds in donor and receiver samples are analyzed by liquid chromatography tandem mass spectrometry (LC/MS/MS). Liquid scintillation is used for analysis of [^{14}C]mannitol.

Solubility experiment

Aqueous solubility was determined with screening method producing crystalline-like solubility values starting from 10 mM solutions in a 96-plate format, called Dried DMSO Solubility test.[2] The Dried DMSO Solubility test determines the amount of test compound dissolved in buffer solution by HPLC-UV/MS or UPLC-UV/MS after incubation of known amount of test compounds concentrated from DMSO solution in 0.1 M sodium phosphate buffer, pH 7.4 for 24 hours at a fixed temperature of 22 °C with mixing on a shaking bed (500 rpm) with StirStix and following separation of a sample solution from not dissolved particles. In the present protocol version, a pre-incubation for at least 4 hours at a fixed temperature of 1°C with StirStix at 500-rpm prior addition of buffer was implemented to generate the most stable solid form. The sample is quantified against the standard of the test compound dissolved in DMSO. The upper limit for the measurement is 400 μM. To ensure that the estimated solubility data are valid, sample

identity and purity are determined also by examining mass spectral data in positive and negative ionization mode respectively chromatographic data, monitored at 220 and 254 nm.

Metabolic Stability (Compounds 5–9)

Compounds (1 μM) were pre-incubated for 15 min at 37°C with pooled human liver microsomes (0.5 mg/mL; Xenotech, Kansas, KS) in 0.1M potassium phosphate buffer pH 7.4 prior to the addition of NADPH (1 mM) to initiate the reaction. Reactions were then incubated for 0, 5, 20 and 40 min and at each time point the reaction was stopped by the addition of acetonitrile. Plates were centrifuged at 3,500 rpm for 20 min at 4°C, and the supernatants were subjected to liquid chromatography/mass spectrometry analysis. The natural logarithm of the analytical peak area ratio (relative to 0 min sample which was considered as 100%) was plotted against time and analyzed by linear regression. *In vitro* half-life time (*t½*, min) and *in vitro* intrinsic clearance (Clint, μl/min/mg) were calculated on the basis of first-order reaction kinetics of the percentage of remaining compound. Dextromethorphan (3 μM) and midazolam (5 μM) were used as positive controls for cytochrome P450 enzymes (CYP) isoforms CYP2D6 and CYP3A4, respectively.

Transcellular Transport and Uptake Experiments (Compounds 5–9)

Caco-2 cells (obtained from American Tissue Collection, Rockville, MD) were maintained in an atmosphere of 90% air and 10% CO_2 as described previously.[5] For transport experiments, 3.0×10^5 cells (passages 98 to 102) were seeded on polycarbonate filter inserts (12 mm diameter; pore size 0.4 μm; Costar, Cambridge, MA) and allowed to grow and differentiate for 21–24 days. The monolayers integrity was assessed by measuring the paracellular marker [^{14}C]-Mannitol (1.0 μCi/mL 57.3 mCi/mmol; Perkin-Elmer Life Sciences, Boston, MA) transport and the transepithelial electrical resistance (TEER) before and after the experiments.

CHO-K1 and CHO-PepT1 cells (control and stably transfected cells, respectively, were kind gifts from Dr. Anna-Lena Ungell, AstraZeneca Mölndal) and were maintained at 37°C in an atmosphere of 90% air and 10% CO_2, with DMEM containing 4.5 g/L glucose, 10 % fetal bovine serum, 1% non essential amino acids and 50 μg/mL of gentamicin sulphate (Invitrogen, Carlsbad, CA). For the uptake

experiments, 1.0 x 10^5 cells/well were seeded in 24-well plates and allowed to grow in antibiotic-free media for 2 days.

Stock solutions (10 mM) of the peptides were prepared in dimethylsulfoxide (DMSO) and diluted to 100 μM (final DMSO concentration of 1%) in Hank's balanced salt solution (HBSS) containing 10 mM MES at pH 6.0 (HBSS pH 6.0) or containing 10 mM HEPES at pH 7.4 (HBSS pH 7.4). Compound **5** and **7**-**9** were further diluted to 25 μM due to poor aqueous solubility. In all experiments, [^{14}C]-Glycylsarcosine ([^{14}C]-GlySar; 1.82 μM, 0.1 μCi/mL; 55 mCi/mmol; ARC, St. Louis, MO) was used as a PepT1 substrate control. For inhibition controls, an excess of unlabeled competitor (10mM; Sigma-Aldrich, St. Louis, MO) was used.

The intestinal epithelial permeability was determined from transport rates across Caco-2 cell monolayers. The cell monolayers were gently rinsed with HBSS pH 6.0 and left to equilibrate in the same solution for 30min at 37°C. The transport experiments were run for 2 h at 37°C, and were started by the application of the compound solution to the donor side, which was the apical chamber in the apical to basolateral (a–b) experiments, and the basolateral chamber in the basolateral to apical (b–a) experiments. Filter inserts were continuously stirred at 500 rpm on IKA-Schüttler MTS4 to obtain data that were unbiased by the aqueous boundary layer. The receiver chambers were sampled in suitable time points and the samples were replaced with equal volumes of pre-heated receiver solution. For transport studies performed under sink conditions, where less than 10% of the compound was transported across the Caco-2 cell monolayers, the apparent permeability coefficients (P_{app}) were calculated from the equation:

$$P_{app} = \frac{(\Delta Q)}{(\Delta t)} \times \frac{1}{A \times C_0}$$

where $\Delta Q/\Delta t$ is the steady-state flux (mol/s), $C0$ is the initial concentration in the donor chamber at each time interval (mol/mL), and A is the surface area of the filter (cm2).

If the fraction transported exceeded 10% the P_{app} coefficients were calculated applying non-sink conditions from the equation:

$$C_R(t) = \frac{M}{V_D + V_R} + \left(C_{R,0} - \frac{M}{V_D + V_R} \right) e^{-P_{app}A(1/V_D + V_R)t}$$

where $CR(t)$ is the time-dependent drug concentration in the receiver compartment (μM), M is the amount of drug in the system (nmol), VD and VR are the volumes of the donor and receiver compartment (mL), respectively, and t is the time that has elapsed from the start of the interval (s).[6] P_{app} was obtained from nonlinear regression of the accumulated dose in the receiver compartment over time, minimizing the sum of squared residuals in the equation.

Uptake studies with CHO cells were performed at 37°C in HBSS pH 6.0. Initially, cells were gently rinsed and left to equilibrate for 30min at 37°C. After the equilibration period, buffer was removed and replaced by compound diluted in HBSS pH 6.0 and cells were incubated for 15 min at 37°C. Uptake was terminated by buffer removal followed by two washes with ice-cold phosphate buffer saline (PBS). Cells were then lysed with acetonitrile/water (60:40, v/v) and centrifuged at 3,500 rpm and 4°C for 20min. In the case of experiments with [^{14}C]-GlySar, sodium hydroxide 1M solution was used for cell lysis. The results were expressed as pmol/mg of protein/min.

Data Analysis (Compound 5–9)

All experiments were performed in, at least, triplicates, and samples were subjected to liquid chromatography/mass spectrometry analysis with a ThermoFinnigan TSQ Quantum Discovery triplequadrupole (electrospray ionization, ESI; Thermo Electron Corp. Waltham, USA) coupled to an Acquity Ultra High Performance LC system (Waters, Milford, MA). For chromatographic separation, an Acquity UPLC C18 column (1.7 μm; Waters, Milford, MA) and a flow rate of 600 μL/min were used. During the analysis 10 μL of the samples were injected with a gradient with 0.1% formic acid in acetonitrile and 0.1% formic acid in water. Electrospray ionization was used in positive mode, and the daughter ion of m/z 91.1 was used for quantification of the respective compounds. The internal standard warfarin (20 nM) was used throughout the analysis.

Radioactive samples ([^{14}C]-GlySar and [^{14}C]-Mannitol) were analyzed with a liquid scintillation counter (TopCount NXT, Perkin-Elmer Life Sciences, Boston, MA). Cellular protein content was determined using a protein assay kit with bovine serum albumin (BSA) as standard (Thermo Scientific, Rockford, IL).

References

(1) Lowry, O. H.; Rosebrough, N. J.; Farr, A. L.; Randall, R. J. Protein measurement with the Folin phenol reagent. *J. Biol. Chem.* **1951**, 193, 265-275.

(2) Alelyunas, Y. W.; Liu, R. F.; Pelosi-Kilby, L.; Shen, C. Application of a Dried-DMSO rapid throughput 24-h equilibrium solubility in advancing discovery candidates. *Eur. J. Pharm. Sci.* **2009**, 37, 172-182.

(3) Sohlenius-Sternbeck, A. K. Determination of the hepatocellularity number for human, dog, rabbit, rat and mouse livers from protein concentration measurements. *Toxicol. In Vitro* **2006**, 20, 1582-1586.

(4) Sohlenius-Sternbeck, A. K.; Afzelius, L.; Prusis, P.; Neelissen, J.; Hoogstraate, J.; Johansson, J.; Floby, E.; Bengtsson, A.; Gissberg, O.; Sternbeck, J.; Petersson, C. Evaluation of the human prediction of clearance from hepatocyte and microsome intrinsic clearance for 52 drug compounds. *Xenobiotica* **2010**, 40, 637-649.

(5) Hubatsch, I.; Ragnarsson, E. G. E.; Artursson, P. Determination of drug permeability and prediction of drug absorption in Caco-2 monolayers. *Nature Protocols* **2007**, 2, 2111-2119.

(6) Tavelin, S.; Grasjo, J.; Taipalensuu, J.; Ocklind, G.; Artursson, P. Applications of epithelial cell culture in studies of drug transport. *Methods Mol. Biol.* **2002**, 188, 233-272.

APÊNDICE 4

Lista de Artigos Publicados durante o do Doutorado (2007-2011)

KRATZ, J.M.; TEIXEIRA, M.R.; KOESTER, L.S.; SIMÕES, C.M.O. An HPLC-UV method for the measurement of permeability of marker drugs in the Caco-2 cell assay. **Brazilian Journal of Medical and Biological Research**, v. 44, p. 531-537, 2011.

KUMINEK, G.; **KRATZ, J.M.**; RIBEIRO, R.; KELMANN, R.G.; ARAUJO, B.V.; TEIXEIRA, H.F.; SIMÕES, C.M.O.; KOESTER, L.S. Pharmacokinetic study of a carbamazepine nanoemulsion in beagle dogs. **International Journal of Pharmaceutics**, v. 378, p. 146-148, 2009.

KRATZ, J.M.; ANDRIGHETTI-FROHNER, C.R.; LEAL, P.C.; NUNES, R.J.; YUNES, R.A.; TRYBALA, E.; BERGSTRÖM, T.; BARARDI, C.R.M.; SIMÕES, C.M.O. Evaluation of Anti-HSV-2 Activity of Gallic Acid and Pentyl Gallate. **Biological and Pharmaceutical Bulletin**, v. 31, p. 903-907, 2008.

KRATZ, J.M.; TERRAZAS, C.B.; MOTTA, M.J.; REGINATTO, F.H.; SIMÕES, C.M.O. Determinação da composição química e dos perfis de dissolução *in vitro* de medicamentos à base de Ginkgo biloba disponíveis no mercado brasileiro. **Latin American Journal of Pharmacy**, v. 27, p. 674-680, 2008.

KRATZ, J.M.; ANDRIGHETTI-FROHNER, C.R.; KOLLING, D.J.; LEAL, P.C.; CIRNE-SANTOS, C.C.; YUNES, R.A.; NUNES, R.J.; TRYBALA, E.; BERGSTRÖM, T.; FRUGULHETTI, I.C.P.P.; BARARDI, C.R.M.; SIMÕES, C.M.O. Anti-HSV-1 and anti-HIV-1 activity of gallic acid and pentyl gallate. **Memórias do Instituto Oswaldo Cruz**, v. 103, p. 437-442, 2008.

APÊNDICE 5

Lista de Resumos Publicados durante o do Doutorado (2007-2011)

SIMÕES, C.M.O.; **KRATZ, J.M.**; TEIXEIRA, M.R.; FERRONATO, K.; CARO, M.; KOESTER, L.S.; Preparation, Characterization and *In vitro* Intestinal Permeability Evaluation of Thalidomide Inclusion Complexes. In: 2nd International Conference on Drug Discovery & Therapy, Dubai. Abstracts, v. 1, p. 256-257,. 2010

TEIXEIRA, M.R.; SILVA, I.T.; **KRATZ, J.M.**; KOESTER, L.S.; SIMÕES, C.M.O. Evaluation of Antiherpes Activity of Pentyl Gallate and their Complexes with Cyclodextrins. In: XXI Encontro Nacional de Virologia / V Encontro de Virologia do Mercosul, Gramado. Virus Review & Research, v. 15, p. 231-231, 2010.

KRATZ, J.M.; TEIXEIRA, M.R.; KOESTER, L.S.; SIMOES, C.M.O. Standardization of an Intestinal Permeability Assay with Caco-2 Cells. In: VII International Congress of Pharmaceutical Sciences, Ribeirão Preto. Abstracts, v. único, p. AF049-AF049, 2009.

KRATZ, J.M.; KELMANN, R.G.; LANG, K.L.; SILVA, I.T.; MASCARELLO, A.; DIAS, D.O.; ARAUJO, F.A.; NUNES, R.J.; TEIXEIRA, H.F.; KOESTER, L.S.; SIMÕES, C.M.O. Anti-HSV-1 Evaluation and Physicochemical Characterization of Isopentyl Gallate. In: VII International Congress of Pharmaceutical Sciences, 2009, Ribeirão Preto. Abstracts, v. único, p. QM014-QM014, 2009.

KRATZ, J.M.; LANG, K.L.; SILVA, I.T.; MASCARELLO, A.; NUNES, R.J.; BARARDI, C.R.M.; SIMÕES, C.M.O. Evaluation of the anti-HSV-1 activity of pentyl and isopentyl gallates. In: XX Encontro Nacional de Virologia, Brasília-DF. Virus Reviews and Research, v. 14, p. 82, 2009.

SIMÕES, C.M.O.; BARARDI, C.R.M.; REGINATTO, F.H.; ANDRIGHETTI-FROHNER, C.R.; SILVA, A.C.; CARRIEL-GOMES, M.C.; MULLER, V.D.M.; **KRATZ, J.M.**; LUCKEMEYER, D.D.; SILVA, I.T.; SAVI, L.; Searching for New Antiviral Agents from Brazilian Biodiversity. In: World Congress of *In vitro* Biology, Tucson,

Arizona. *In vitro* Cellular & Development Biology, v. 44, p. S21-S21, 2008.

FERRONATO, K.; **KRATZ, J. M.**; ARAUJO, F.A.; TEIXEIRA, H.F.; SIMÕES, C.M.O.; KOESTER, L.S. Desenvolvimento de um Método Analítico para Caracterização dos Complexos de Talidomida com HPBCD e MEBCD por HPLC. In: XX Salão de Iniciação Científica da UFRGS, Porto Alegre/RS. Abstracts, p. 605-605, 2008.

ANDRIGHETTI-FROHNER, C.R.; **KRATZ, J.M.**; LEAL, P.C.; BARARDI, C.R.M.; SIMÕES, C.M.O.; NUNES, R.J.; BERGSTRÖM, T. Anti-Herpes Simplex Virus type 2 Activity of Gallic Acid and Pentyl Gallate. In: VI International Congress of Pharmaceutical Sciences, 2007, Ribeirão Preto/SP. Abstracts, v. único, p. QM033-QM033, 2007.

KRATZ, J.M.; ANDRIGHETTI-FROHNER, C.R.; LEAL, P.C.; NUNES, R.J.; YUNES, R.A.; BARARDI, C.R.M.; SIMÕES, C.M.O. Molecular investigation of the *in vitro* anti-HSV-1 activity of gallic acid and pentyl gallate. In: XVIII Encontro Nacional de Virologia, Búzios/RJ. Virus Reviews and Research, v. 12, p. 125-126, 2007.

ANDRIGHETTI-FROHNER, C.R.; **KRATZ, J.M.**; LEAL, P.C.; NUNES, R.J.; YUNES, R.A.; BARARDI, C.R.M.; SIMÕES, C.M.O. Evaluation of the *in vitro* anti-HSV-2 activity of gallic acid and pentyl gallate. In: XVIII Encontro Nacional de Virologia, Búzios/RJ. Virus Reviews and Research, v. 12, p. 126-126, 2007.

LUCKEMEYER, D.D.; SILVA, I.T.; ANDRIGHETTI-FROHNER, C.R.; **KRATZ, J.M.**; LEAL, P.C.; SOUZA, L.B.P.; SILVA, L.L.; JOUSSEF, A.C.; BARARDI, C.R.M.; SIMÕES, C.M.O. Antiherpes screening of N,N'-diarylurea, pyridazinone and glutamic acid derivatives. In: XVIII Encontro Nacional de Virologia, Búzios/RJ. Virus Reviews and Research, v. 12, p. 127-127, 2007.

FERRONATO, K.; **KRATZ, J.M.**; SIMÕES, C.M.O.; TEIXEIRA, H.F.; KOESTER, L.S. Talidomida: validação de método analítico por espectrofotometria no ultravioleta e avaliação preliminar da complexação com ciclodextrinas. In: XIX Salão de Iniciação Científica da UFRGS, Porto Alegre/RS. CDROM, p. 367, 2007.